US Army Corps of Engineers

TECHNICAL REPORT HL-92-11

(2)

HYDRODYNAMICS AT MOUTH OF COLORADO RIVER, TEXAS, PROJECT

Numerical Model Investigation

by

Larry M. Hauck

Hydraulics Laboratory

DEPARTMENT OF THE ARMY
Waterways Experiment Station, Corps of Engineers
3909 Halls Ferry Road, Vicksburg, Mississippi 39180-6199

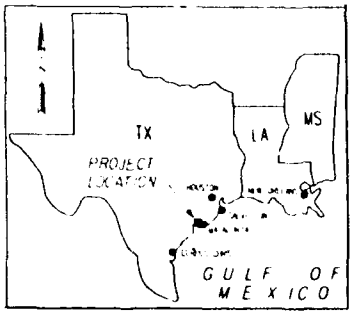

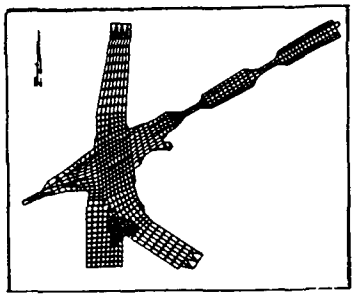

September 1992

Final Report

Prepared for US Army Engineer District, Galveston
Galveston, Texas 77553

HYDRAULICS LABORATORY

Destroy this report when no longer needed. Do not return it to the originator.

The findings in this report are not to be construed as an official Department of the Army position unless so designated by other authorized documents.

The contents of this report are not to be used for advertising, publication, or promotional purposes. Citation of trade names does not constitute an official endorsement or approval of the use of such commercial products.

REPORT DOCUMENTATION PAGE

Form Approved
OMB No. 0704-0188

1. AGENCY USE ONLY *(Leave blank)*	2. REPORT DATE	3. REPORT TYPE AND DATES COVERED
	September 1992	Final report

4. TITLE AND SUBTITLE

Hydrodynamics at Mouth of Colorado River, Texas, Project; Numerical Model Investigation

5. FUNDING NUMBERS

6. AUTHOR(S)

Larry M. Hauck

7. PERFORMING ORGANIZATION NAME(S) AND ADDRESS(ES)

USAE Waterways Experiment Station, Hydraulics Laboratory, 3909 Halls Ferry Road, Vicksburg, MS 39180-6199

8. PERFORMING ORGANIZATION REPORT NUMBER

Technical Report HL-92-11

9. SPONSORING/MONITORING AGENCY NAME(S) AND ADDRESS(ES)

USAE District, Galveston, PO Box 1229, Galveston, TX 77553

10. SPONSORING/MONITORING AGENCY REPORT NUMBER

11. SUPPLEMENTARY NOTES

Available from National Technical Information Service, 5285 Port Royal Road, Springfield, VA 22161.

12a. DISTRIBUTION/AVAILABILITY STATEMENT

Approved for public release; distribution is unlimited.

12b. DISTRIBUTION CODE

13. ABSTRACT *(Maximum 200 words)*

The Mouth of Colorado, Texas, Project includes a diversion channel of the Colorado River into the eastern arm of Matagorda Bay, a dam on the present Colorado River channel downstream of the diversion channel, a dam at Culver Cut, and a navigation bypass channel from the Gulf of Mexico to the city of Matagorda, TX. The project will create an intersection of the Gulf Intracoastal Waterway (GIWW) with the navigation bypass channel, which is the emphasis of this study. The freshwater flow diversion is expected to alter existing current patterns and tidal propagation in an area with navigational and recreational concerns.

The US Army Engineer District, Galveston, required that preliminary results from steady-state numerical simulations be produced initially and be followed by field investigations and long-term dynamic numerical simulations of hydrodynamics. Both the field data collection effort and the ship simulation study are described in separate reports.

(Continued)

14. SUBJECT TERMS

Bypass channel; Matagorda Bay; TABS System; Freshwater diversion; Navigation; Hydrodynamic model; Numerical simulation

15. NUMBER OF PAGES 100

16. PRICE CODE

17. SECURITY CLASSIFICATION OF REPORT	18. SECURITY CLASSIFICATION OF THIS PAGE	19. SECURITY CLASSIFICATION OF ABSTRACT	20. LIMITATION OF ABSTRACT
UNCLASSIFIED	UNCLASSIFIED		

13. ABSTRACT (Continued).

This report describes the hydrodynamic steady-state preliminary results, verification to prototype measurements, and long-term tidally influenced simulations using the vertically integrated two-dimensional numerical model, RMA-2V.

PREFACE

The numerical modeling of hydrodynamic conditions for the Mouth of the Colorado River, Texas, Project, as documented in this report was performed for the US Army Engineer District, Galveston.

The study was conducted in the Hydraulics Laboratory (HL) of the US Army Engineer Waterways Experiment Station (WES) from April to December 1990 under the direction of Messrs. Frank A. Herrmann, Jr., Chief, HL; Richard A. Sager, Assistant Chief, HL; William H. McAnally, Jr., Chief, Estuaries Division (ED); and David R. Richards, Chief, Estuarine Simulation Branch (ESB), ED.

The work was performed and the report was prepared by Mr. Larry M. Hauck (ESB) with technical support from Messrs. John Cartwright and Mark Bardwell (ESB). Mr. Ed Reindl was liaison for the Galveston District.

At the time of publication of this report, Director of WES was Dr. Robert W. Whalin. Commander and Deputy Director was COL Leonard G. Hassell, EN.

CONTENTS

CONVERSION FACTORS, NON-SI TO SI (METRIC) UNITS OF MEASUREMENT

Non-SI units of measurement used in this report can be converted to SI (metric) units as follows:

Multiply	By	To Obtain
cubic feet	0.02831685	cubic metres
cubic feet per second	0.02831685	cubic metres per second
degrees (angle)	0.01745329	radians
feet	0.3048	metres
feet per second	0.3048	metres per second
inches	2.54	centimetres
miles (US statute)	1.609347	kilometres
miles per hour	1.609347	kilometres per hour
pounds (force) - second per square foot	47.88026	pascals-second

HYDRODYNAMICS AT MOUTH OF COLORADO RIVER, TEXAS, PROJECT

Numerical Model Investigation

PART I: INTRODUCTION

Background

1. The Mouth of Colorado River, Texas, Project is located on the Texas coast of the Gulf of Mexico about midway between the ports of Galveston and Corpus Christi (Figure 1, USAE District 1981). The project consists of a diversion channel of the Colorado River into the eastern arm of Matagorda Bay, a dam on the present Colorado River channel downstream of the diversion channel, a dam at Parker's (Tiger Island) Cut, and a navigation bypass channel (bypass channel) from the Gulf of Mexico to the city of Matagorda, Texas (Figure 1). As authorized, the project consists of navigation, recreation, and river diversion features.

2. The Gulf Intracoastal Waterway (GIWW) is a salient feature in the project area. The east and west Colorado River locks on the GIWW serve to control sediment and facilitate barge crossing during times of excessive velocities at the GIWW-Colorado River intersection.

3. The Mouth of Colorado River project will divert the freshwater flow of the Colorado River into Matagorda Bay and alter current patterns and tidal propagation in the project area through construction of two dams and two channels. Navigation interests are concerned that the project will alter current patterns at the GIWW-Colorado River intersection and at the proposed intersection of the bypass channel and the GIWW.

Purpose

4. This investigation was conducted to develop hydrodynamic conditions (water levels and velocities) for use in a tow-simulation study of the influence of the Mouth of Colorado River, Texas, Project on the GIWW. Emphasis was placed upon the proposed intersection of the bypass channel at the GIWW between the east lock and the F.M. 2031 pontoon bridge crossing of the GIWW. The tow-simulation study was performed by the Waterways Division of the

Hydraulics Laboratory at the US Army Engineer Waterways Experiment Station (WES), and is reported separately (Thevenot and Daggett, in preparation).

Approach

5. The investigation was designed to provide preliminary information that could be used quickly in tow-simulation studies, and be followed with field investigations and long-term dynamic simulation of currents and water levels. The sequential steps to the approach are discussed below.

a. Numerical meshes were developed and steady-state hydrodynamic conditions were simulated for five intersection configurations of the project and the GIWW. These steady-state results provided ranges of currents for use in a tow-simulation study.

b. Currents were measured in the prototype for 25 hr (one tidal cycle) in the vicinity of the intersection of the GIWW with the Colorado River, and water levels were recorded for approximately five weeks in the project area. Currents were measured during high amplitude tides, which produced high tidal currents. These measurements were made to allow numerical model verification and to provide boundary conditions for the numerical model.

c. A numerical mesh of the present project area and contiguous water areas was developed, and the numerical model was verified to prototype current measurements and water levels.

d. The numerical mesh was modified to reflect alternative designs of the navigation channel and other Mouth of Colorado River project features. (The diversion channel for the project has been dredged, while other features of the project were not constructed at the time of this study.) These alternative design meshes were operated to simulate the hydrodynamics for 27 days during the period of prototype water-level records. From the 27-day simulation, tidal current duration (or frequency) graphs were developed for the proposed bypass channel-GIWW intersection.

e. An unverified model of McCabe Cut was operated for 27 days. McCabe Cut was a channel directly connecting the GIWW to the Gulf of Mexico. The McCabe Cut model results were compared with results from step d. Located east of East Matagorda Bay, McCabe Cut was closed due to an increase in its size, development of dangerous crosscurrents affecting navigation in the GIWW, and sedimentation problems in the GIWW. Limited comparisons were made of currents at the McCabe Cut-GIWW intersection and the proposed navigation channel-GIWW intersection.

PART II: HYDRODYNAMIC MODEL AND MESHES

The TABS-2 Modeling System

6. TABS-2 is a modular system composed of distinct computer programs linked by preprocessors and postprocessors. Each of the major computer programs solves a particular type of problem: hydrodynamics (RMA-2V), sediment transport (STUDH), or water quality (RMA-4). These programs employ the finite element method to solve the two-dimensional vertically averaged governing equations. Only the RMA-2V model was required for this study, and a brief description of RMA-2V appears in Appendix A. The RMA-2V model has been successfully used in over 50 US Army Corps of Engineers applications in inland and coastal waters.

Two-Dimensional Hydrodynamic Model

7. RMA-2V is a finite element solution of the Reynolds form of the Navier-Stokes equations for turbulent flows in two dimensions (vertical averaging). Friction is calculated with Manning's equation, and eddy viscosity coefficients are used to define turbulent exchange characteristics. A velocity form of the basic equation is used with side boundaries treated as either slip (parallel flow) or static (zero flow). The model recognizes computationally wet or dry elements and corrects the mesh accordingly. Boundary conditions may be water-surface elevations, velocities, or discharges and may occur inside the mesh as well as along the outer boundaries.

Numerical Meshes

8. A numerical mesh was developed for each system to which RMA-2V was applied. The scope of this study necessitated the development of numerous meshes, including meshes for steady-state simulations and for dynamic simulations.

Steady-state meshes

9. In the steady-state simulations, the preproject and postproject Colorado River-GIWW intersections were evaluated. Also, three alternative designs of the postproject intersection at the bypass channel and the GIWW

were evaluated. These steady-state results were used in the tow-simulation study.

10. The mesh of the preproject Colorado River-GIWW intersection is provided in Figure 2. The postproject Colorado River-GIWW intersection with diversion channel and river channel dam is depicted in Figure 3. Three alternative designs of the postproject intersection of the bypass channel and the GIWW are depicted in Figures 4-6. Alternative design 1 (Figure 4), which was the initial design, provided for a 50-deg* angle of intersection of the bypass channel with the GIWW. To reduce the crosscurrent (current component perpendicular to the GIWW), the alternative design 2 (Figure 5) provided for an angle of intersection of about 25 deg. Alternative design 3 (Figure 6) also had an angle of intersection of about 25 deg and the bypass channel width had been increased in an attempt to reduce currents in the intersection area. The meshes were used in step a described in Part I.

11. The horizontal plane representation for the meshes was obtained from maps provided by the USAE District, Galveston (SWG). The sole exception was the alternative design 3 bypass channel, which was developed by the Waterways Division at WES. Bathymetric information was obtained from the design drawings for the Mouth of Colorado River project and from cross-section information provided by SWG of which the greatest source was the GIWW predredge survey drawings of February 1990.

Dynamic meshes

12. To include tidally influenced areas that would affect velocities in the project area and to include convenient boundary condition locations, the dynamic meshes had to incorporate much greater geographical regions than in the steady-state meshes. Four meshes were developed: one represented the present (partial project) condition, two represented various designs of the postproject intersection at the navigation bypass channel and the GIWW, and one included the former McCabe Cut. Generally, the dynamic meshes were developed by expanding the appropriate steady-state mesh(es).

13. The present condition mesh used in verification to prototype data (step c described in Part I) is provided in Figure 7. A dynamic mesh was developed for steady-state alternative design 2 and for steady-state

* A table of factors for converting non-SI units of measurement to SI (metric) units is presented on page 3.

alternative design 3. Both postproject meshes, which were used to evaluate various bypass channel designs under dynamic (tidally varying) conditions, have no discernible difference at the scale required to show the entire mesh area. As for the steady-state meshes, these meshes vary only in the alignment and width of the bypass channel. A representative mesh is provided in Figure 8. In addition to the bypass channel, these postproject meshes included the two proposed Mouth of Colorado Project dams. When the near-river gate on the east navigation lock is closed, as assumed in all project simulations, the project area is hydrodynamically separated from Matagorda Bay and the Colorado River by the project dams and existing gate. These meshes were used in step d described in Part I.

14. The McCabe Cut mesh involved expansion and modification of the verification mesh. The mesh was expanded to the east to include McCabe Cut, San Bernard River, and other relevant features in the vicinity of the cut (see Figure 9). This mesh was used in step e described in Part I.

15. Horizontal plane representation and bathymetric information were obtained from maps and charts provided by SWG. The following National Ocean Service/National Oceanic and Atmospheric Administration nautical charts were used extensively:

Chart No.	Location	Scale	Date
11319	Cedar Lakes to Espiritu Santo Bay	1:40,000	Dec 1985
11322	Galveston Bay to Cedar Lakes	1:40,000	Jan 1985

These were supplemented with numerous US Geological Survey (USGS) 7-1/2-minute quadrangle maps and SWG cross-section information along the GIWW.

PART III: STEADY-STATE HYDRODYNAMIC MODEL APPLICATION

16. The development of steady-state currents for the tow simulator required use of the five meshes representing the various intersection conditions (Figures 2-6). These meshes were operated with the RMA-2V model to produce various levels of current for assessment in the tow-simulator study.

17. The RMA-2V model was operated at several current levels for each of the five intersection condition meshes (Table 1). The intent was to generate a reasonable range of steady-state velocities for use in the simulator study. For the preproject and postproject Colorado River-GIWW intersection, only downstream (ebb) flows were generated, which reflected the condition of river flow and ignored tidal influences. Tidal influences were ignored since the project dams should reduce tidal influences in this area and pilot experience indicated greatest difficulties occurred during high river inflow. The four velocity cases were 0.5, 1.0, 2.0, and 3.0 fps, in which the average velocity was determined in the Colorado River channel immediately upstream of the GIWW. The corresponding river flows to cause the velocities are provided in Table 1.

18. The simulations of the bypass channel-GIWW intersection were conducted for ebb and flood conditions. The eight velocity cases were 0.5, 1.0, 2.0, and 3.0 fps each for ebb and flood conditions. The average velocity was determined in the bypass channel immediately downstream of the GIWW for alternative design 1. The differences in average channel velocity for the same flow (Table 1) result from the different channel cross-sectional areas of the alternative 1, 2, and 3 designs. (The desired 3.0-fps velocity case was just low at 2.9 fps.)

19. The desired flow boundary condition for each mesh was specified at the upstream boundary, and a constant water-level boundary condition equal to mean lower low water (mllw) was specified at the downstream end. This was the appropriate boundary specification procedure for subcritical flow. The upstream and downstream boundaries were reversed when flow was flood as opposed to ebb.

20. Based upon experience in other Gulf coast estuarine systems, the bottom roughness coefficients (Manning's n) were selected to reflect a slight

Table 1

Steady-State Hydrodynamic Condition Cases

Intersection Condition	Flow cfs	Flow Direction	Average Channel Velocity fps	Eddy Viscosity lb-sec/ft^2
Preproject Colorado River–GIWW	2,000	Ebb	0.5	1
	4,000	Ebb	1.0	1
	8,000	Ebb	2.0	2
	12,000	Ebb	3.0	3
Postproject Colorado River–GIWW	2,000	Ebb	0.5	1
	4,000	Ebb	1.0	1
	8,000	Ebb	2.0	2
	12,000	Ebb	3.0	3
Bypass channel–GIWW Alternative 1	1,000	Ebb	0.5	1
	2,050	Ebb	1.0	1
	4,100	Ebb	2.0	2
	6,150	Ebb	2.9	3
	1,000	Flood	0.5	1
	2,050	Flood	1.0	1
	4,100	Flood	2.0	2
	6,150	Flood	2.9	3
Bypass channel–GIWW Alternative 2	1,000	Ebb	0.5	1
	2,050	Ebb	1.1	1
	4,100	Ebb	2.2	2
	6,150	Ebb	3.3	3
	1,000	Flood	0.5	1
	2,050	Flood	1.1	1
	4,100	Flood	2.2	2
	6,150	Flood	3.3	3
Bypass channel–GIWW Alternative 3	1,000	Ebb	0.3	1
	2,050	Ebb	0.6	1
	4,100	Ebb	1.3	2
	6,150	Ebb	1.9	3
	1,000	Flood	0.3	1
	2,050	Flood	0.6	1
	4,100	Flood	1.3	2
	6,150	Flood	1.9	3

inverse relationship with depth as follows:

Depth, ft	Manning's n
0–5	0.022
5–10	0.020
>10	0.018

The other coefficient requiring specification in RMA-2 was the eddy viscosity or turbulent exchange coefficient. The eddy viscosity coefficient is directly proportional to both element size and velocity. Since element size was similar throughout all meshes, a constant eddy viscosity value was assigned for a specified flow and the values were increased as flow was increased (see Table 1). The eddy viscosity was adjusted to produce reasonable current patterns in the study areas. These patterns included eddies and velocity variations laterally across channels. However, the size of the channels and the length of the tows in the simulator study (300 ft minimum) make the tow simulations relatively insensitive to the detailed current adjustments obtained with reasonable eddy viscosity coefficients.

21. The current pattern for a particular direction of flow through a mesh was similar for the four levels of velocity (or flow). Therefore, only the current pattern for the highest velocity case is provided. The 12,000-cfs ebb current pattern for preproject Colorado River-GIWW intersection (Figure 10) showed a strong flow across the GIWW with weak eddies formed in the intersection on both sides of the flow. A similar current pattern was predicted for the 12,000-cfs flow in the postproject Colorado River-GIWW intersection (Figure 11) with a third eddy formed to the north of the dam on the old Colorado River Channel.

22. The flood and ebb current patterns for the 6,150-cfs condition are presented for each of the three alternative designs of the bypass channel-GIWW intersection. The flood and ebb current patterns for alternative design 1 are presented in Figures 12 and 13, respectively. The most notable feature of the flood current pattern was the well-defined eddy in the GIWW. On the ebb current pattern, crosscurrents were generated in the GIWW as the flow made the relatively sharp turn into the bypass channel. The flood and ebb current patterns for alternative design 2 are presented in Figures 14 and 15; design 2 was smoother and the eddy in the GIWW was greatly reduced. The flood and ebb

patterns of design 3 (Figures 16 and 17, respectively) were similar to design 2, except the widened channel of design 3 resulted in reduced velocities and an easier flow transition from the GIWW to the bypass channel. The influences on navigation of these designs is reported in Thevenot and Daggett (in preparation).

PART IV: HYDRODYNAMIC MODEL VERIFICATION

23. The dynamic RMA-2V model was verified to water levels and currents measured by WES during the period 25-26 May 1990. These field measurements were the only available detailed and synoptic data of currents for the conditions in the project area during mid-1990.

24. The process of verification of RMA-2V required adjustment of eddy viscosity coefficients, which control turbulence exchange due to velocity gradients; Manning's n values, which define bed friction; and wind shear stress formulation, which controls wind stress on the water surface. In addition, accurate boundary conditions must be supplied at the open water edges (or boundaries) of the numerical mesh. Water-level boundary conditions were specified where the Colorado River enters the Gulf of Mexico, at the western extremity of the mesh in Matagorda Bay, at Caney Fork Cut located at the eastern extremity of East Matagorda Bay, and at the upstream end of the Colorado River.

Verification Approach

25. The RMA-2V was verified through adjustment of model coefficients and comparison with field measurements, a process common to the majority of numerical model applications. (The WES field investigation is reported in Fagerburg, Coleman, Parman, and Fisackerly (1992.) However, the verification process required modification of emphasis because (a) the proposed project will drastically alter pathways and connections of tidal propagation in the study area (see Figure 1) and (b) the prototype current measurements indicated extremely complex flow patterns and eddy formation at the existing (May-June 1990) five-channel intersection of the upper and lower Colorado River, east and west GIWW segments, and the diversion channel. To resolve the complexity of flow patterns measured in the existing intersection would have necessitated a greatly refined mesh, which was not warranted for this study since this intersection will be hydrodynamically isolated (not included) from the proposed navigation bypass channel-GIWW intersection by dams and lock gates. However, the existing intersection and prototype measurements in its vicinity provided a convenient means to verify that the model properly simulated tidal propagation through the study area. Therefore the emphasis of the

verification process was to properly reproduce cross-sectionally averaged flows, especially in the east segment of the GIWW, rather than to accurately reproduce the lateral current variations.

Model Coefficients

26. The process of model verification resulted in one final set of model coefficients representing Manning's n values, eddy viscosity, and wind stress. These coefficients were selected by adjustment within the range of realistic values until the optimum comparison of RMA-2V-predicted water levels and currents with field-measured values was obtained.

Eddy viscosity and Manning's n

27. Eddy viscosity coefficients and Manning's n values used in this study were as follows:

Location	Eddy Viscosity lb-sec/ft^2	Manning's n
Upper Colorado River	1,000-2,000	0.020-0.040
Lower Colorado River	25	0.018-0.022
Diversion channel	25	0.018-0.022
Open shallow bays	100	0.020-0.022
Colorado River at GIWW	8-15	0.018-0.022
GIWW, east of Colorado River	3	0.018-0.022
Miscellaneous one-dimensional areas	1,000-2,000	0.020-0.040
GIWW, one-dimensional	1,000	0.020
Culver Cut	3,000	0.040

Element sizes largely dictated the selected eddy viscosities, since these values are directly proportional to element size and velocity. The Manning's n values reflected expected differences in bottom roughness and a slight inverse relationship of n value to water depth which ranged from as deep as 20 ft to as shallow as 2 to 3 ft in portions of East Matagorda Bay. To represent the head loss through the dendritic pattern at Culver Cut without including the enormous detail necessary to represent the cut, elevated eddy viscosity and Manning's n values of 3,000 lb-sec/ft^2 and 0.040, respectively, were used. With these values, peak ebb and flood velocities through the cut were 2 to 3 fps, which were in the range of values measured in field studies by the US Geological Survey in the 1970's (Hahl and Ratzlaff 1971 and Smith 1977).

28. As discussed previously, complex flow patterns were measured in the prototype system at the existing Colorado River-GIWW intersection. The eddies

and associated turbulence exchange in the prototype system required eddy viscosities of 8 to 15 lb-sec/ft^2 in the model, whereas a value of 3 lb-sec/ft^2 was used in the GIWW east of the Colorado River for similar element sizes and velocities. (The eddy viscosity of 3 lb-sec/ft^2 was also used in the GIWW east of the Colorado River for simulations with the navigation bypass channel, as presented in Part V.)

Wind stress formulation

29. The Wu wind stress formulation was used in this application. The formula has the following form:

$$\tau = \rho_a C W^2 \tag{1}$$

where

τ = horizontal stress

ρ_a = density of air

C = nondimensional drag coefficient, $C = 0.0005\ W^{0.5}$

W = wind speed, generally measured at a height of 10 m

Good agreement exists among researchers on wind stress formulation, in particular, the formulation of C . While the Wu formulation results in a horizontal stress slightly higher than the majority of formulations, the Wu formulation has been successfully applied to Gulf of Mexico regions such as the Mississippi Sound area. Because the orientation of East Matagorda is nearly perpendicular to the prevailing southeast winds, the model results indicated insignificant response to the wind stress formulation applied for the verification period. By using the Wu wind stress formulation, a conservative (high) yet reasonable response of the model to various sensitivity simulations with east, west, and north winds was assured.

One-Dimensional Elements

30. Extensive use of one-dimensional (1D) elements was made in the mesh to represent the upper Colorado River to approximately the head of tide, the GIWW removed from the areas of emphasis, the numerous creeks and bayous that enter the north side of the GIWW, and the eastern extremity of East Matagorda Bay, including Caney Fork Cut. In RMA-2V, 1D elements allow specification of a trapezoidal cross-section (bottom width and side slopes) and side storage, which can represent marsh areas. By using 1D elements, areas removed from the

study area, where extreme detail was not required, can be included with the necessary detail and with minimal computational burden.

Boundary Conditions

31. RMA-2V was operated with boundary conditions at all external water edges to the mesh, i.e., the Colorado River at the Gulf of Mexico, Matagorda Bay, Caney Fork Cut, and the upstream end of the Colorado River. The measurements from water-level recorders in Matagorda Bay and the Colorado River at the Gulf were the source of the time-dependent water-surface elevations at these locations. The water-level measurements on the Colorado River at the Gulf were applied unadjusted at Caney Fork Cut. While some phasing and amplitude differences probably exist between the two areas, Caney Fork Cut is a minor Gulf opening, removed from the project area, and consequently the water levels at Caney Fork Cut are of minimal importance to currents in the project area. Prototype water levels in the Colorado River at the Gulf are shown in Figure 18 for the period immediately prior to and including the intensive field survey. Part of these data were used as the Gulf boundary condition for model verification.

32. Both the eastern and western ends of the GIWW in the mesh were not provided boundary conditions. The eastern end of the GIWW was too far removed from the project area for the boundary condition at this location to have any impact on the project. The next eastward Gulf opening, the San Bernard River, is 15 miles to the east of Caney Fork Cut, which would indicate that most of the tidal variation in the GIWW at the eastern end of the mesh propagates through Caney Fork Cut.

33. The western GIWW end was a more important issue, due to proximity to the project area. Because of the direct connection with Matagorda Bay through Culver Cut (see Figure 1) and the nearer access of this section of the GIWW to tidal propagation from the Colorado River, only minor tidal propagation was expected from the west. The nearest Gulf opening to the west is a major opening, the Matagorda Ship Channel, which is approximately 25 miles west of Culver Cut. Based on the predominant tidal propagation occurring up the Colorado River into this section of the GIWW and the relatively minor flows in this reach of the GIWW, as indicated from the field study, a boundary condition was not specified at the western end of the GIWW.

34. Information before and during the field survey was provided by SWG on the USGS streamflow gaging stations on the Colorado River at Bay City, TX, and at Wharton, TX (Meyers*). This information, which indicated steady flows, was used to give the 900-cfs flow at upstream boundary on the Colorado River.

35. The wind speed and direction for use in determining the wind stress were provided by the published records from the Victoria, TX, National Weather Service (NWS). The field investigation wind station malfunctioned, which prevented use of that data source. The limited direction data salvaged from the wind station indicated excellent agreement with the Victoria NWS data.

36. During the field survey, the Victoria NWS data indicated winds peaking in midafternoon at 18 to 20 mph and decreasing to 5 to 6 mph by early morning. Wind direction was from the south to southeast, which is typical of the prevailing late spring-summer patterns along the Texas coast.

Comparison with May 1990 Field Measurements

37. RMA-2V was operated for the May 1990 verification period with the eddy viscosities, Manning's n values, wind stress formulation, wind speed and direction, water-level boundary conditions, and flow boundary condition previously discussed. The water levels and currents predicted with RMA-2V were compared with the field measurements, which were taken at the stations depicted in Figure 19. RMA-2V was operated with a 1-hr time-step, which has proven to be acceptable for several studies with RMA-2V along the Gulf of Mexico. A 29-hr initial period was used to allow the transients induced by initialization of RMA-2V to dissipate and for the model solution to respond correctly to the imposed boundary conditions. The simulations were initiated at midnight on 23 May and the verification field measurements had begun at approximately 7:00 am on 25 May. For the field measurements, arrangements had been made with SWG for all gates on the navigation locks to be left open beginning at midnight on 23 May and to remain open until completion of the survey at approximately 8:00 am on 26 May. The open gates avoided the complexity of gate operation on the hydrodynamics, and allowed uninterrupted

* Personal communications from R. Meyers, 1990, US Army Engineer District, Galveston, Galveston, TX.

tidal propagation to the east as would occur with the project bypass channel. During this period, high amplitude (tropic) tides occurred producing high tidal currents.

38. Comparisons of water level predicted by RMA-2V with the two interior (nonboundary) water-level recorder measurements are presented in Plate 1. The water-level comparisons indicated good agreement between model results and field measurements. At sta S3, GIWW at the Colorado River, the phasing and amplitude were very good. At sta S4, in the GIWW 5 miles east of the Colorado River and near the first cut into East Matagorda Bay, the phasing was correct. The simulated amplitude at sta S4 was very damped compared with the amplitude at sta S3 as was indicated in the measurements. Though the damping from the prototype record was somewhat greater, the model water levels were within 0.2 ft of the prototype data.

39. Comparisons of velocities predicted by RMA-2V with field-measured values are provided in Plates 2-11. At all survey stations, the vertical depth profile from the field survey was averaged to obtain a single value for comparison with the vertically integrated RMA-2V results. RMA-2V-predicted velocities generally compared favorably with the vertically averaged field measurements. However, the RMA-2V results did not totally reproduce the significant lateral variations across some channels resulting from complex eddy patterns that occurred in the GIWW-Colorado River area.

40. At sta 1A, 1B, and 1C (Plates 2 and 3), the model velocity direction and magnitude accurately reproduced the prototype data, though peak velocities are underpredicted by approximately 0.5 fps. At this location tidal propagation occurred with a strong standing wave component. (For a pure standing wave, velocity phasing precedes water-level phasing by approximately 90 deg (6 hr)).

41. At sta 2A, 2B, and 2C (Plates 3 and 4), RMA-2V reproduced the general pattern at the cross section. However, the prototype data indicated stronger lateral variations than predicted with the model. The same pattern occurred at sta 3A, 3B, and 3C (Plates 5 and 6). The prototype lateral variations were even more extreme at cross section 3, as compared with cross section 2. At cross section 3, prototype currents were generally feeble and less than 1.0 fps, and at sta 3C an eddy formed on the ebb tide which resulted in local velocities of less than 0.5 fps generally in the flood direction. This eddy was not resolved by RMA-2V.

42. At sta 4A, 4B, and 4C (Plates 6 and 7), prototype velocities were again feeble and always less than 1.0 fps. Because of freshwater inflow, the flow direction was predominately ebb at this cross section. Lateral variation was less pronounced at this cross section as compared with cross sections 2 and 3, and the model provided good results on velocity direction and magnitude.

43. At sta 5A, 5B, and 5C (Plates 8 and 9), the model results reproduced the average cross-section currents, i.e., the model and prototype results for the center of the channel (sta 5B) were in very good agreement. An eddy developed in the prototype on the ebb tide at sta 5A, which produced the highest ebb velocity at sta 5C. This lateral variation was not reproduced by the numerical model.

44. Even in the straight section of the GIWW between the east lock and the pontoon bridge, noticeable lateral variation occurred. At cross section 6 (Plates 9 and 10), the flood current moved toward the north bank (sta 6A) and on the ebb the current moved to the south bank (sta 6C). As occurred at several of the previous cross sections, the model properly simulated current velocities and tidal phasing for the center station (sta 6B), but the lateral variations were not properly simulated. The cause of current variation at cross section 6 could not be explained by available bathymetric data or by channel alignment and shape.

45. Limited prototype measurements were made at cross section 7, which was located in the GIWW approximately 5 miles east of the Colorado River. Cross section 7 was immediately west of the most westerly pass from the GIWW into East Matagorda Bay. Because the numerical mesh was 1D in this region (laterally and vertically integrated), simulated results are compared with cross-section averaged prototype measurements for sta 7 (Plate 11). The simulated results are about 0.5 fps too high. Portions of this difference were the result that (a) the 1D conveyance channel in the model includes area adjacent to the GIWW only as storage and as not capable of carrying flow, i.e., the hydraulic cross section is underestimated in the model, and (b) the vertical prototype measurements were made only at two points along the cross section (right and left channel edges), which would tend to slightly underestimate average channel velocity. Based on the above sources of velocity differences and the proper simulation of water level damping near this

location (sta S4), the model appeared to properly simulate flow in this portion of the GIWW.

46. While the strong standing wave component in both prototype and numerical data, as previously discussed for cross section 1, was also observed at cross sections 2, 3, and 4, a strong progressive wave influence was indicated at cross sections 5 and 6. At these two cross sections, both the prototype and numerical tides behaved as a progressive wave, e.g., maximum flood current occurred in phase with high water (model hr 35). The ability of the model to reproduce this behavior increased confidence that important features to the east of the Colorado River dictating tidal exchange were properly represented.

47. The inability of the numerical model and mesh to reproduce the complicated lateral variations and eddies of the prototype system was apparent. Possible explanations include: (a) three-dimensional flow patterns in the prototype system, which were measured, but cannot be reproduced by a two-dimensional model, (b) low spatial resolution in the mesh, even though element sizes in the study area are typically less than 100 ft by 100 ft, and (c) too much turbulence exchange because of eddy viscosity coefficients that are too large. The complex flow patterns and various directions of exchange between the five intersecting channels required eddy viscosity coefficients a factor of three to five times larger than in the area of the GIWW east of the river locks.

48. While the inability of RMA-2V to reproduce the lateral variations in the prototype system was apparent, this weakness must be kept in perspective, as discussed previously in the verification approach. Proper simulation of average cross-section flow for the Colorado River-GIWW intersection would indicate proper coefficients and tidally affected areas in the model. In fact, the model demonstrated the ability to accurately reproduce average cross-section flows as indicated by comparisons of model simulated currents with average flows (Plate 12-14). The prototype data were averaged at each cross section for those times when measurements occurred at all three lateral stations. The prototype averaged data and the centerline channel model results showed good agreement in phasing and magnitude at all six cross sections.

49. The ability of the model to properly simulate flow through the channel was demonstrated for the verification period, even if lateral variations

were not totally resolved. Water levels and current magnitudes and phasing were, in general, correctly simulated. Very importantly, the progressive wave characteristic and average currents in the GIWW east of the Colorado River were properly simulated, which provided confidence in the ability of the model to simulate the navigation bypass channel condition.

PART V: DYNAMIC MODEL APPLICATIONS

50. Hydrodynamic conditions for two alternative designs of the navigation bypass channel were developed from the verified model. The mesh for the verified model was modified to include the proposed project dams in Culver Cut and on the lower Colorado River south of the GIWW Also, the nearest gate to the Colorado River on the east lock was assumed closed a sufficient percentage of the time to effectively act as a dam. Therefore, the verification mesh was modified to include the navigation bypass channel and to exclude Matagorda Bay, the upper Colorado River, and the GIWW west of the Colorado River (see Figure 8). A second application of the verification mesh involved closing Caney Fork Cut and adding areas to the east of the mesh to allow inclusion of McCabe Cut.

Dynamic Mesh Configurations

51. The configurations of the navigation bypass channel evaluated were the same as those for the steady-state designs and are described below:

a. Alternative design 2: Provided angle of intersection of approximately 25 deg, bypass channel width constant at 100 ft (see Figure 20).

b. Alternative design 3: Provided angle of intersection of approximately 25 deg, bypass channel gradually widened from 100 ft to 175 ft at GIWW (see Figure 21).

Alternative design 1 was not evaluated due to excessive crosscurrent development in the GIWW during the steady-state simulations.

52. The mesh with McCabe Cut was developed to evaluate the situation of a Gulf outlet occurring very near the GIWW. In the model, the McCabe Cut-GIWW area is depicted in Figure 22. McCabe Cut, which has been closed, was originally constructed at a width of 40 ft and depth of 3.5 ft below mean low water (mlw). Swift currents, often associated with freshwater floods, enlarged the cut appreciably beyond the project dimensions. The size of the cut apparently varied with time, but dimensions of 100 ft wide and 20 ft deep were reported by Texas A&M (1988). The engineering drawing for closing the cut gave the following dimensions: bottom width of 70 ft, top width of 150 ft, and relatively flat bottom at a depth of 13 ft below mlw. McCabe Cut was specified in the model as having an average depth of 8 ft below mlw, a width of 125 ft, and

a length from the Gulf to the GIWW of 1,400 ft. This represented an approximate average cross section between the design size and observed extremes.

Simulated Navigation Bypass Channel Conditions

53. To evaluate the frequency of occurrence of velocities in the GIWW and bypass navigation channel (and McCabe Cut) the simulated period needed to encompass a reasonable range of tides. Based on the fact that Texas coastal tides are dictated by the declination of the moon, a tropic month period was selected, which is 27.3 days. (A tropic month is the duration of the average declination cycle of the moon.) Allowing 1 day for the model to overcome imposed initial conditions, 28 days were simulated. The selected period was midnight 31 May 1990 to midnight 28 June 1990, a period during which water-level recorders were positioned in the study area. The unfiltered (unsmoothed) recorded hourly values of water levels used as the driving Gulf tide in the model are depicted in Figure 23. During this tropic month, two periods of high amplitude diurnal (maximum declination or tropic) tides occurred. The first period (approximately model hours 100 to 240) had lower amplitude than the second period (approximately model hours 460 to 580). The feeble semidiurnal (equatorial) tides occurred twice, around model hours 360 and 660. The Victoria NWS wind speed and direction were used to supply the information to determine surface wind stress. During most of the period, the wind direction was from the southeast at a daily average speed of 10 mph.

54. Sensitivity simulations to 23-mph (20-knot) wind events were undertaken for a frontal passage (norther), constant east winds, and constant west winds. Since the east and west winds occur basically along the primary axis of East Matagorda, the system did respond to this type of wind forcing. The frontal passage included an abrupt water level plunge of 1.5 ft over a couple of hours coincident with ebb tide. The 1.5-ft water level decrease incorporated wind stress on the system, barometric pressure increases, and strong setdown in the Gulf with the frontal passage. Without extended tidal records during the winter months, the degree of setdown associated with frontal passages was difficult to assess. However, based on limited information available for Sabine Pass, TX (Ward and Chambers 1978), the 1.5-ft setdown appeared to be a reasonable response to a well-defined rapidly moving frontal passage.

Hydrodynamic Simulations for Navigation Bypass Channel

55. The dynamic current patterns at the intersection area of the GIWW-navigation bypass channel were very similar to the steady-state patterns previously presented. The reader is referred to the steady-state patterns (Figures 13-16).

56. For alternative design 2, the 27-day time-history of velocities for a central bypass channel location (node 2811) and a GIWW location (node 830) are presented in Plate 15. Node locations are provided in Figure 20. The time-history of water level at the intersection (node 794) is also provided in Plate 16. In Plates 15 and 16, the variation of the astronomical tide during the 27-day period is apparent as reflected in the variation of tide range and peak velocities. Tidal velocity duration for node 2811 is provided in Figure 24 and for node 830 in Figure 25. The duration plots indicate for a given tidal velocity direction (flood or ebb) the percent of the time the velocity is less than a particular value. To obtain the percentage of the total simulated time that the velocity is less than a particular value (direction and magnitude), the percent from the plot must be multiplied by the percentage of time that direction occurred (which is provided on the chart). For example, at node 830 an ebb velocity less than 1.0 fps occurs 44 percent of the time of ebb flow, and occurs 22 percent of the total time (44 percent times 49 percent).

57. For alternative design 3, the 27-day time-history of velocities for a central bypass channel location (node 3205) and a central GIWW location (node 861) are presented in Plate 17. Node locations are provided in Figure 21. The time-history of water level at the intersection (node 794) is also provided in Plate 18. Tidal velocity duration for node 3205 is provided in Figure 26 and for node 861 in Figure 27.

58. To properly assess the velocity duration plots, the tidal amplitudes of 2-28 June 1990 must be considered in relation to seasonal and annual patterns of tides. The National Ocean Service/National Oceanic and Atmospheric Administration (NOS/NOAA) considers 37 harmonic constituents as composing an astronomical tide, and these constituents vary periodically over a 19-year cycle. For the Gulf of Mexico at the Pleasure Pier, Galveston, TX (the closest site of detailed harmonic analysis), the major high frequency constituents are (in descending order of importance): K_1 (lunisolar diurnal

constituent), O_1 (lunar diurnal constituent), M_2 (principal lunar semidiurnal constituent), S_2 (principal solar semidiurnal constituent, and N_2 (larger lunar elliptic semidiurnal constituent). The cyclic variation of these constituents based on a normalized amplitude value of unity was obtained from Shureman (1958) and is presented in Figure 28. Generally, the cycle of the diurnal and semidiurnal constituents are 180 deg out of phase. Also in Figure 28, a normalized maximum amplitude tide is provided based on the normalized constituents, the relative importance of each from the NOS/NOAA harmonic analysis, and assuming all constituents are in phase to give a maximum amplitude. The normalized maximum tide for the Pleasure Pier ranges from 0.92 to 1.08 with a value of 1.05 for the year 1990. This indicates that tidal amplitudes in 1990 were higher than the average.

59. In addition to the annual variations, there is variation in amplitudes within each year. The maximum mean monthly amplitudes occur at the summer and winter soltices (June and December) when the sun's gravitational vector is more nearly parallel to the earth's in subtropical and higher latitudes (see Mason 1981). Conversely, the minimum mean monthly amplitudes occur at the equinoxes (September and March). Since the simulated period was 2-28 June during the summer soltice, tidal amplitudes during this period were higher than the average for 1990. This intra-annual amplitude variation is approximately 5 percent.

60. Based on the above information, the conclusion is that the simulated period was for a month with high mean monthly amplitudes during a year of somewhat higher tidal amplitudes than the average. Therefore, the tidal currents during the period, ignoring meteorological factors, provided conservative (high) values as compared to the expected average. The currents would be estimated to be 5 to 10 percent higher during 2-28 June 1990 than the average.

61. Alternative design 2 mesh was tested under various scenarios of wind direction to indicate sensitivity of the system to wind stress. The response of alternative design mesh 3 would have been very similar. As previously mentioned, the system's response to the predominant southeasterly wind was not as great as experienced in many Texas coastal systems, probably because the major East Matagorda Bay axis is aligned almost perpendicular to the southeast. The three-day period of greatest tropic tides was selected for these simulations.

62. For this first sensitivity testing, simulations were made with a

constant east wind of 20 knots (23 mph) and with a constant west wind of 20 knots. All other model coefficients and boundary conditions were kept identical to the verification and 27-day simulations, except the eddy viscosity coefficients in the area of the bypass channel-GIWW intersection were increased from 3 lb-sec/ft^2 to 4 lb-sec/ft^2 because of higher velocities. The comparison of the east (solid line) and west (dotted line) simulated currents for navigation bypass channel node 2811 and GIWW node 830 is provided in Plate 19 for hours 24-72. The plots show a difference between the two wind direction scenarios of 0.5 to 1.0 fps, with the greatest differences in the flood direction. The east winds produced the expected greater ebb velocities, and the west wind the greater flood velocities, in response to wind stress on East Matagorda Bay. There is also a 0.3-ft difference in water level at the intersection (node 794) between the two wind scenarios in Plate 20. Sustained winds of 20 knots in either east or west direction are extremely rare based upon wind roses provided for the Victoria NWS (Larkin and Bowmar 1983). However, the simulations demonstrate sensitivity of model response as wind direction approaches the primary axis of East Matagorda Bay.

63. The frontal passage from the north is a relatively frequent event occurring approximately 70 times per year with the highest frequency in the winter months (DiMego, Bosart and Enderson 1976). These frontal passages vary in intensity and celerity. Based on studies found in Ward and Chambers (1978) on meteorological forcing in upper Sabine Pass, TX, a reasonable frontal passage scenario was constructed in lieu of actual prototype measurements. The frontal passage scenario consisted of 20-knot south winds reversing to 20-knot north winds at the time of frontal passage. The passage was timed to coincide with the ebb tide, to maximize ebb velocities. The wind and barometric pressure gradient setdown on the gulf boundary of the model was assumed to result in an additional drop in water level of 1.5 ft within 2 hr of frontal passage. This designed frontal passage was estimated to represent a typical strong frontal passage event. Inherent in the design was isolation from other frontal passages, i.e., prior frontal passages occurred sufficiently in advance of this front so that water levels in the Gulf and bays had recovered. (This is often not the case when multiple fronts pass through one after the other.)

64. The simulated frontal passage is depicted in Plate 21 for the Gulf boundary water level (node 1461) and the water level at the intersection

(node 794), and in Plate 22 for velocity in the navigation bypass channel (node 2811) and velocity in the GIWW (node 830). The frontal passage was simulated to occur at model hour 37, and the duration of the simulation was not extended to sufficient length to include recoveries of water levels to prepassage levels. Typically, this recovery is more gradual than the frontal passage so that the recovery flood currents are not enhanced to the degree that ebb currents are enhanced by the frontal passage. The peak ebb velocities in both the bypass channel and GIWW for the frontal passage (Plate 22) are increased about 0.5 fps above those for the east and west wind scenarios (Plate 19) and the 27-day simulations (Plate 15).

65. Great difficulties exist in determining a frequency for the type of current conditions simulated for the frontal passage. In lieu of analysis of several years of water-level records for the area, only generalizations could be made. High amplitude, tropic tides occur approximately one half the time, with the ebb currents occurring during one half of that period. As previously mentioned, DiMego, Bosart, and Endersen (1976) determined that approximately 70 frontal passages occur per year. If it is assumed that one half of these fronts would be too weak or occur too abruptly after another front to produce pronounced setdown of Gulf waters, then roughly 10 to 15 events per year would involve a strong frontal passage coincident with strong astronomically induced ebb currents.

Simulated McCabe Cut Conditions

66. Tidal conditions at McCabe Cut were simulated for the same 27-day water levels used in evaluating the navigation bypass channel. For the McCabe Cut simulations, the water levels, which were recorded in the mouth of the Colorado River near the Gulf, were used as the boundary conditions at the Colorado River, McCabe Cut, and San Bernard River. Relative phasing of the tides along this portion of the Texas coast was not available; however, differences between the three tidal inlets are expected to be minor. In addition, the Gulf-Colorado River tide had little effect at McCabe Cut because of distance and positioning of East Matagorda Bay between the two passes.

67. Because no hydrodynamic data of even the most rudimentary nature existed for McCabe Cut, the model of this area was applied unverified. However, the verification process for the Mouth of the Colorado River project

area and similarities between channels in the two locations would indicate that the simulations of McCabe Cut would provide reasonable and meaningful results that could be compared with those in the project area. Because of the added roughness due to an expected high percentage of sands in McCabe Cut, as compared with silts and clays in the project area, the Manning's n in McCabe Cut ranged from 0.020 to 0.025 as compared with 0.018 to 0.022 in the navigation bypass channel. Similar complexities of flow patterns, as experienced in the verification of the Colorado River–GIWW intersection and the high velocities due to proximity to the Gulf, resulted in turbulence exchange as represented through eddy viscosity coefficients ranging from 12 to 25 lb-sec/ft^2 at McCabe Cut and the intersection at the GIWW.

68. A time sequence of vector plots at 3-hr increments is depicted for a high amplitude, tropic tide (model hours 507-528) in Figures 29-36. The vector plots show expected behavior, and the unusual vector pattern at hour 507 (Figure 29) appeared to be the result of initiation of westerly flow in the western section of the GIWW and the momentum of the high currents (5 fps) in McCabe Cut. The plots also indicate a predominance of flow exchange with East Matagorda Bay and lesser exchange to the east with the Cedar Lakes area. This pattern of exchange seemed reasonable, since the Gulf opening at the San Bernard River would also provide for exchange with the Cedar Lakes, and East Matagorda Bay has a much larger surface area (potential tidal prism) than Cedar Lakes.

69. The flow exchange pattern depicted in the vector plots is confirmed by the time-history velocity plots at specific locations. The plot for a center location of McCabe Cut (node 5171), the center of the GIWW west of McCabe Cut (node 4037), and the center of the GIWW east of McCabe Cut (node 4185) are provided in Plates 23 and 24. Water levels at the intersection (node 4363) are depicted in Plate 24. (McCabe Cut node locations are presented in Figure 22.) Strong ebb and flood velocities in excess of 5 fps during the tropic tides are predicted in McCabe Cut (node 5171). Peak velocities in the GIWW to the west of McCabe Cut (node 4037) were simulated as 2 fps or less. In the GIWW to the east (node 4185), peak flood velocities of approximately 1.5 fps were predicted while ebb velocities rarely exceeded 1.0 fps. The predicted east directed dominance of flow in the GIWW cannot be verified by this limited study.

70. A relevant comparison to be made with the McCabe Cut simulations was

to determine navigability of the GIWW at the Cut to that of the GIWW at the navigation bypass channel. This was accomplished by using the centerline crosscurrent of the GIWW as an indicator of navigability. (The tow simulation studies for the Mouth of the Colorado Project indicated crosscurrent as the major factor influencing navigability). Comparative plots of crosscurrents in the GIWW for the bypass channel design 2 and McCabe Cut are provided for maximum flood and ebb currents in Figure 37. On the flood current, the crosscurrents from McCabe Cut were approximately double in magnitude to those from bypass channel design 2. These crosscurrents from McCabe Cut probably attributed to the navigation problems encountered in this area prior to closing the cut. The peak crosscurrents on ebb tide are approximately 20 percent greater from McCabe Cut than the bypass channel. Apparently the greatest navigation difficulties were often encountered during the enhanced ebb flows from freshwater flooding in Caney Creek (USAE District, Galveston, 1987), an event not included in this study. Based on this limited assessment, navigation in the GIWW at McCabe Cut would have been more difficult than in the GIWW at the navigation bypass channel for peak currents simulated for the 2-28 June 1990 period.

PART VI: SUMMARY AND CONCLUSIONS

71. Using the two-dimensional vertically integrated RMA-2V model, steady-state currents were developed for three alternative designs of the intersection of the navigation bypass channel at the GIWW. Steady currents were also developed for both the preproject and postproject intersection of the Colorado River and GIWW. These hydrodynamic conditions were used in a tow-simulator study conducted at WES.

72. RMA-2V was successfully verified to synoptic prototype measurements obtained by WES in the vicinity of the Colorado River-GIWW intersection. The measurements included hourly vertical velocity profiles at three stations each across seven channel cross sections and water levels at four recorder locations. Water-level measurements were taken for approximately six weeks and velocity measurements for 25 hr (one tidal cycle) during a period of high amplitude (tropic) tides (25-26 May 1990). The comparison of model results with prototype velocities indicated good agreement with average cross-section flow; however, the complex lateral variations in the prototype due to eddy formation could not be resolved. Water-level comparisons were very good. Because the primary objective of the verification process (to reproduce the average channel flows) was realized, the inability of the model to reproduce the complexities of flows at the confluence of five channels was not considered a major deficiency.

73. The verified model was modified to reflect the conditions of the Mouth of the Colorado River Project, including project dams and the navigation bypass channel. Two navigation bypass channel designs that were tested under steady-state conditions in the tow-simulation study were evaluated dynamically. Each evaluation consisted of 27 days of simulated tidal fluctuations (water levels and currents). The 27-day period simulated was 2-28 June 1990 when water-level recorders were in operation. (A 27-day period represents a tropic month, which is the average declination cycle of the moon.) Tidal velocity duration plots were developed and current patterns at certain times of the simulation were supplied for the WES tow-simulator study. Sensitivity testing to 20-knot east and west winds and to a typical frontal passage was also conducted.

74. A now-closed Gulf opening, McCabe Cut, was also simulated for the same 27 days. Maximum crosscurrent patterns in the GIWW at McCabe Cut were

compared with those in the GIWW at the navigation bypass channel. The cross-current patterns in the GIWW from McCabe Cut were greater than from the navigation bypass channel, especially for flood currents. This indicates greater navigation difficulties in the GIWW at McCabe Cut than at the bypass channel for the conditions simulated.

REFERENCES

DiMego, G. J., Bosart, L. F., and Enderson, G. W. 1976 (June). "An Examination of the Frequency and Mean Conditions Surrounding Frontal Incursions into the Gulf of Mexico and Caribbean Sea," Monthly Weather Review, Vol 104, pp 709–718.

Fagerburg, T. L., Coleman, C. J., Parman, J. M., and Fisackerly, G. M. 1992 (Mar). "Field Data Collection Report, Mouth of Colorado River, Texas," US Army Engineer Waterways Experiment Station, Vicksburg, MS.

Hahl, D. C., and Ratzlaff, K. W. 1971. "Provisional Data Lavaca-Tres Palacios Estuary March 4–5, 1971. US Geological Survey Houston, TX. (unpublished data).

Larkin, T. J., and Bomar, G. W. 1983 (December). "Climatic Atlas of Texas," LP-192, Texas Department of Water Resources, Austin, Texas.

Mason, C. 1981. "Hydraulics and Stability of Five Texas Inlets," Miscellaneous Report No. 81-1. US Army Engineer Coastal Engineering Research Center.

Shureman, P. 1958. "Manual of Harmonic Analysis and Prediction of Tides," Special Publication No. 98. US Department of Commerce, Washington, D.C.

Smith, R. E. 1977. Unpublished data. US Geological Survey, Houston, TX.

Texas A&M University. 1988 (Spring). "The Unkindest Cut," Texas Shores Magazine, College Station, TX.

Thevenot, M. M., and Daggett, L. L. In preparation. "Mouth of Colorado River Navigation Study, Matagorda, Texas," US Army Engineer Waterways Experiment Station, Vicksburg, MS.

USAE District, Galveston. 1981 (March). "Mouth of Colorado River, Texas, Phase I General Design Memorandum and EIS," Galveston, Texas.

USAE District, Galveston. 1987 (August). "Section 205, Initial Reconnaissance Report on Flood Control Improvements, East Matagorda Bay," Galveston, Texas.

Ward, G. H., and Chambers, C. L. 1978 (April). "Meteorologically Forced Currents in Upper Sabine Pass, Texas," Document No. 7869, Espey, Huston & Associates, Inc., Austin, Texas.

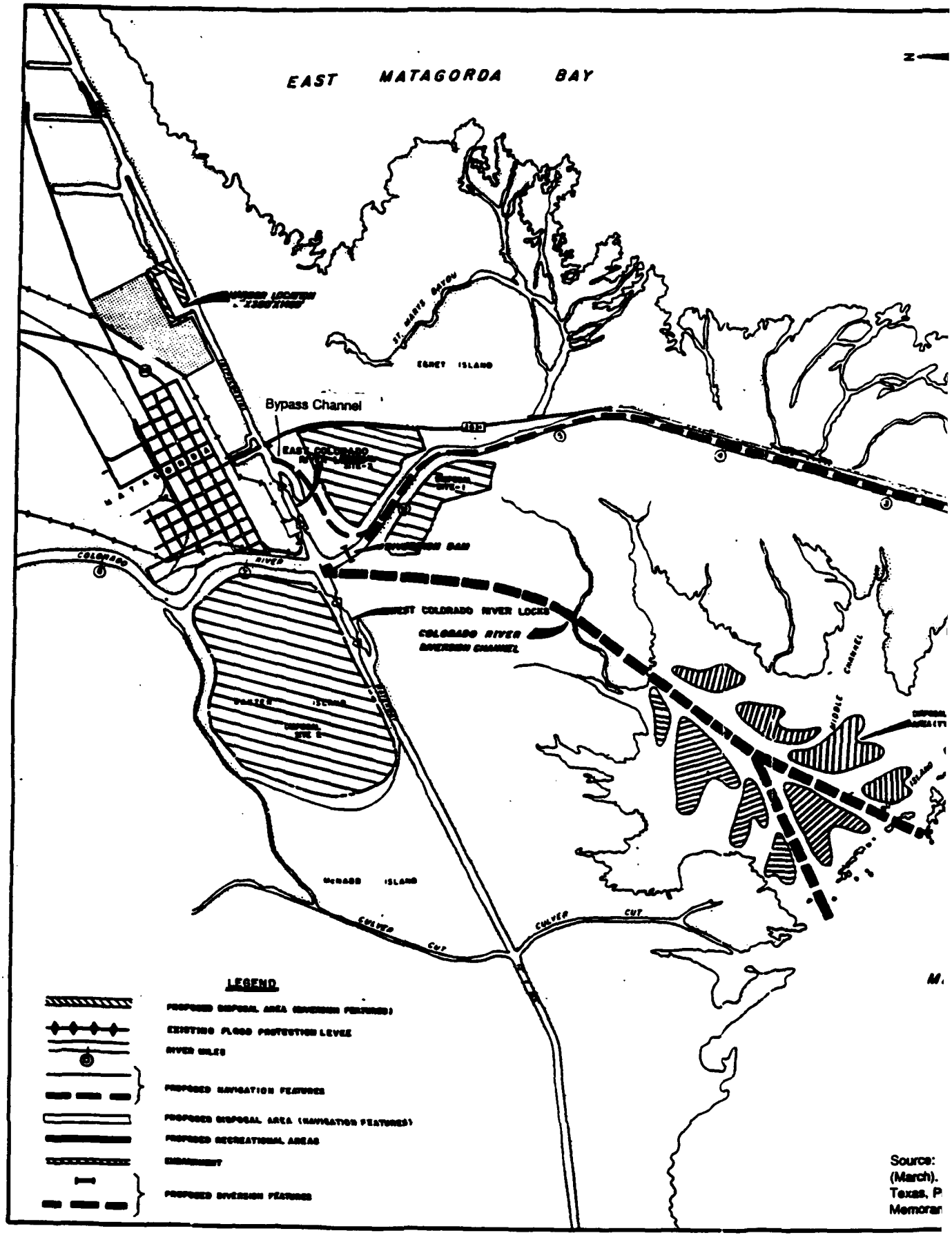

Source:
(March).
Texas, P
Memoran

Figure 1. Propos

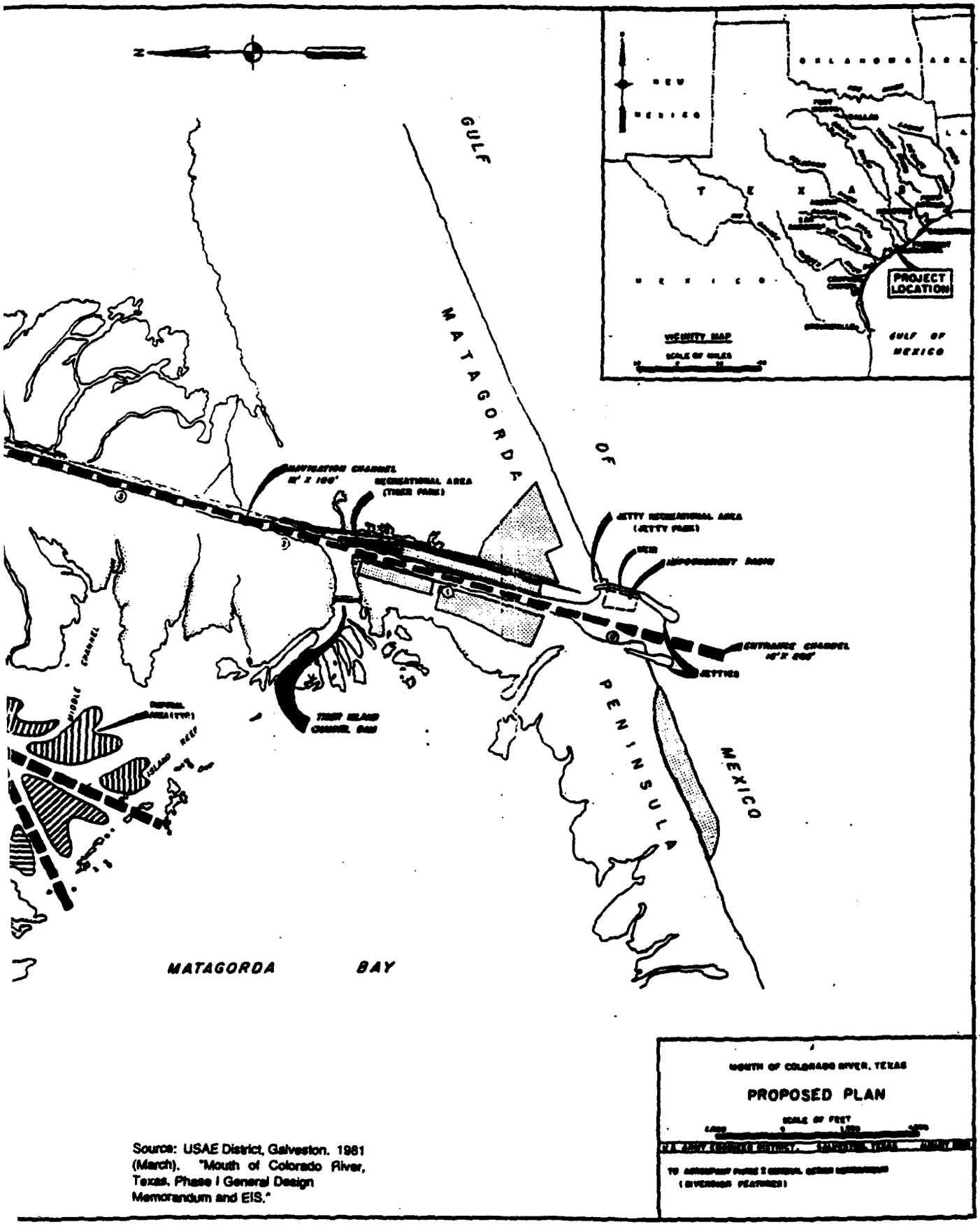

Source: USAE District, Galveston. 1981 (March). "Mouth of Colorado River, Texas. Phase I General Design Memorandum and EIS."

gure 1. Proposed plan

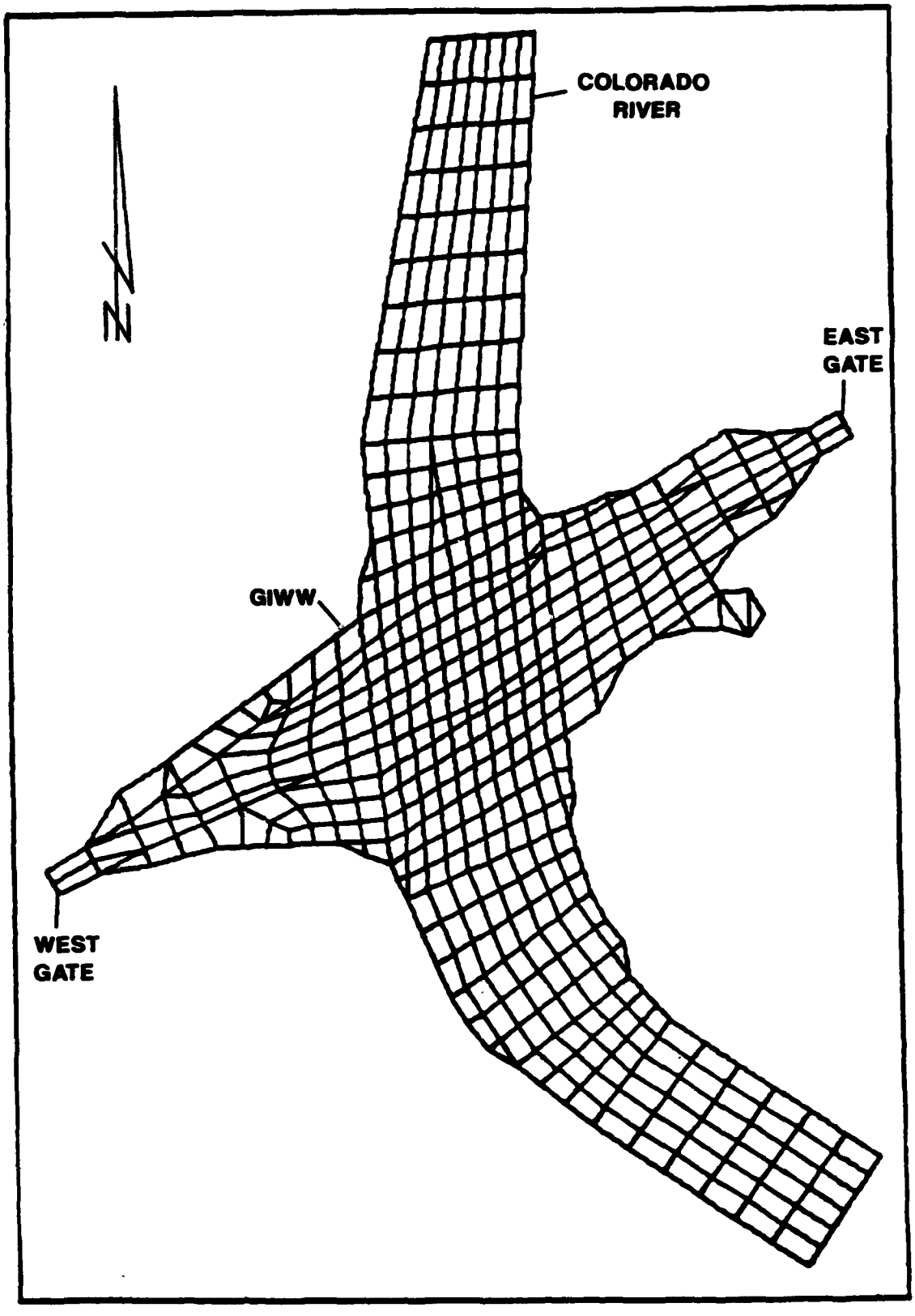

Figure 2. Computational mesh of preproject Colorado River–GIWW intersection for steady state-simulations

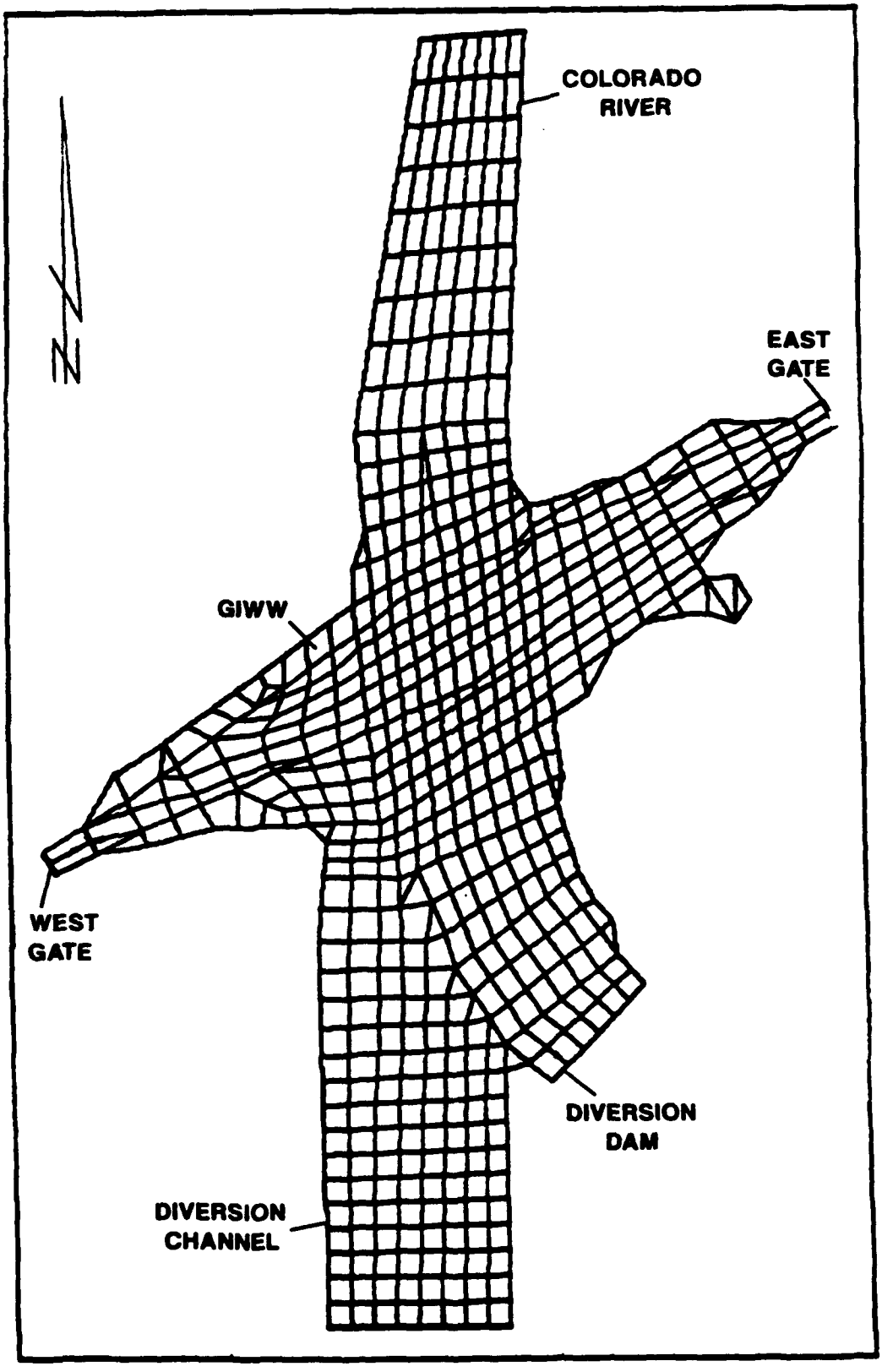

Figure 3. Computational mesh of postproject Colorado River-GIWW intersection for steady-state simulations

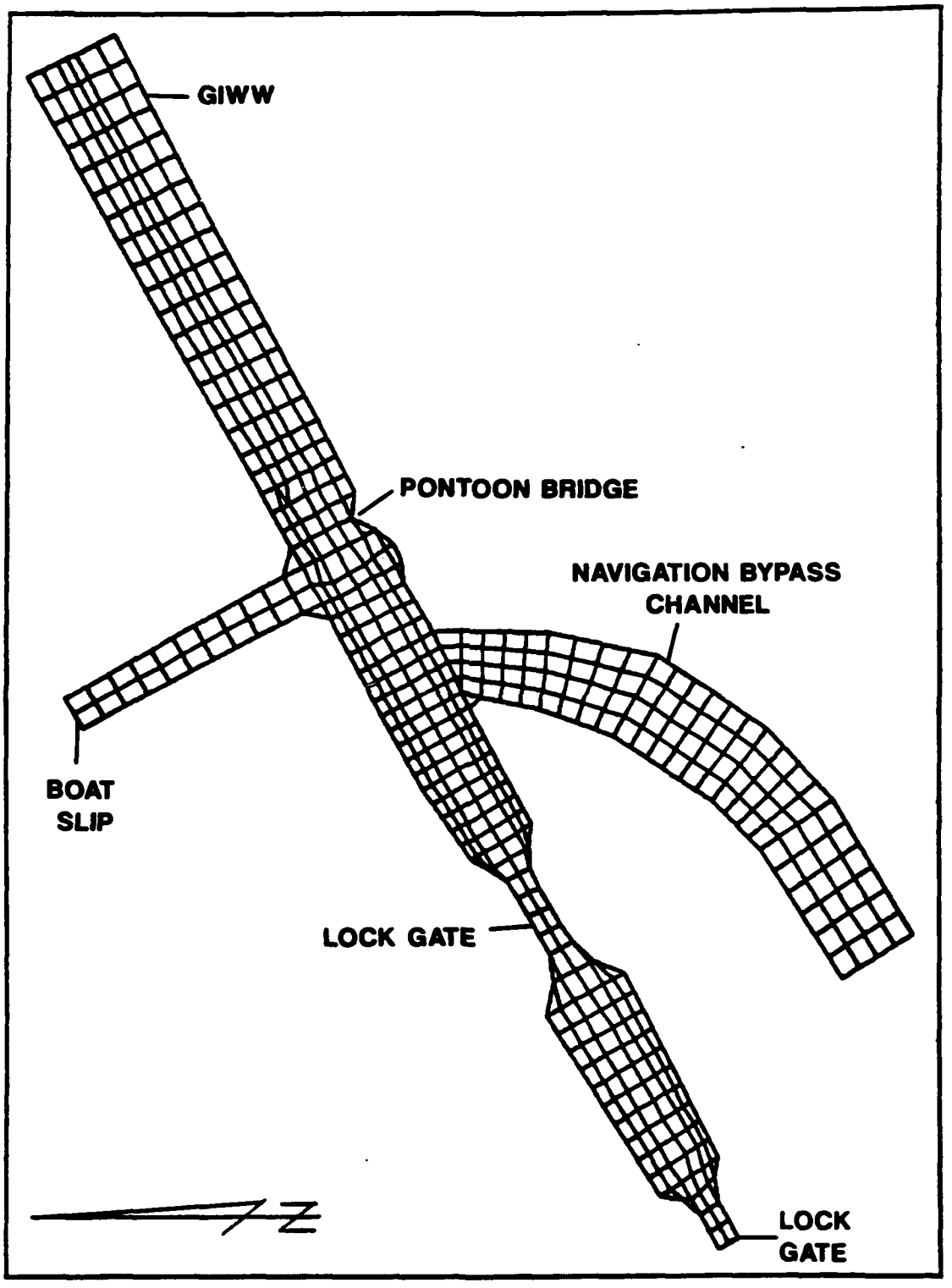

Figure 4. Computational mesh of navigation bypass channel-GIWW intersection (design 1) for steady-state simulations

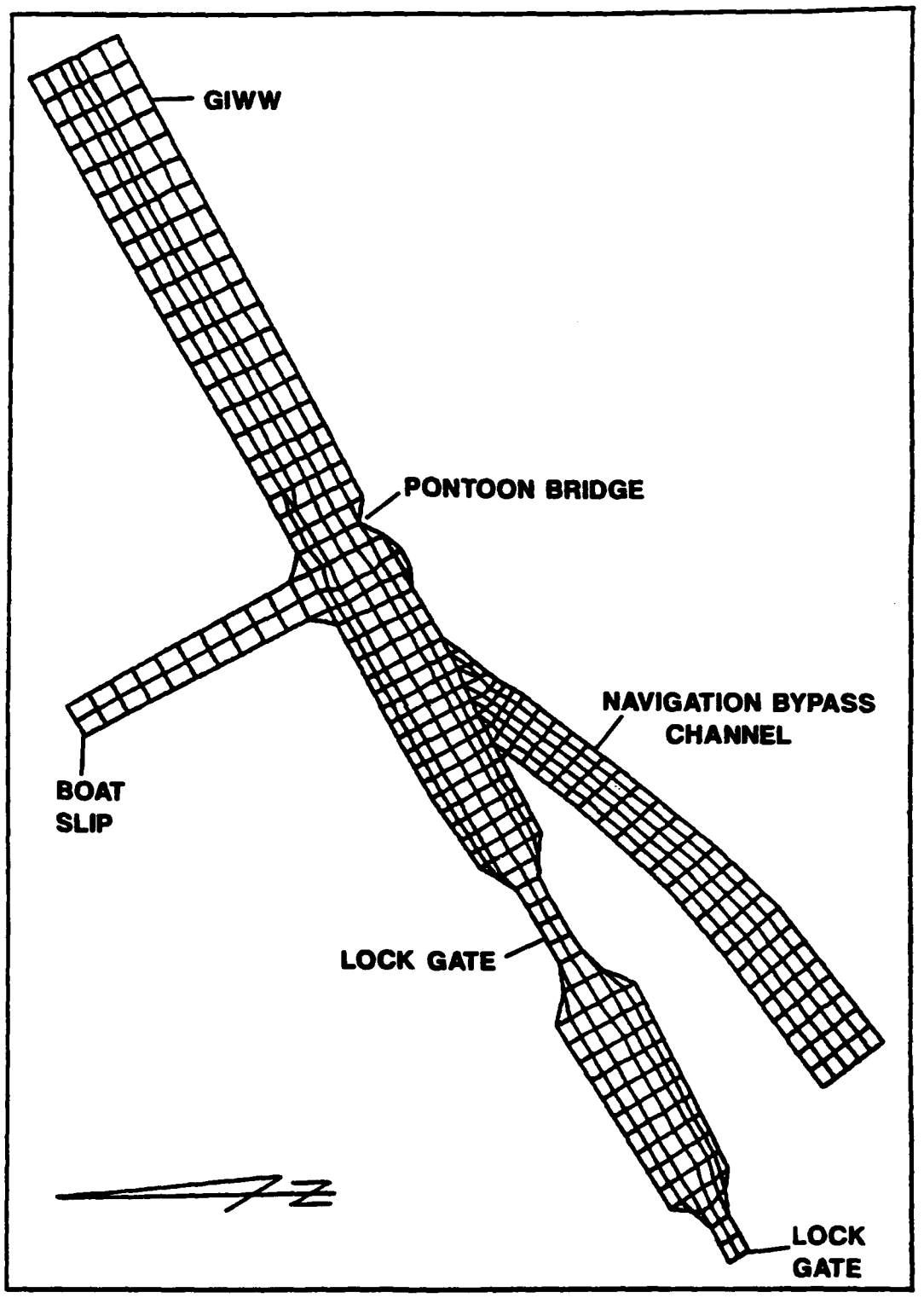

Figure 5. Computational mesh of navigation bypass channel-GIWW intersection (design 2) for steady-state simulations

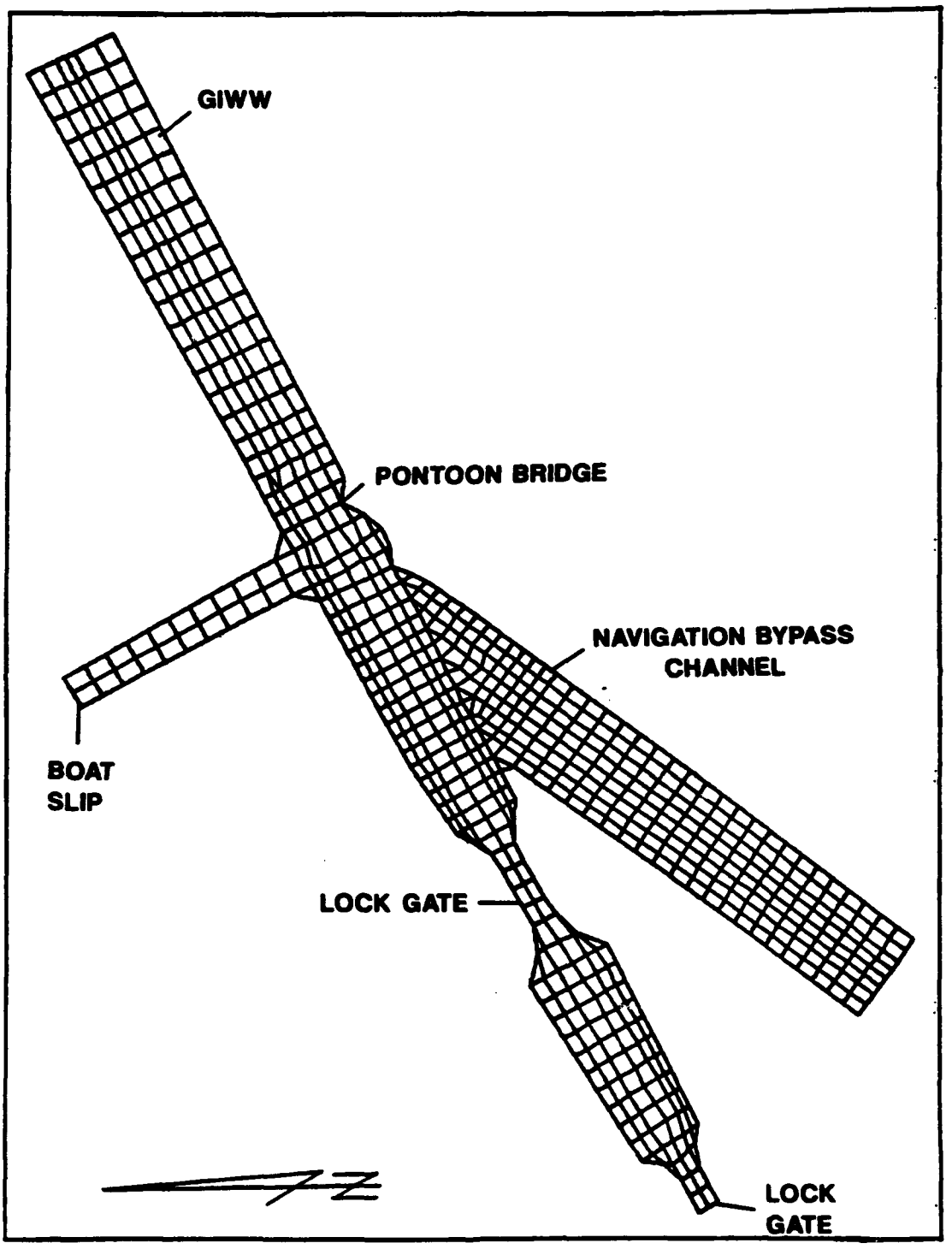

Figure 6. Computational mesh of navigation bypass channel–GIWW intersection (design 3) for steady-state simulations

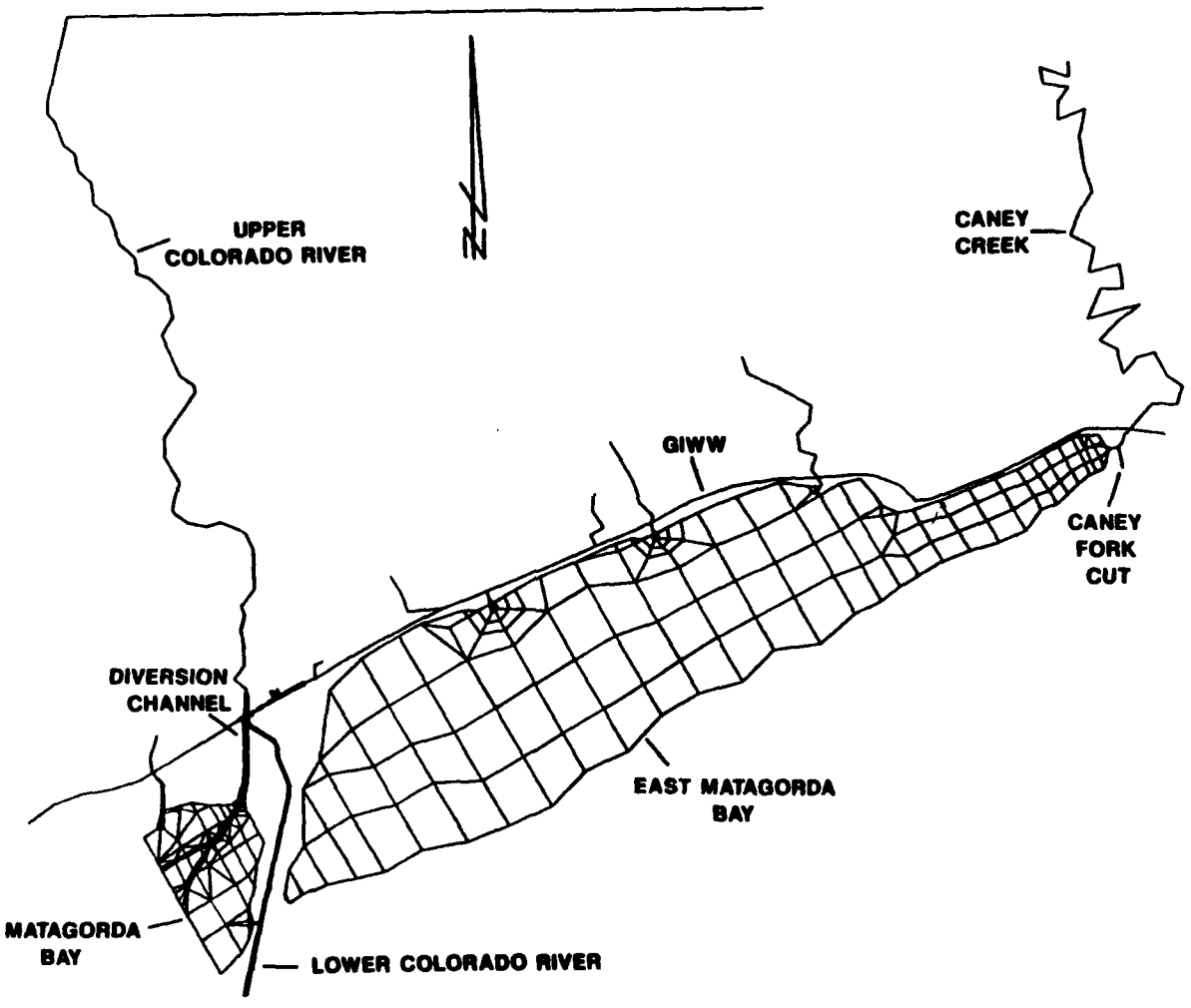

Figure 7. Computational mesh for Mouth of Colorado Project dynamic verification

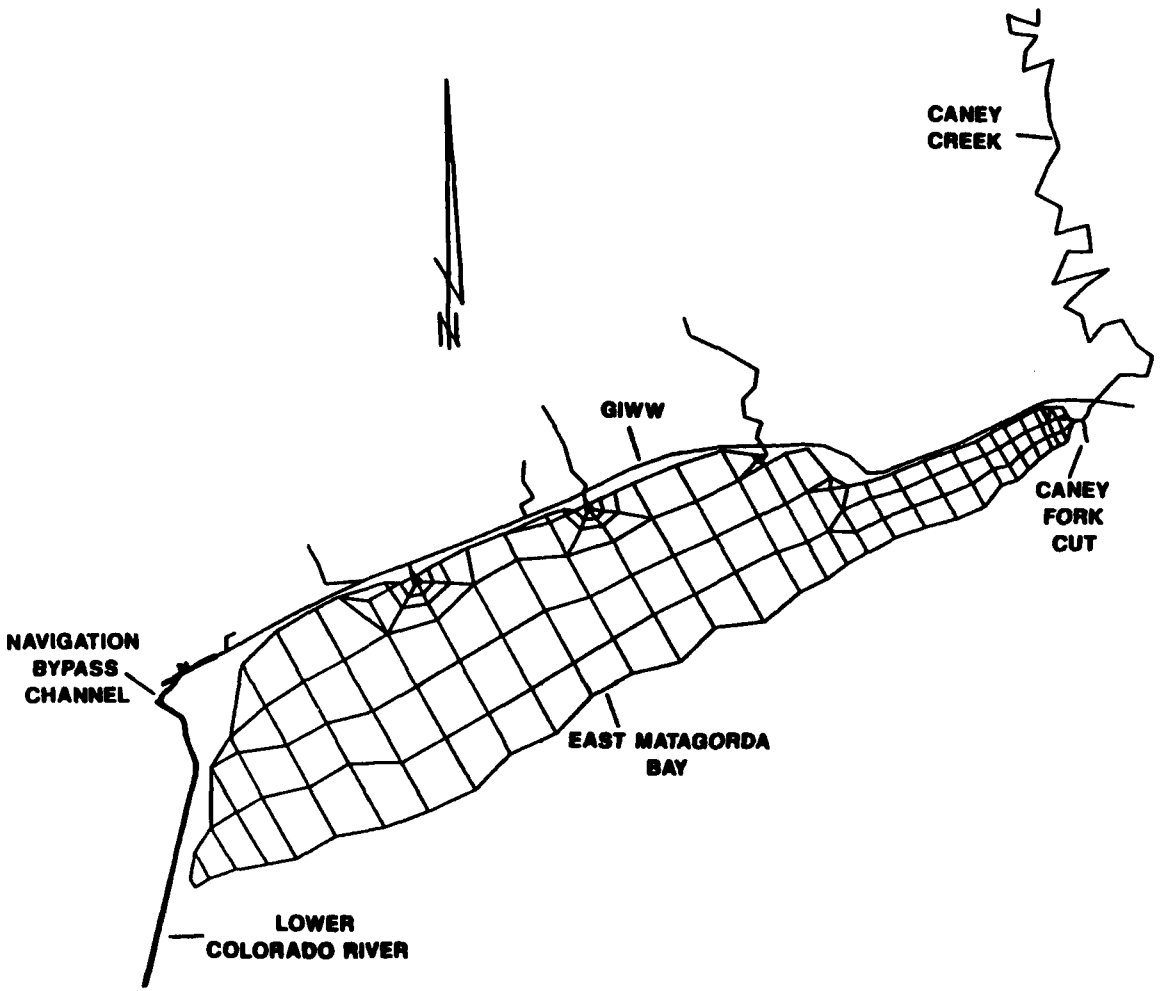

Figure 8. Computational mesh of navigation bypass channel for dynamic simulations

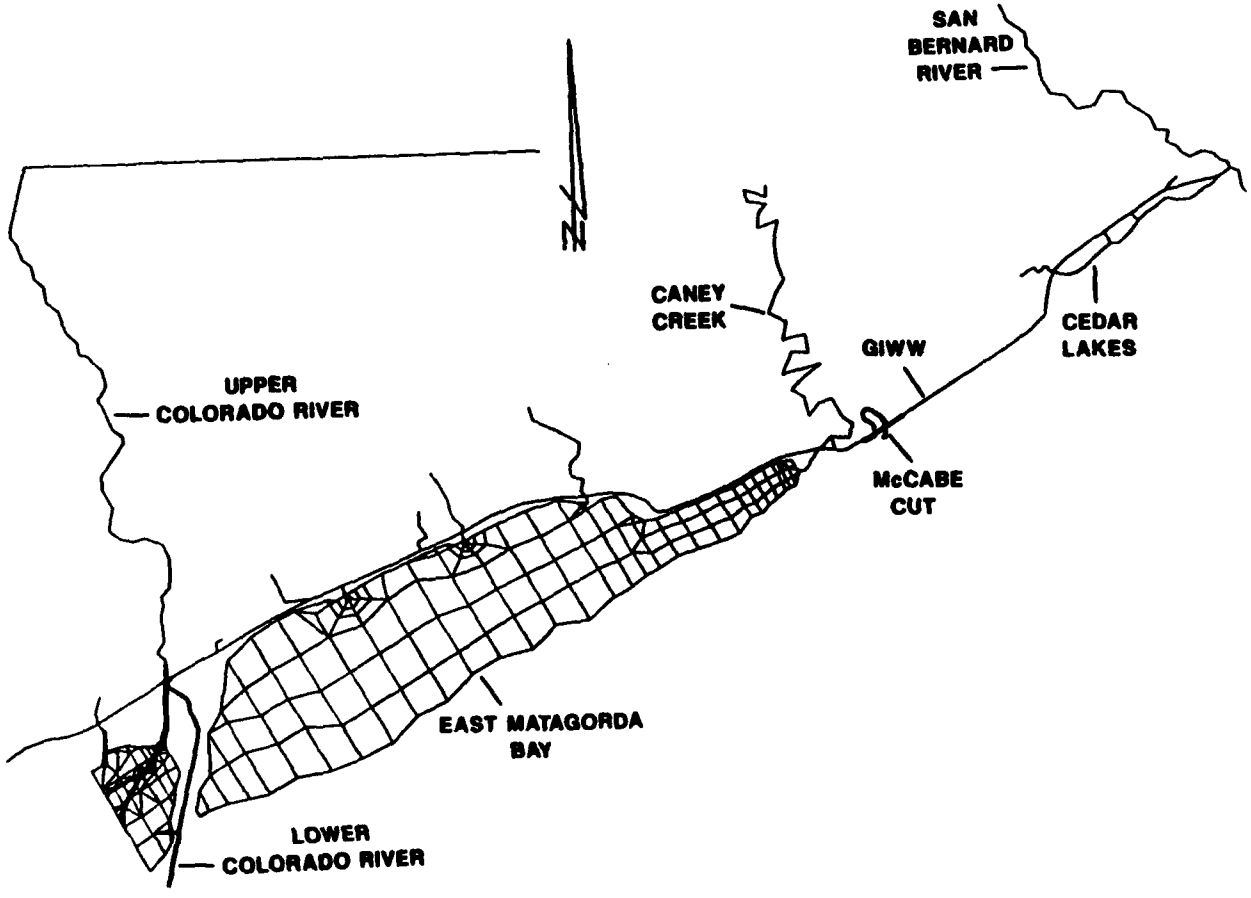

Figure 9. Computational mesh for McCabe Cut dynamic simulations

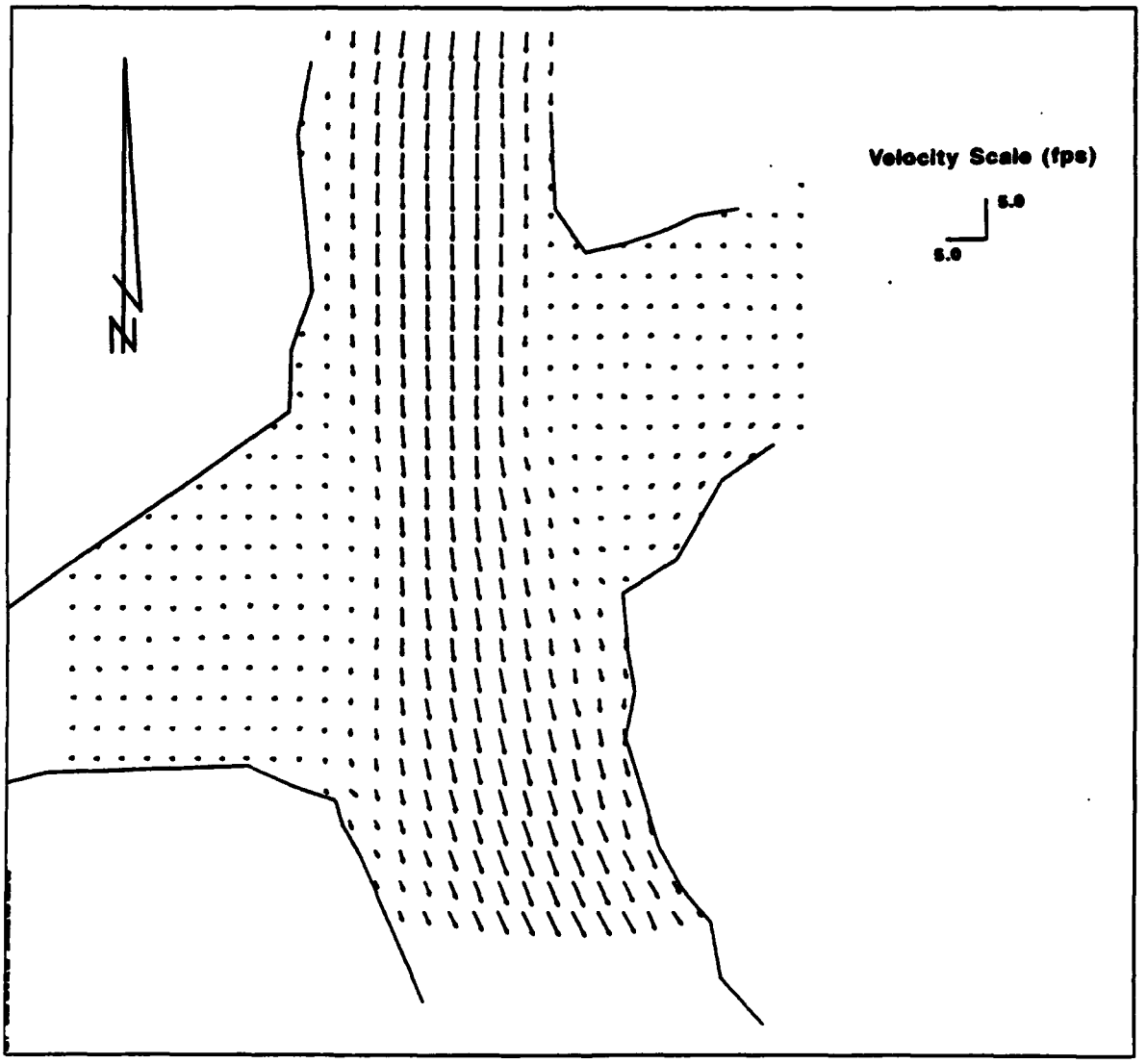

Figure 10. Current pattern at 12,000 cfs for preproject Colorado River–GIWW intersection

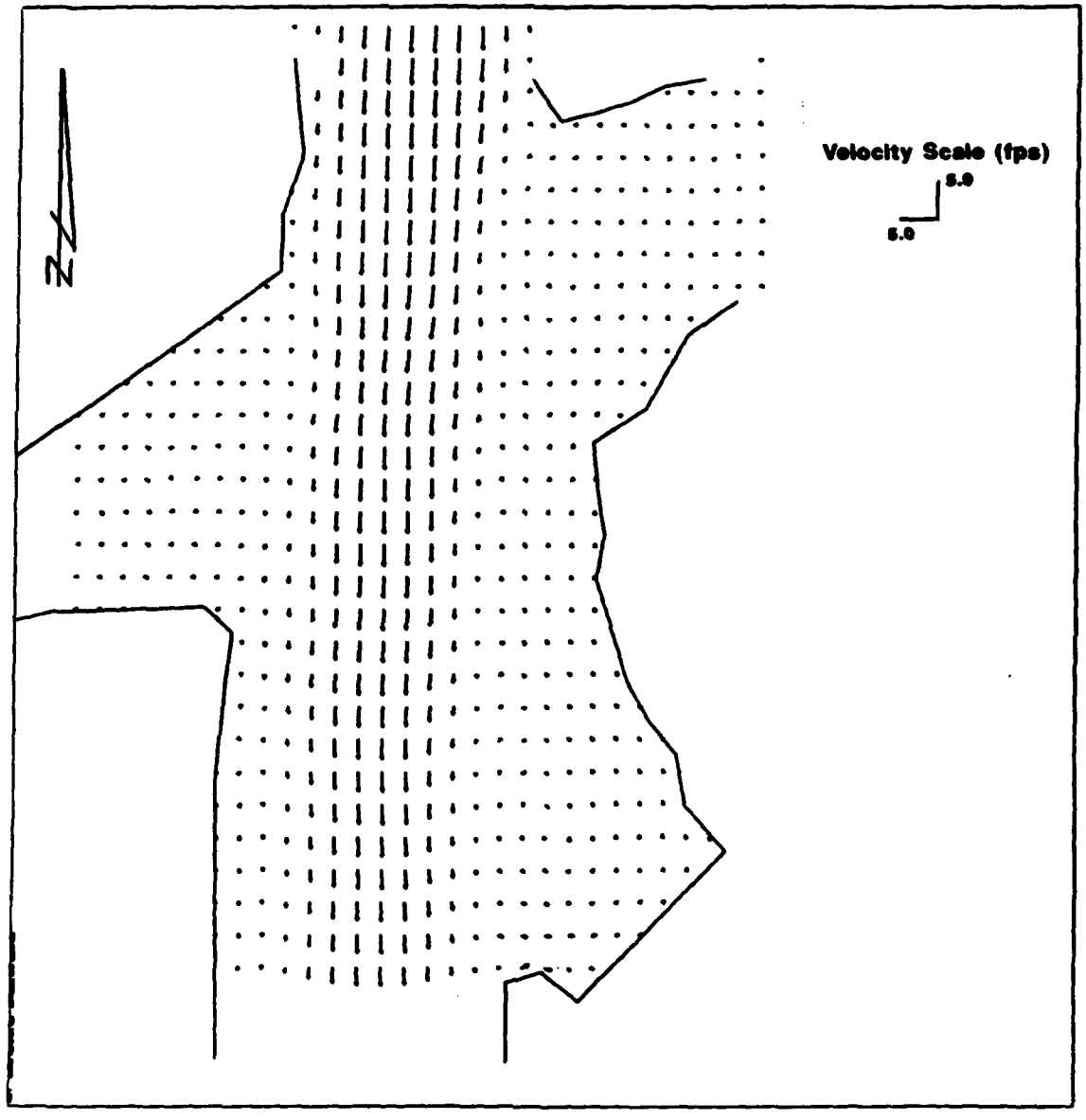

Figure 11. Current pattern at 12,000 cfs for postproject Colorado River-GIWW intersection

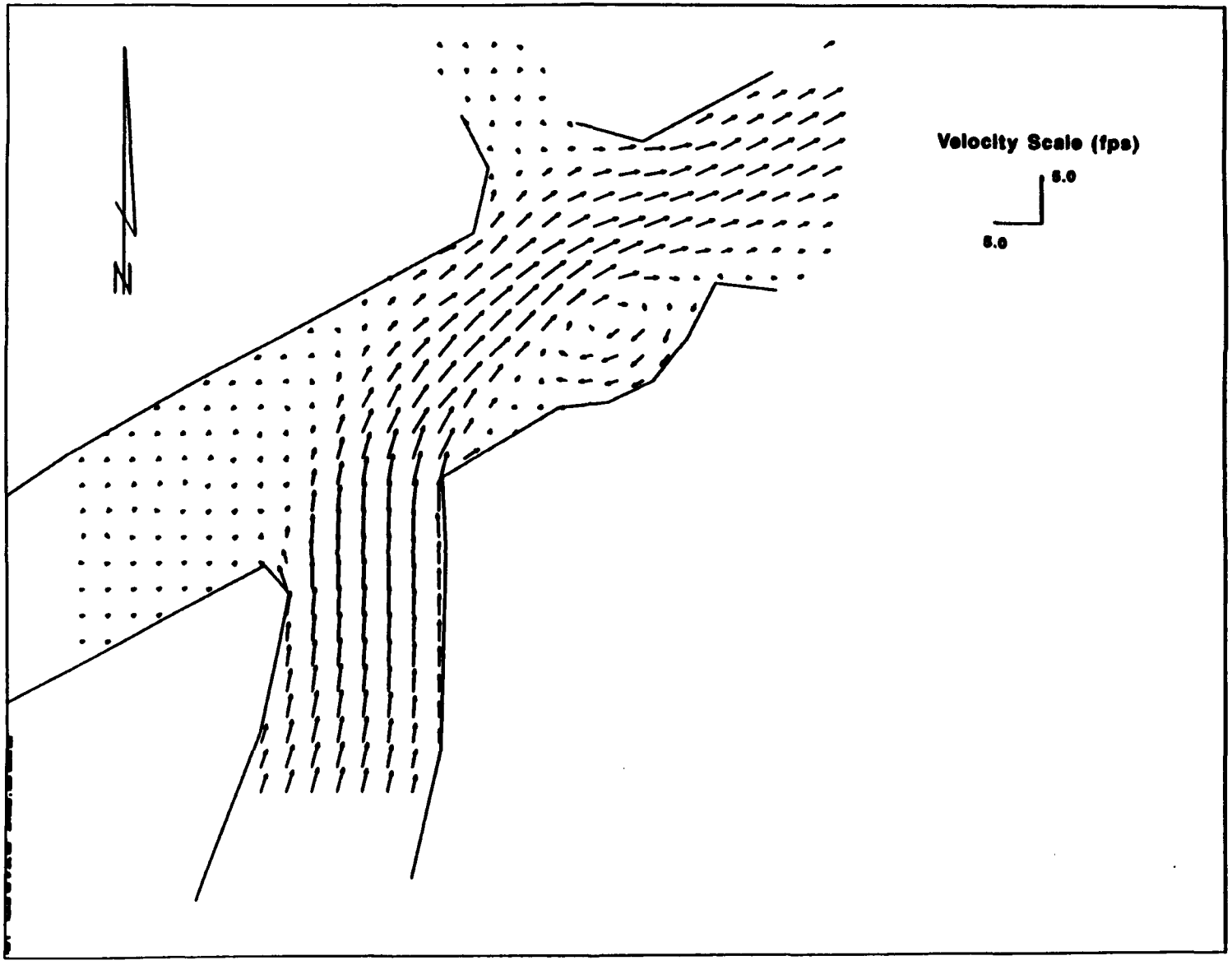

Figure 12. Flood current pattern at 6,150 cfs for navigation bypass channel-GIWW intersection (design 1)

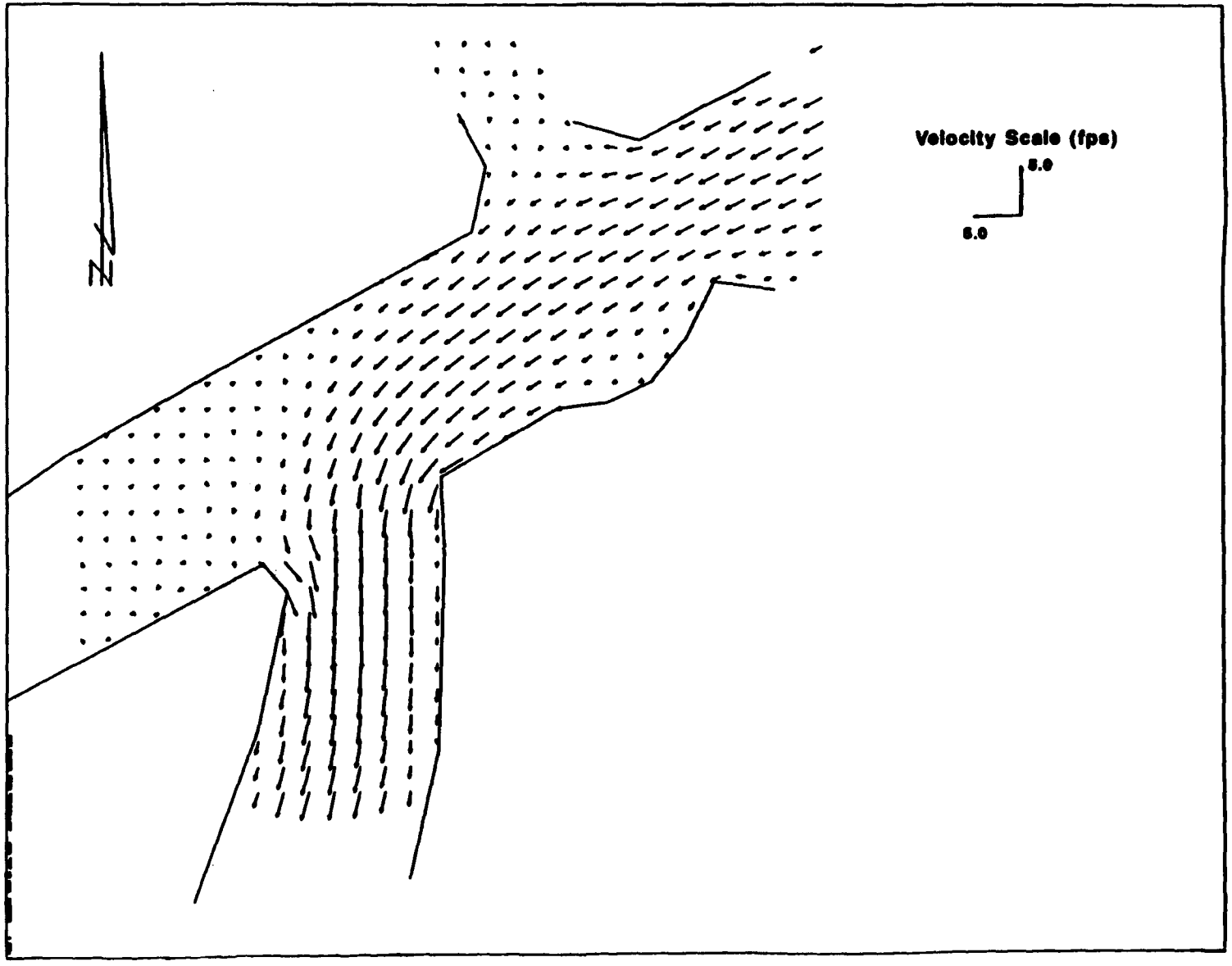

Figure 13. Ebb current pattern at 6,150 cfs for navigation bypass channel-GIWW intersection (design 1)

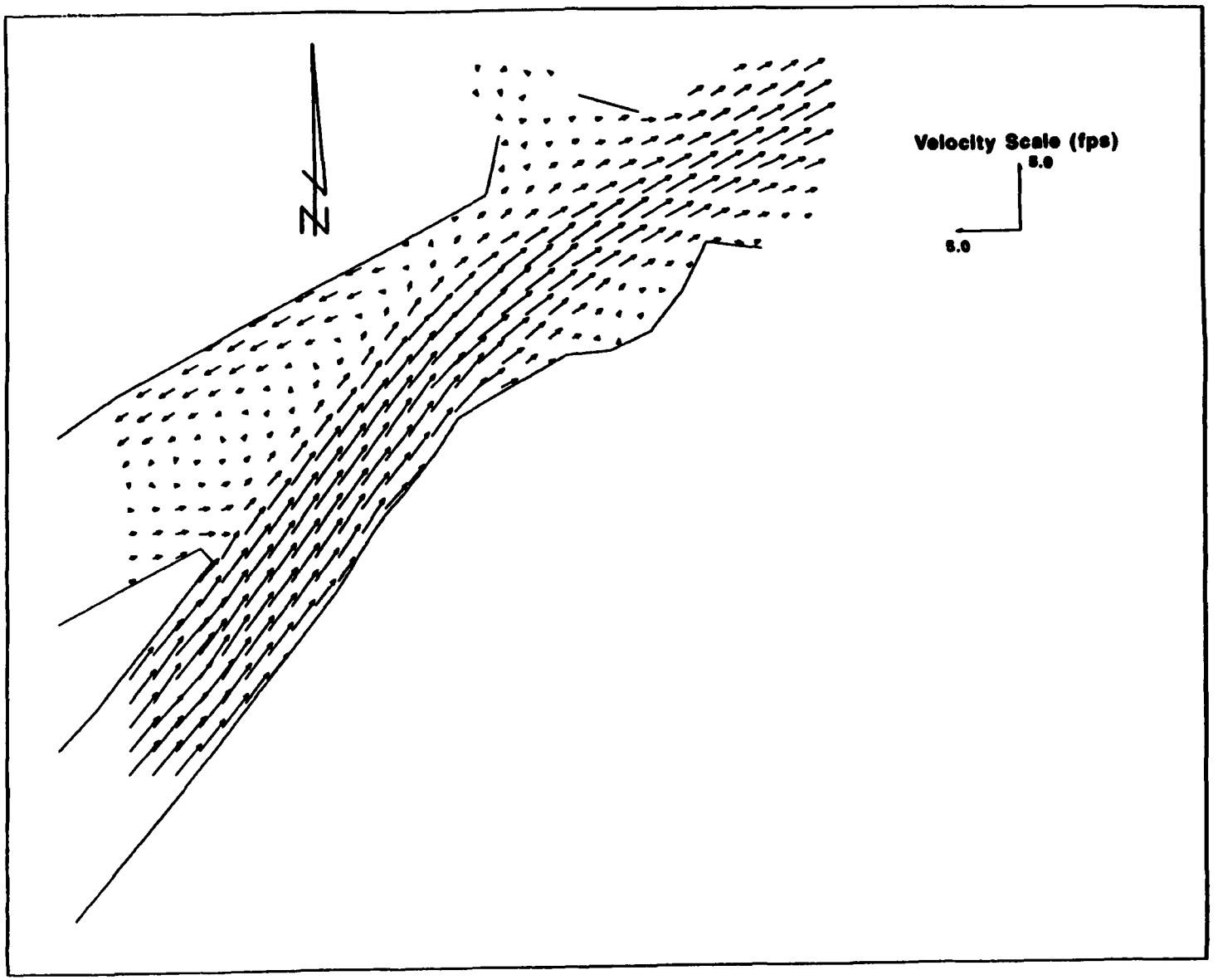

Figure 14. Flood current pattern at 6,150 cfs for navigation bypass channel-GIWW intersection (design 2)

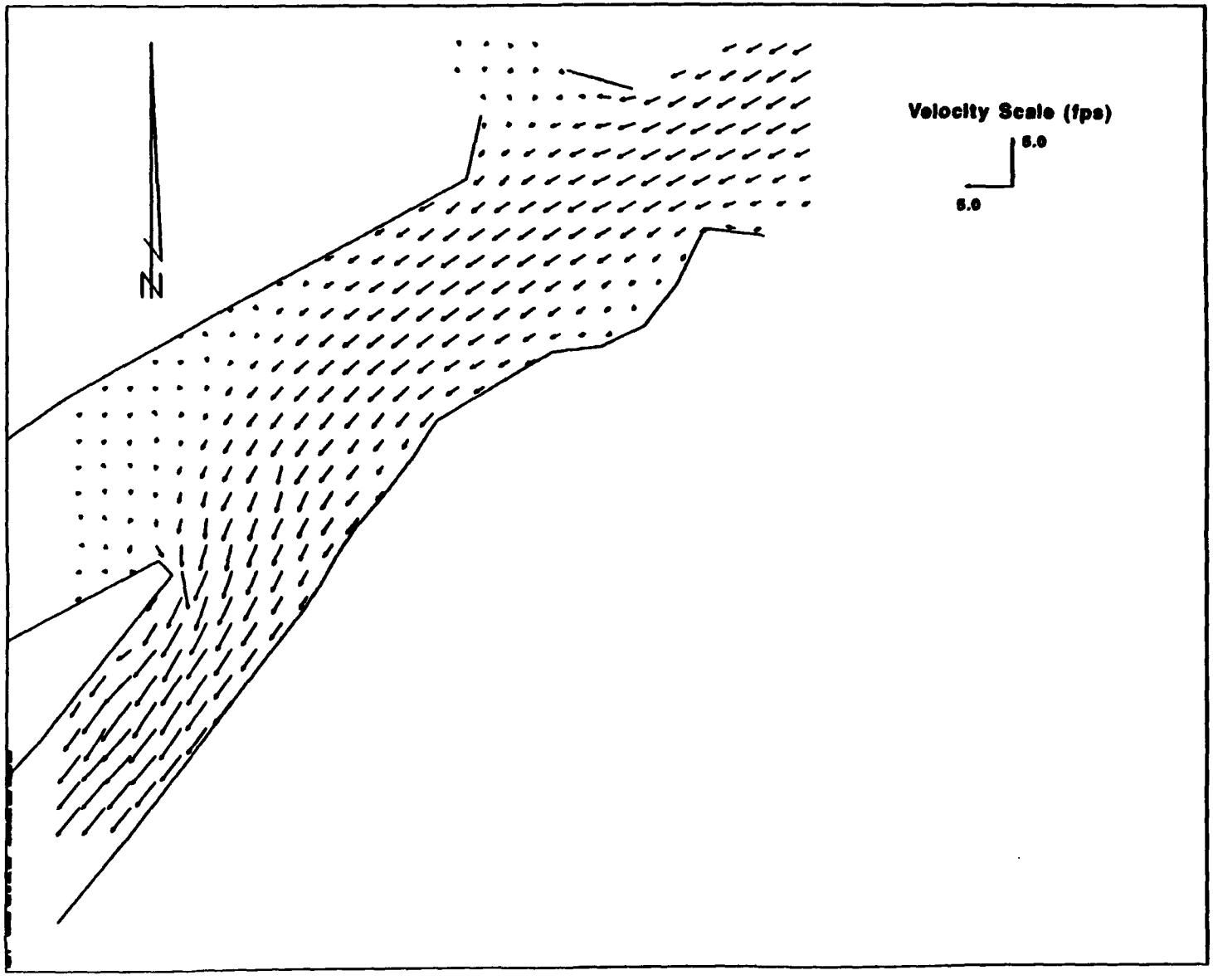

Figure 15. Ebb current pattern at 6,150 cfs for bypass channel-GIWW intersection (design 2)

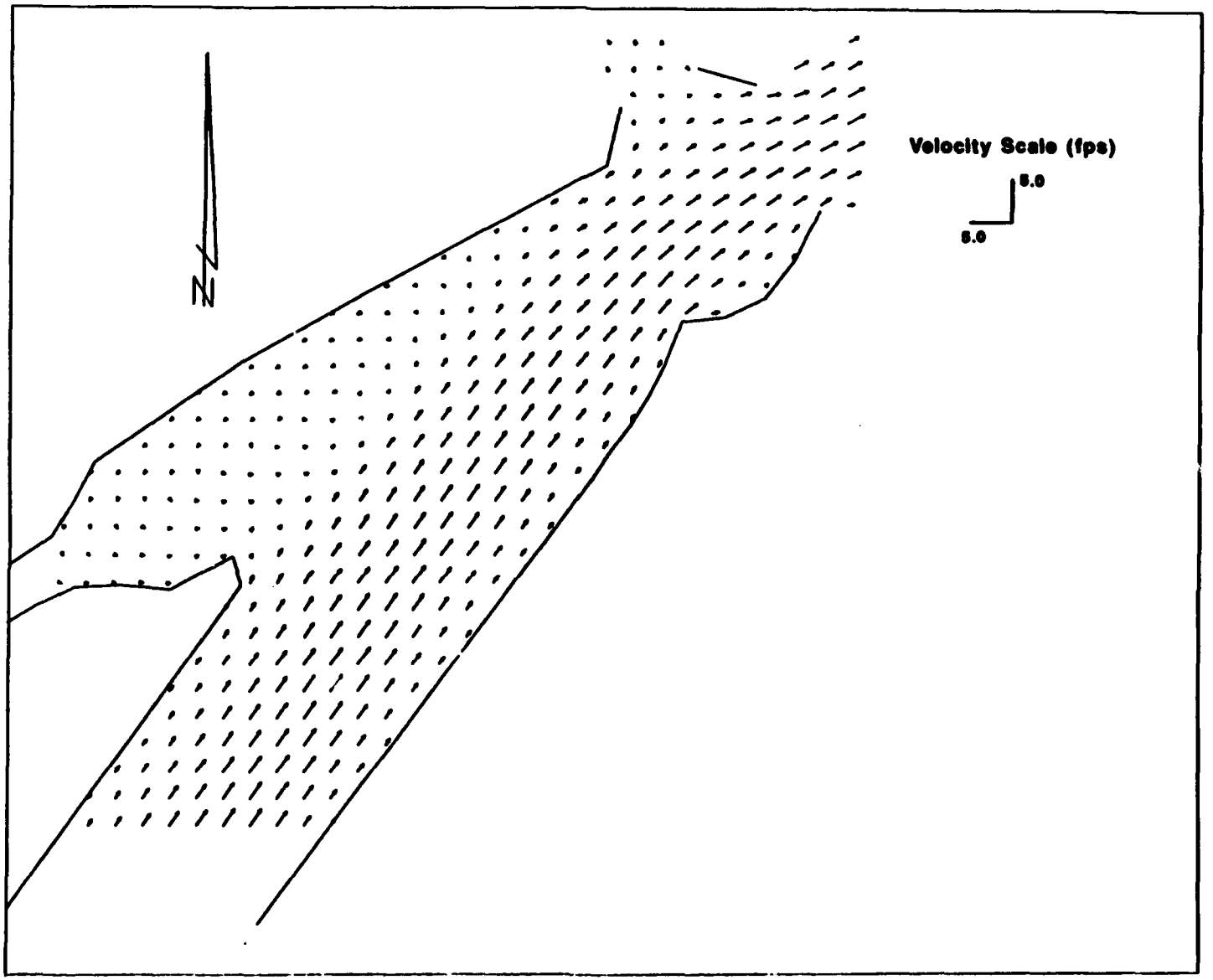

Figure 16. Flood current pattern at 6,150 cfs for bypass channel-GIWW intersection (design 3)

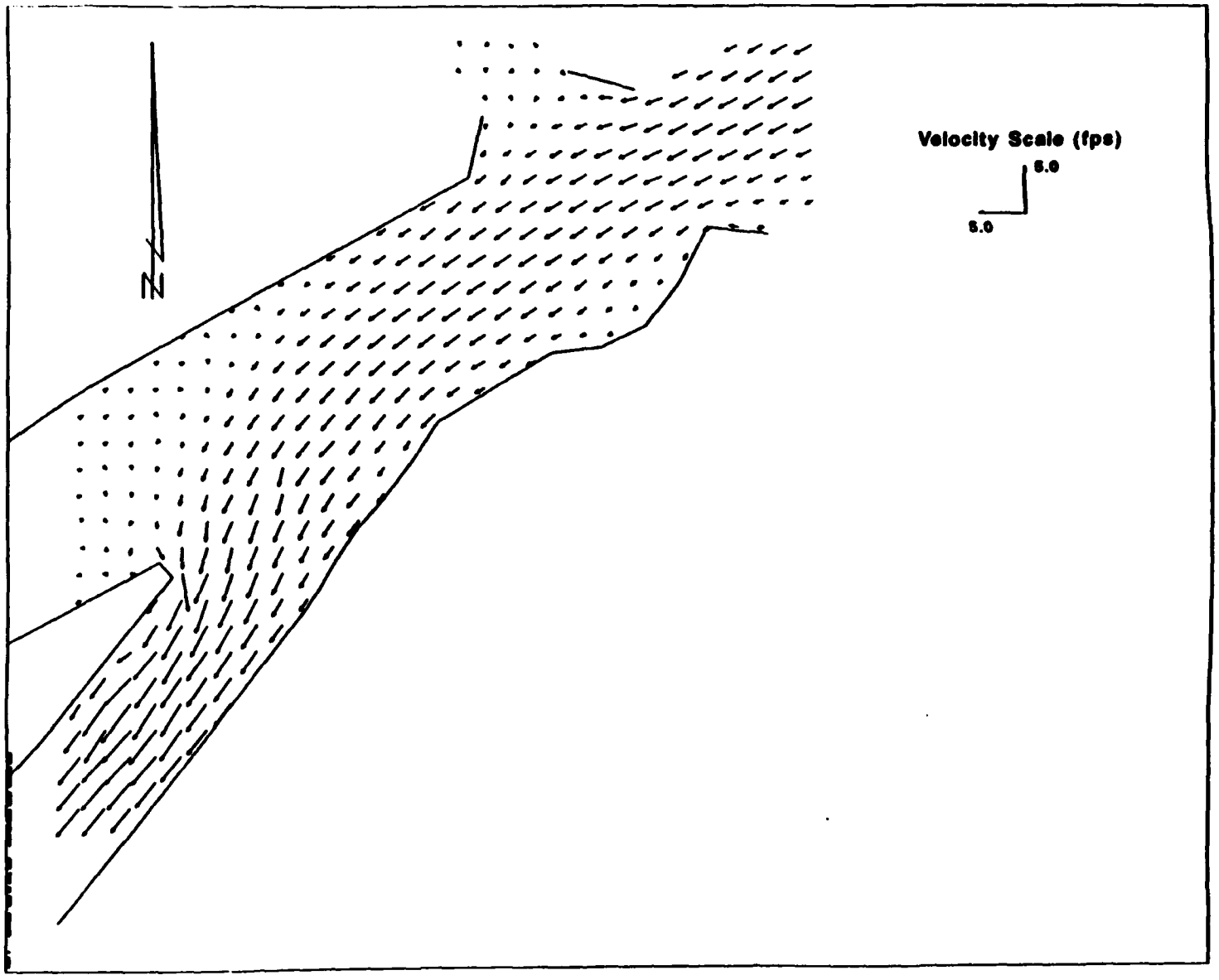

Figure 17. Ebb current pattern at 6,150 cfs for bypass channel-GIWW intersection (design 3)

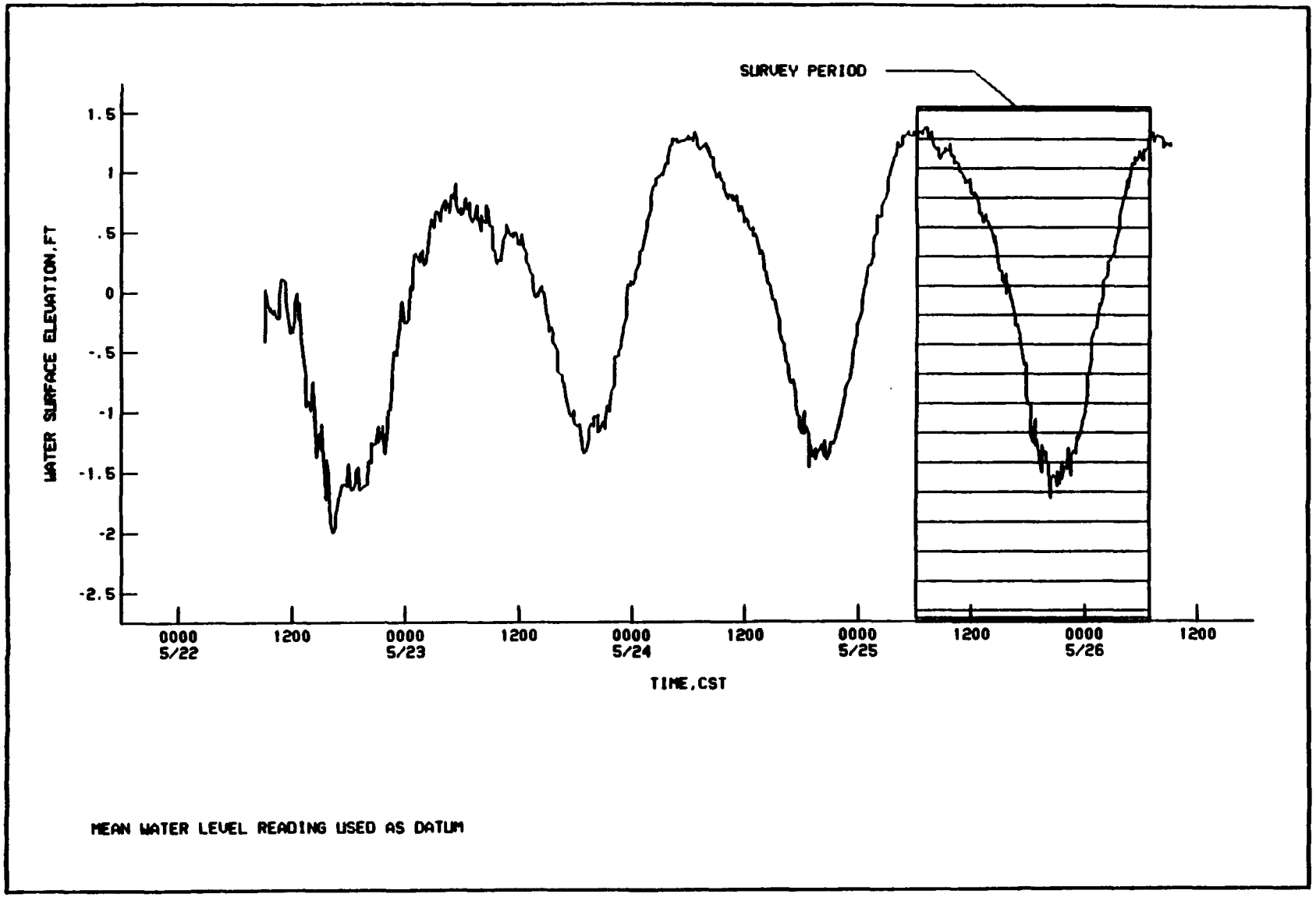

Figure 18. Prototype water levels in the Colorado River at the Gulf of Mexico 22-26 May 1990

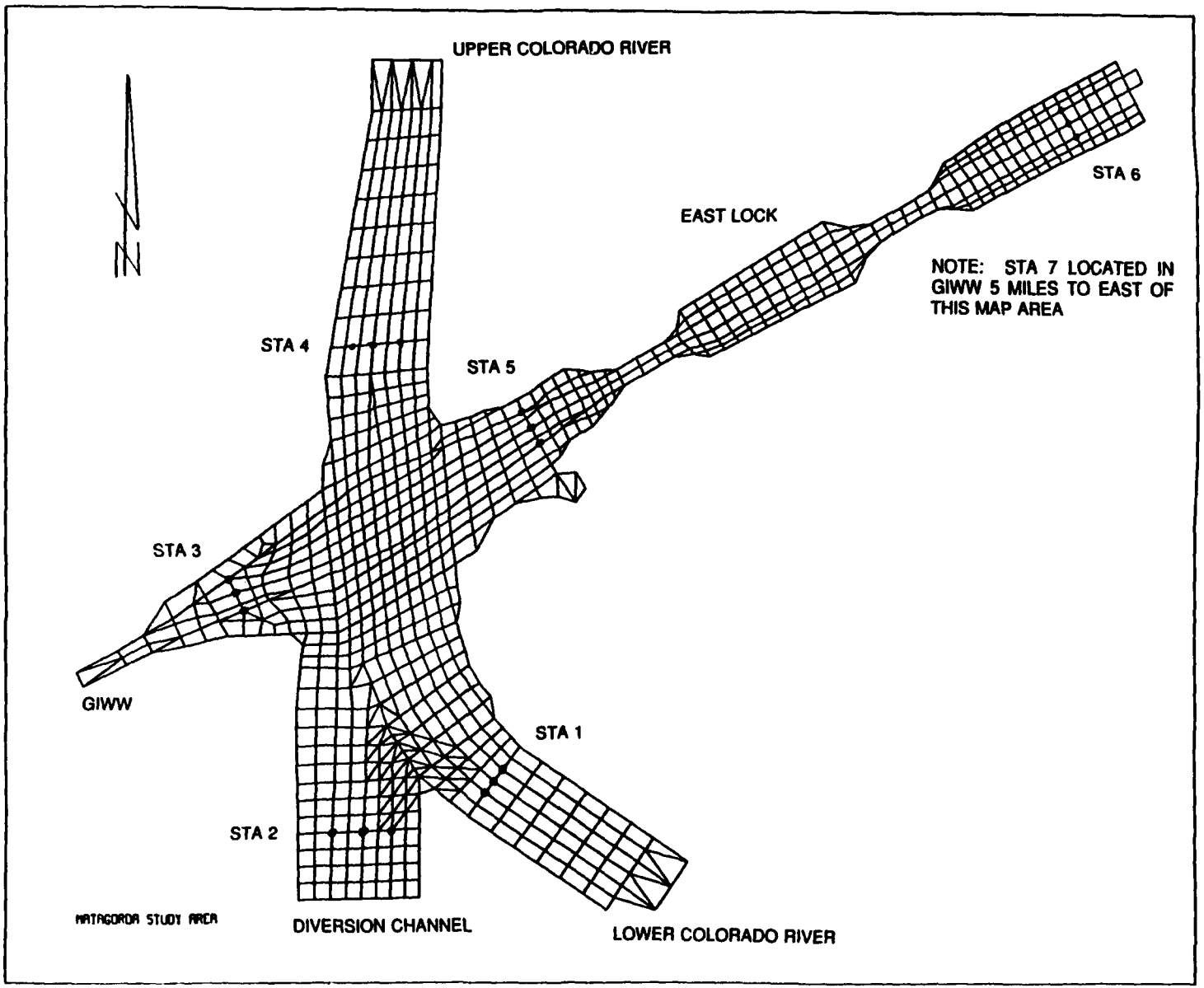

Figure 19. Detailed region of dynamic verification mesh with prototype station identification

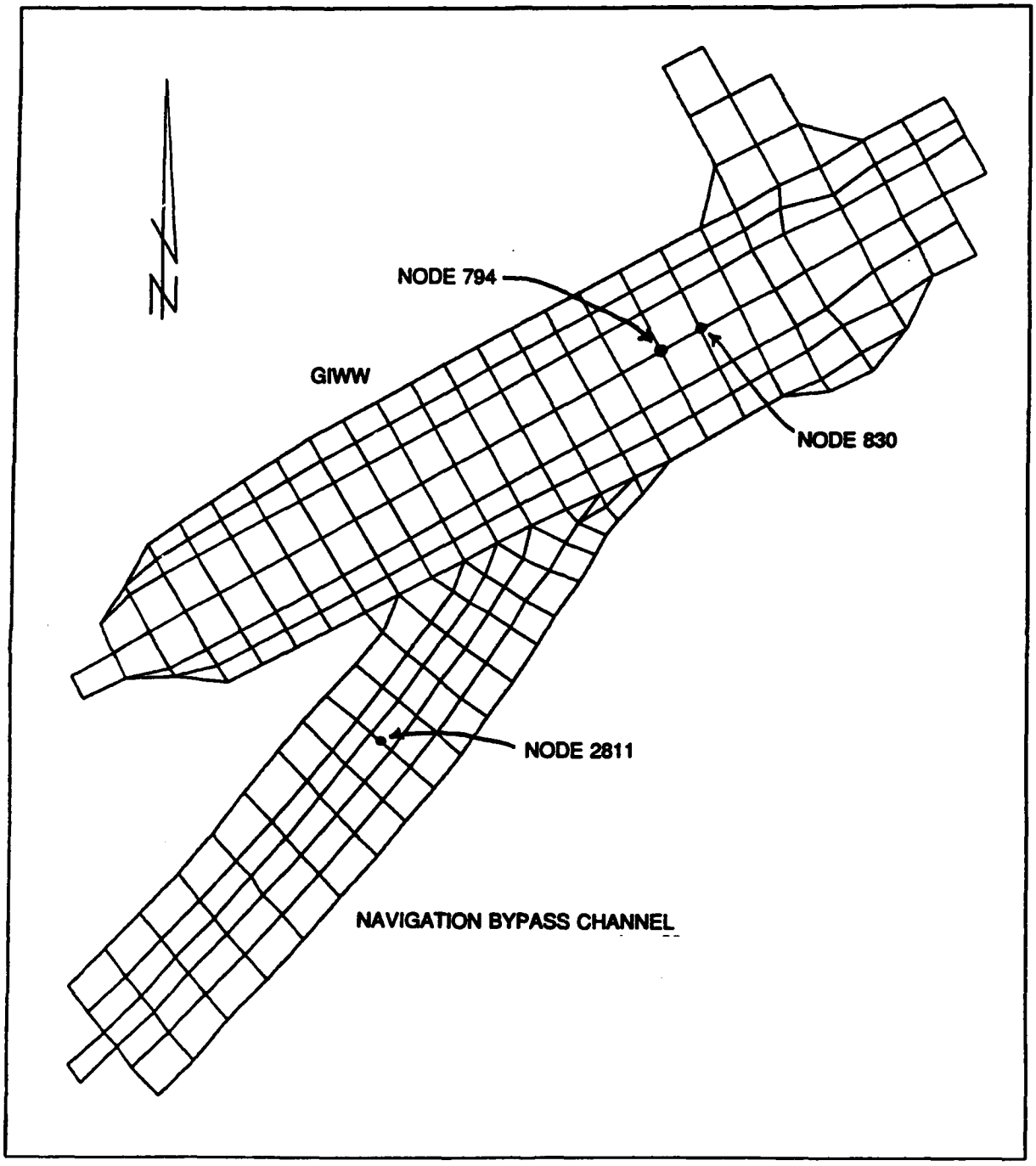

Figure 20. Detailed region of navigation bypass channel-GIWW design 2 computational mesh with reference nodes

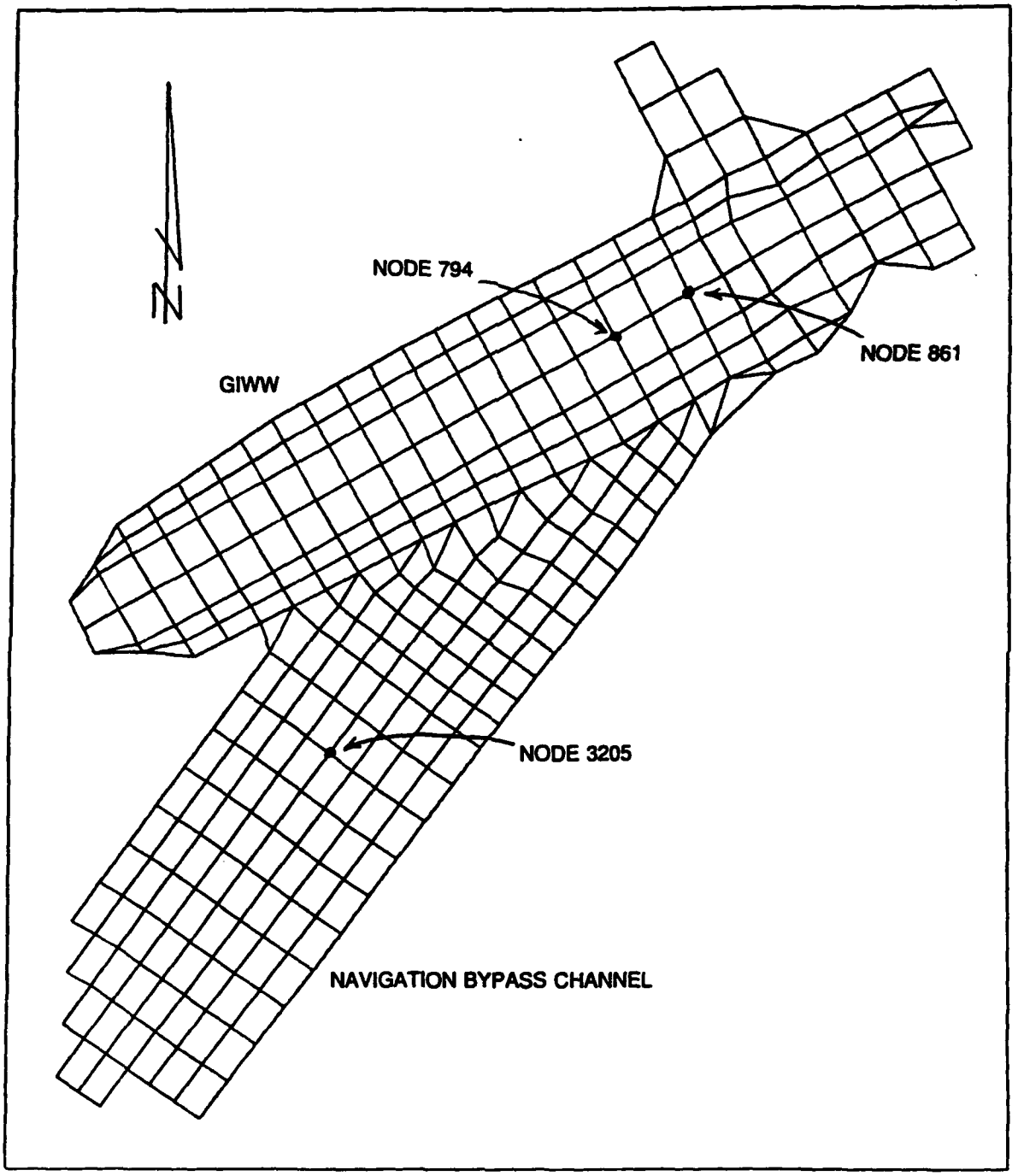

Figure 21. Detailed region of navigation bypass channel–GIWW design 3 computational mesh with reference nodes

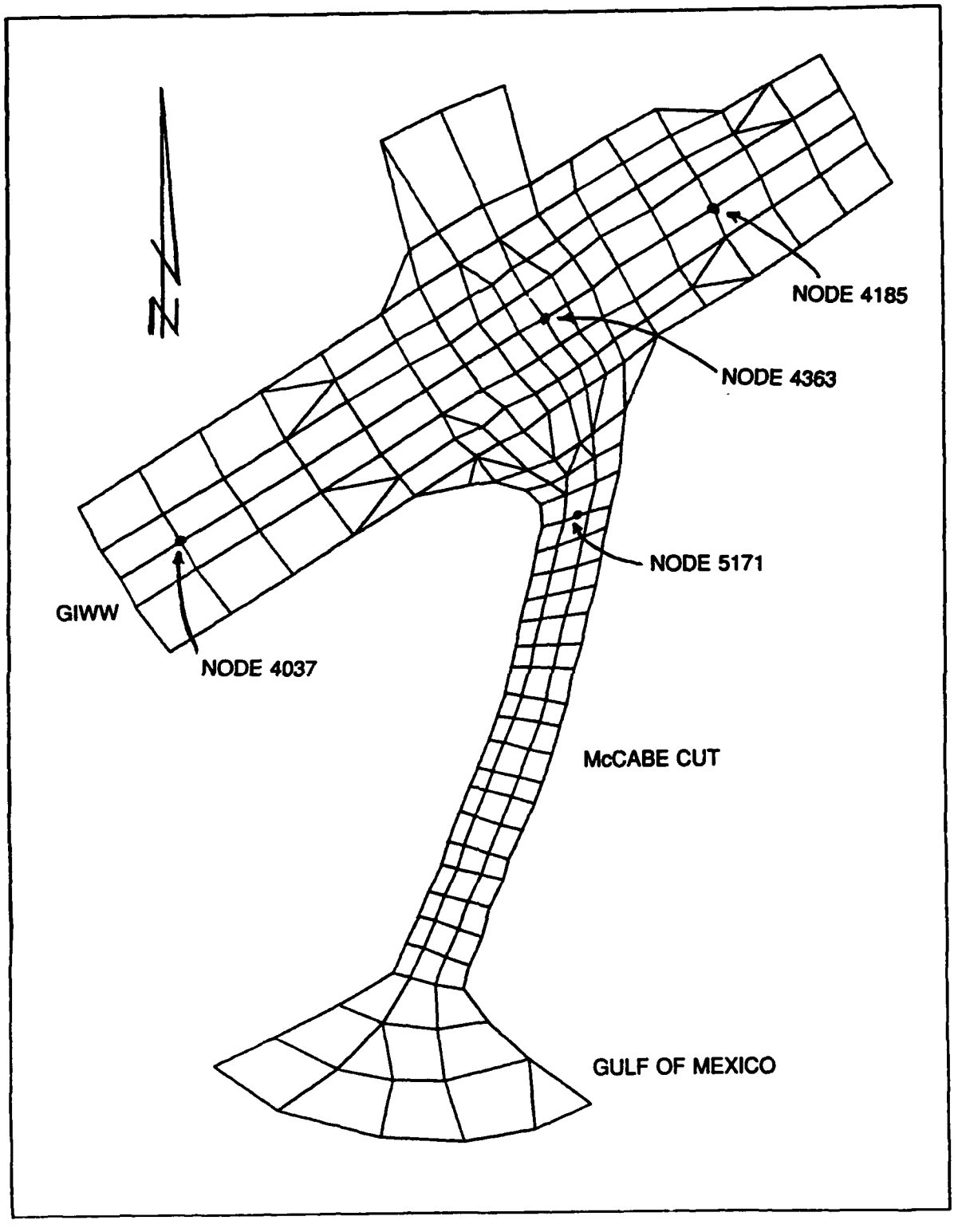

Figure 22. Detailed region of McCabe Cut computational mesh with reference nodes

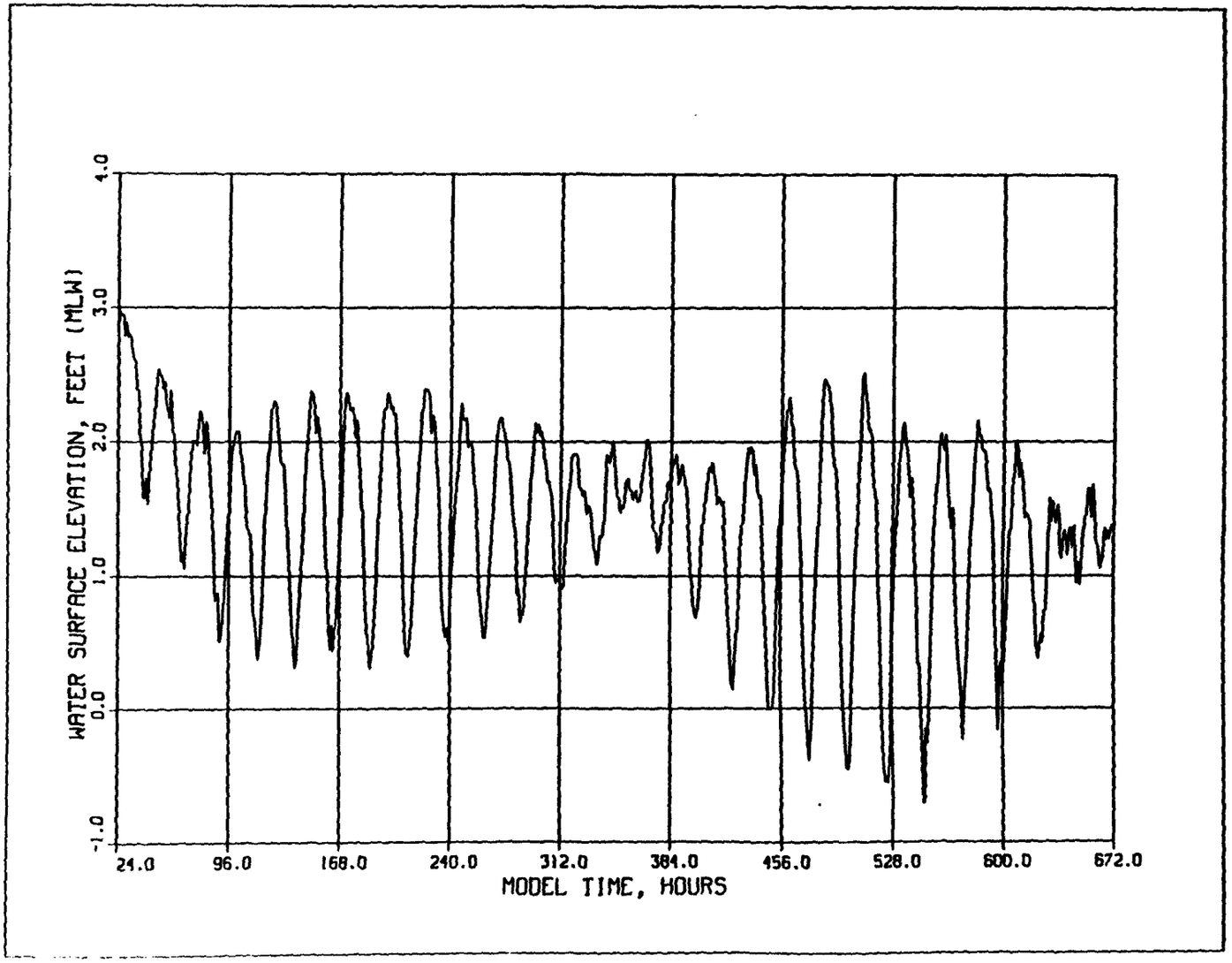

Figure 23. Recorded hourly water-level record in the Colorado River at the Gulf of Mexico used as boundary condition

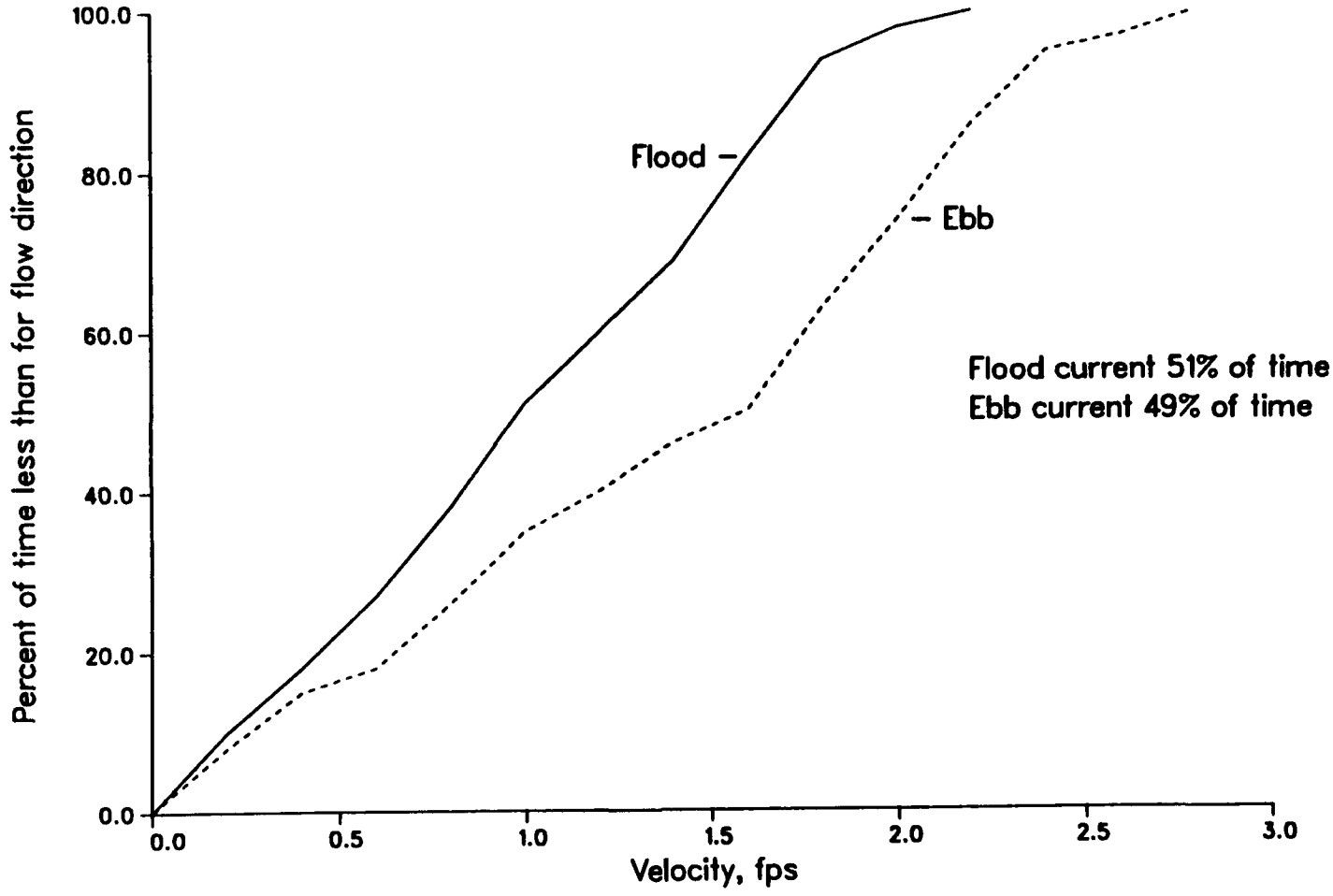

Figure 24. Simulated tidal current duration, 2-28 June 1990, at node 2811, design 2

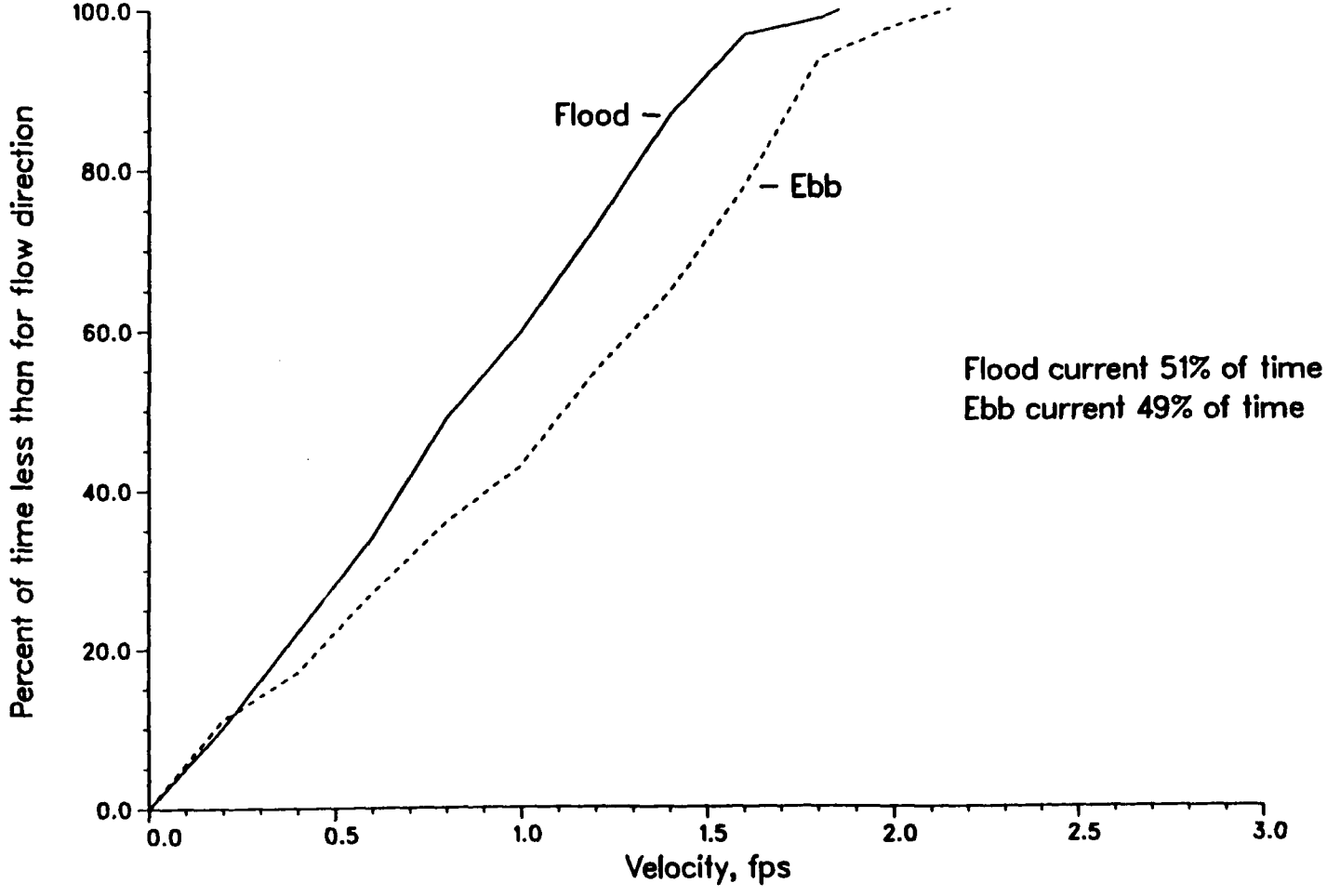

Figure 25. Simulated tidal current duration, 2-28 June 1990, at node 830, design 2

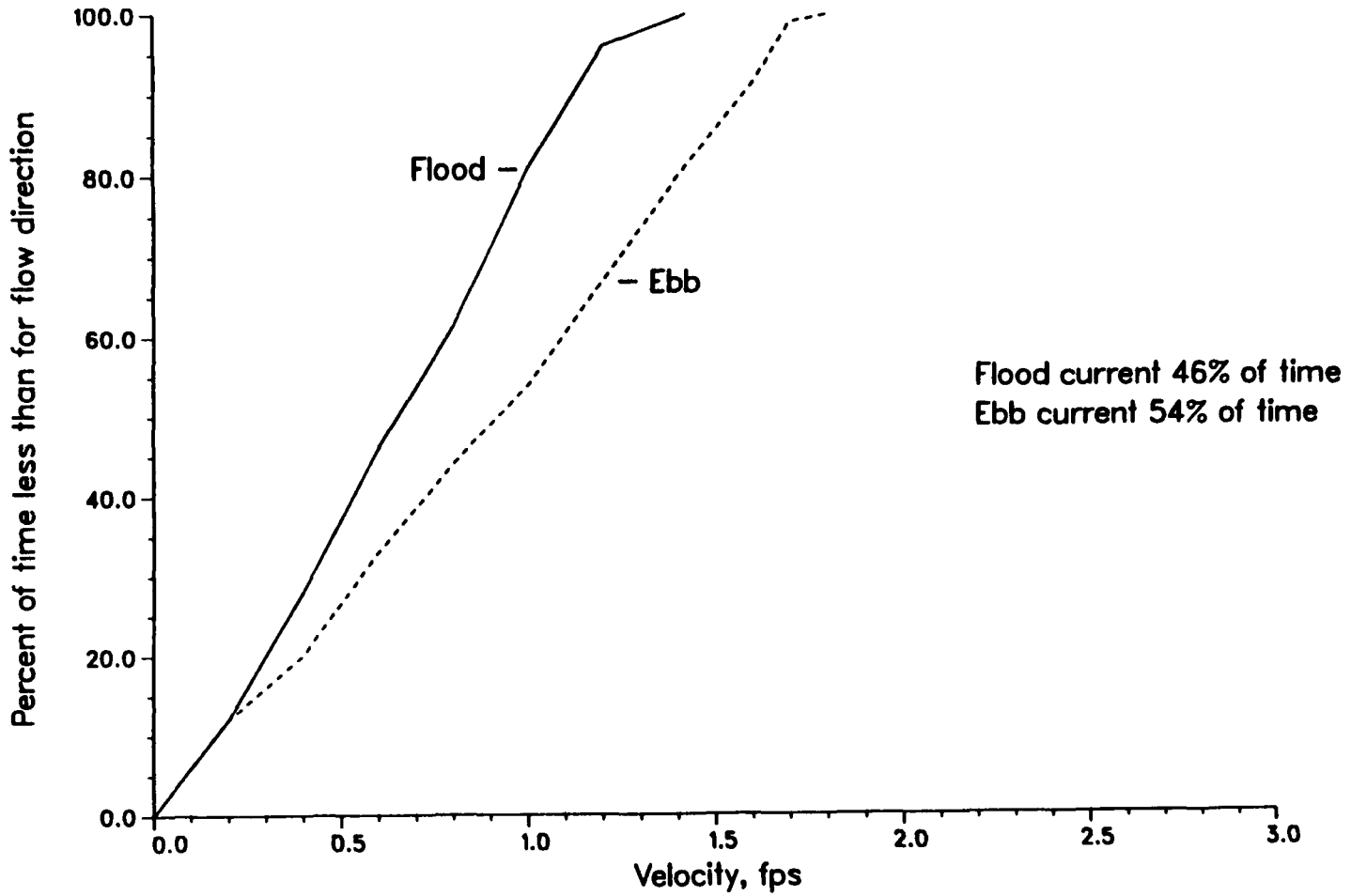

Figure 26. Simulated tidal current duration, 2-28 June 1990, at node 3205, design 3

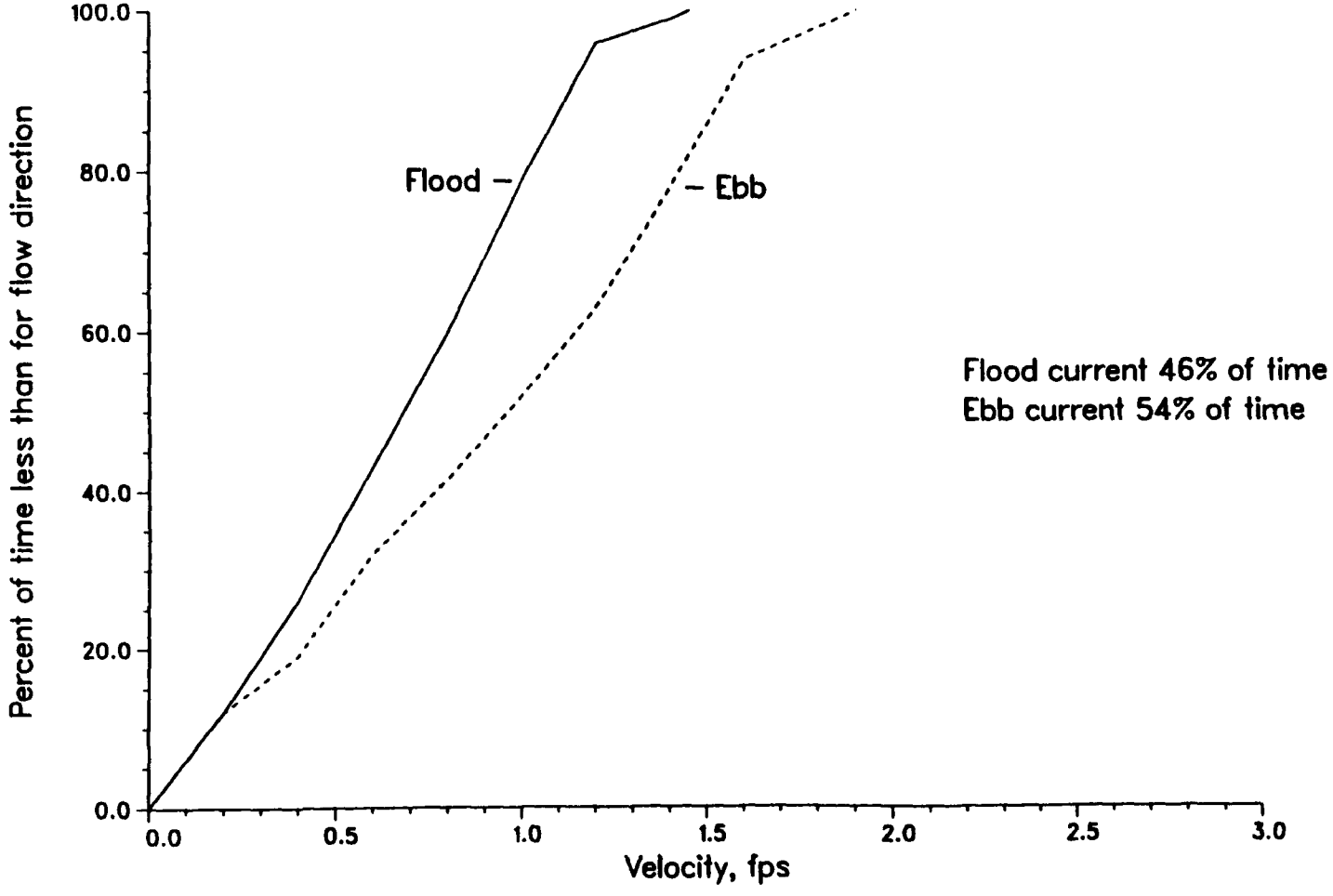

Figure 27. Simulated tidal current duration, 2-28 June 1990, at node 861, design 3

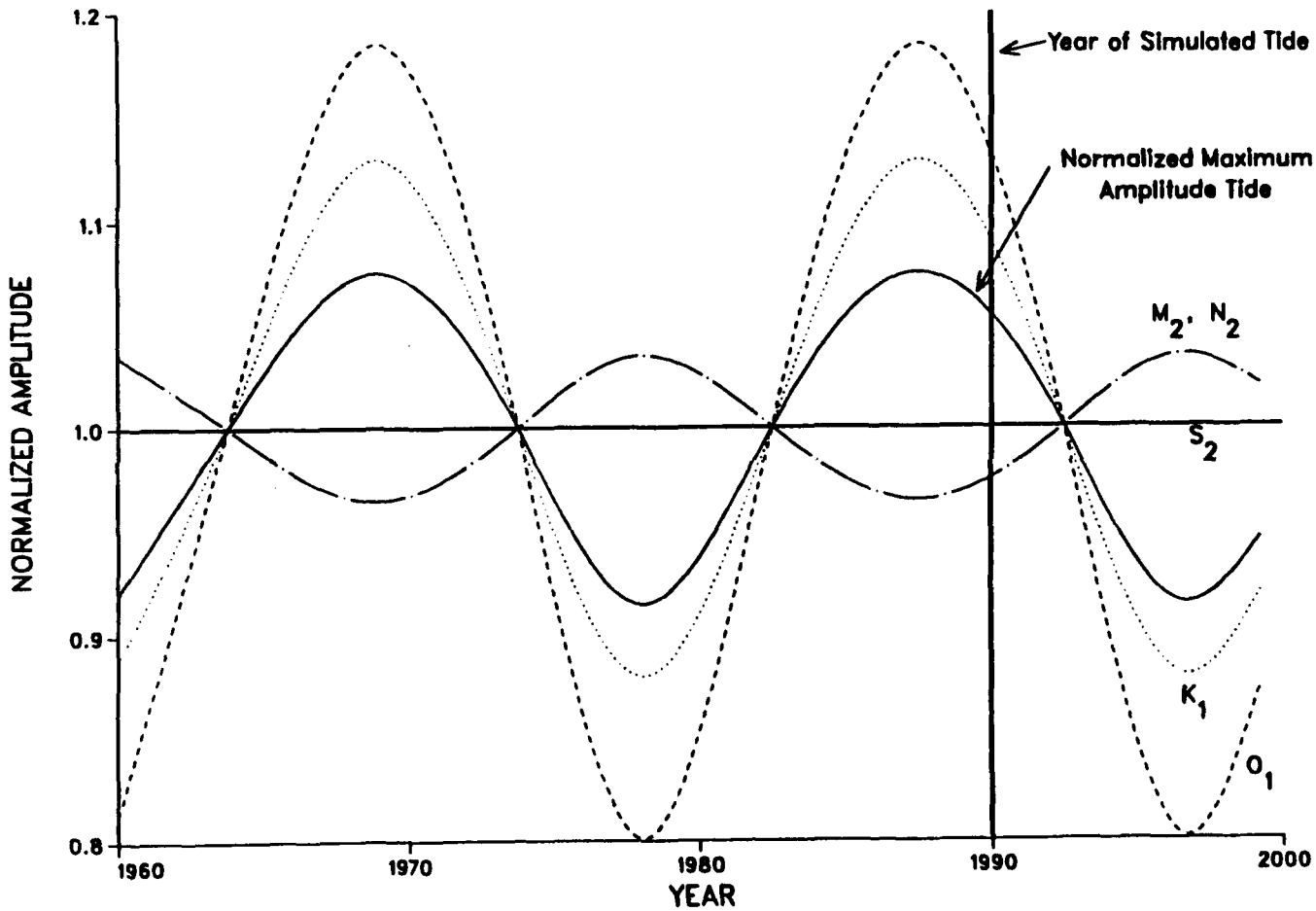

Figure 28. Cyclic variation of tidal constituents and tidal amplitudes, Pleasure Pier, Galveston, TX

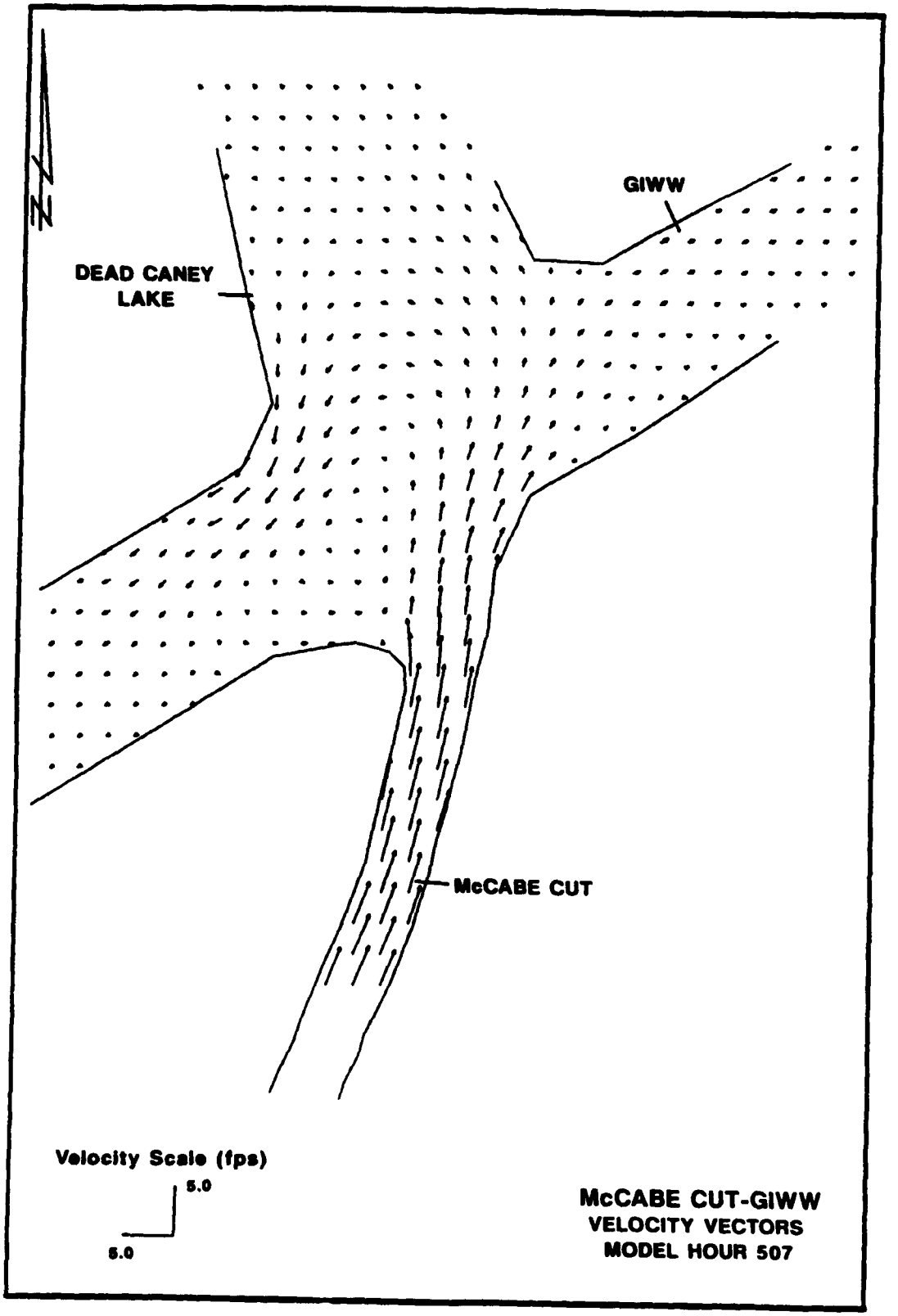

Figure 29. McCabe Cut–GIWW area simulated velocity vectors for hour 507

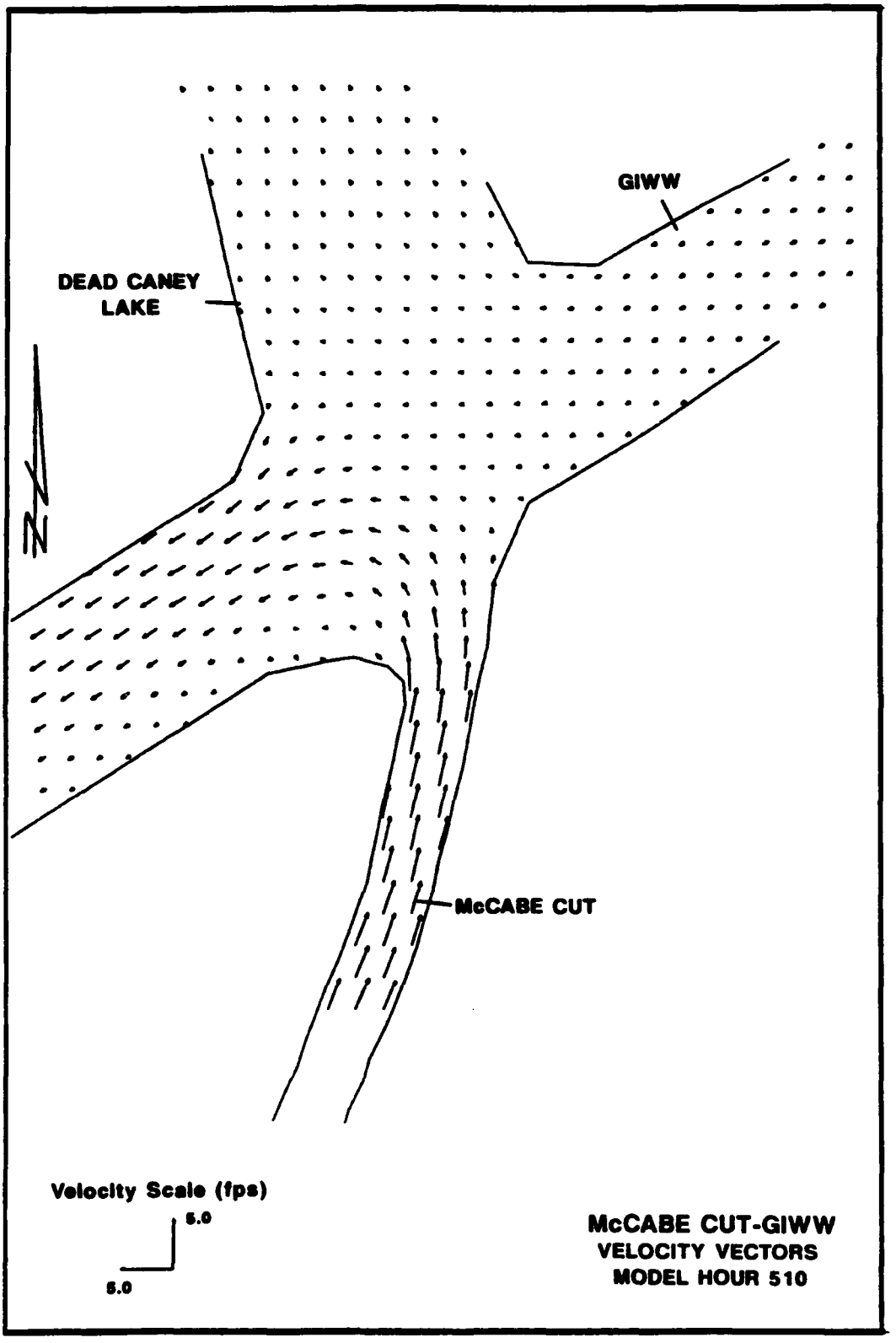

Figure 30. McCabe Cut–GIWW area simulated velocity vectors for hour 510

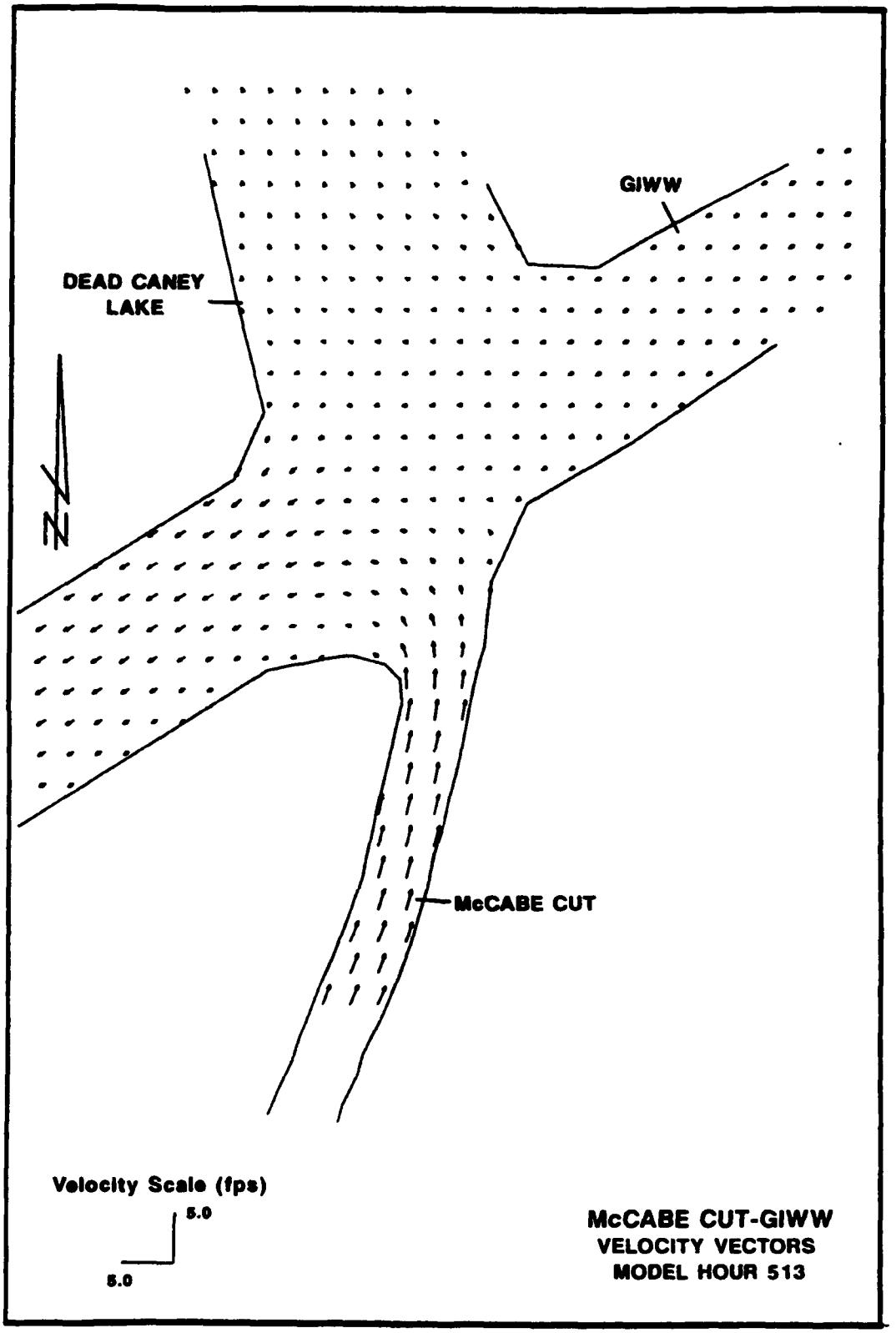

Figure 31. McCabe Cut–GIWW area simulated velocity vectors for hour 513

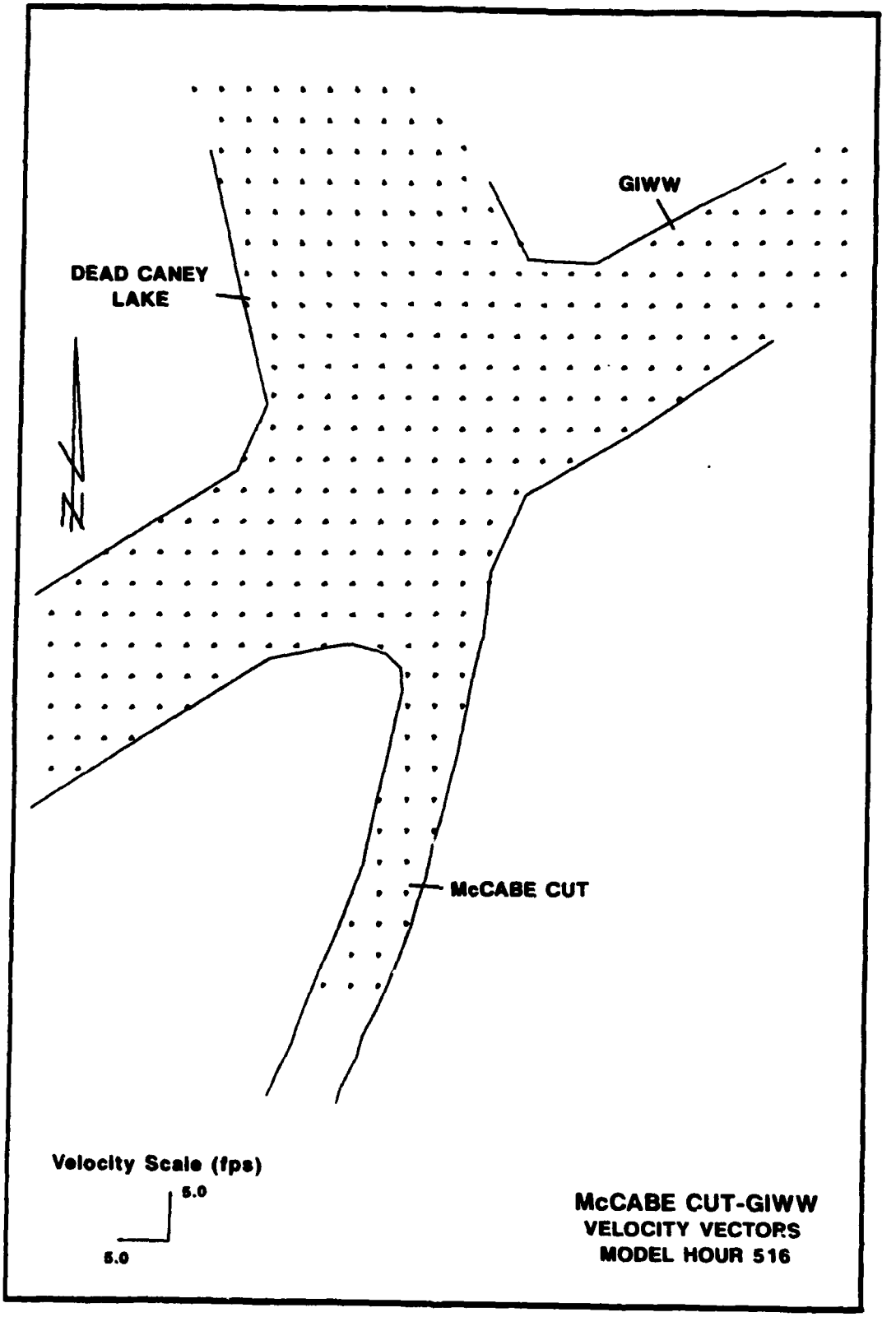

Figure 32. McCabe Cut-GIWW area simulated velocity vectors for hour 516

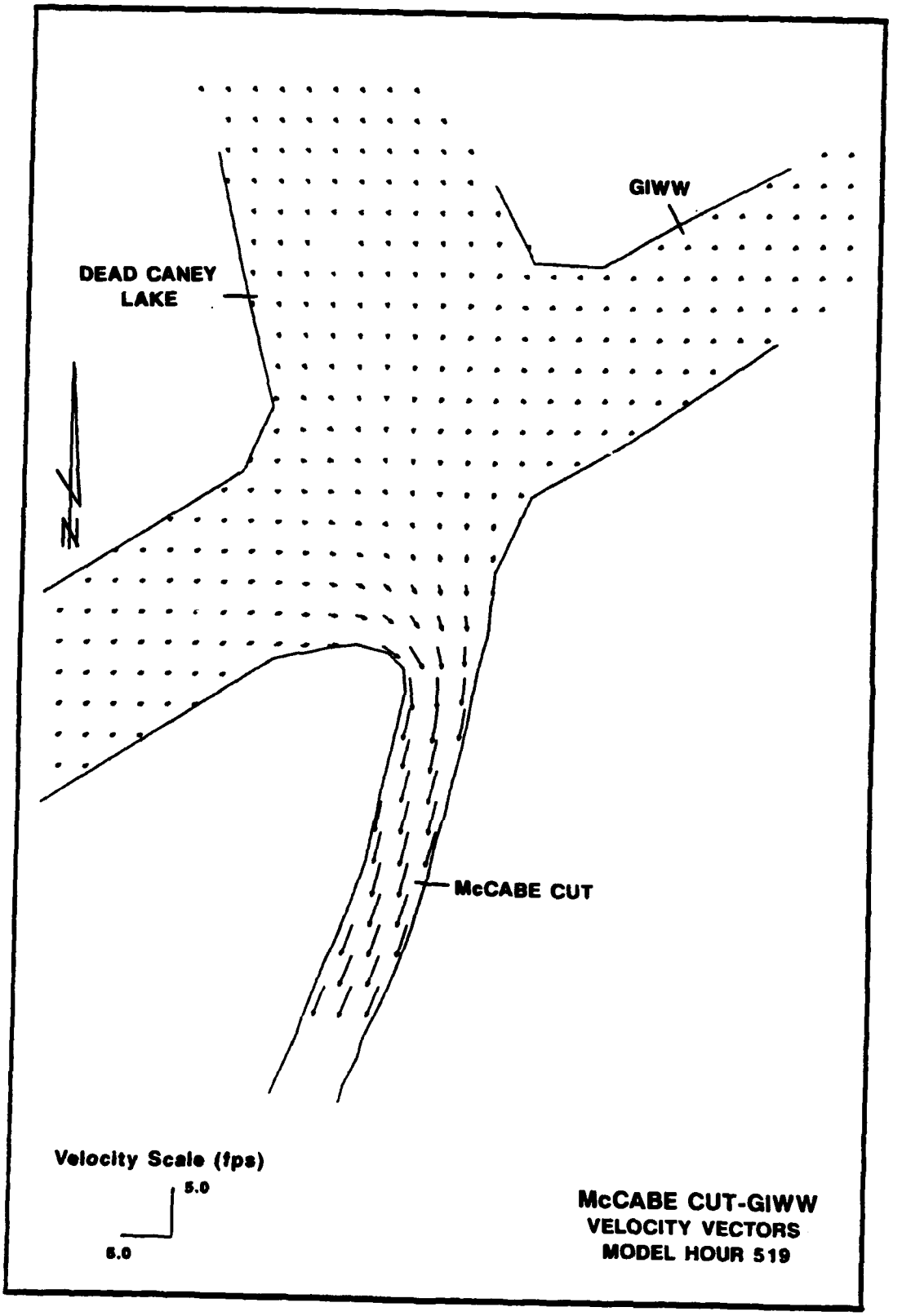

Figure 33. McCabe Cut–GIWW area simulated velocity vectors for hour 519

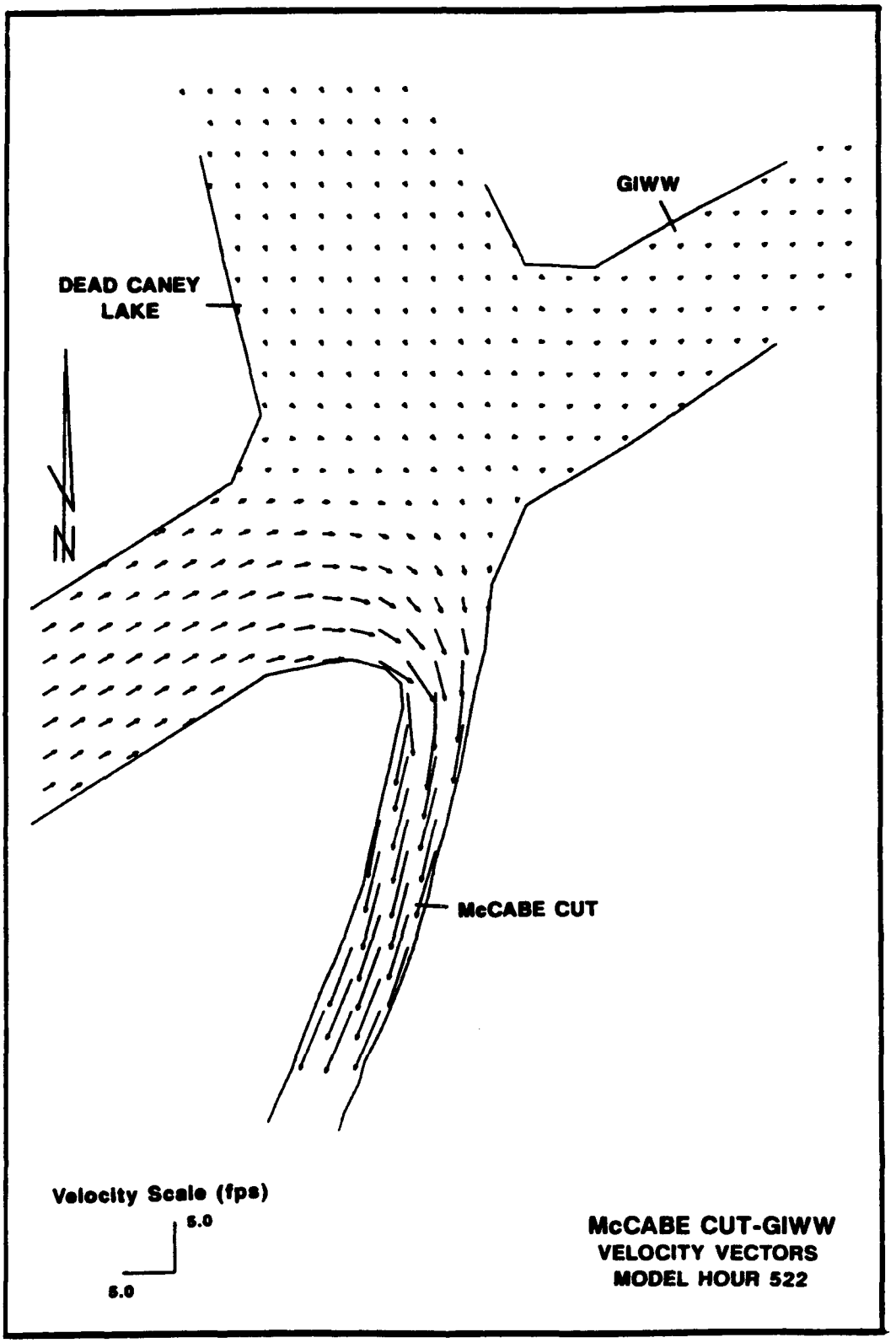

Figure 34. McCabe Cut–GIWW area simulated velocity vectors for hour 522

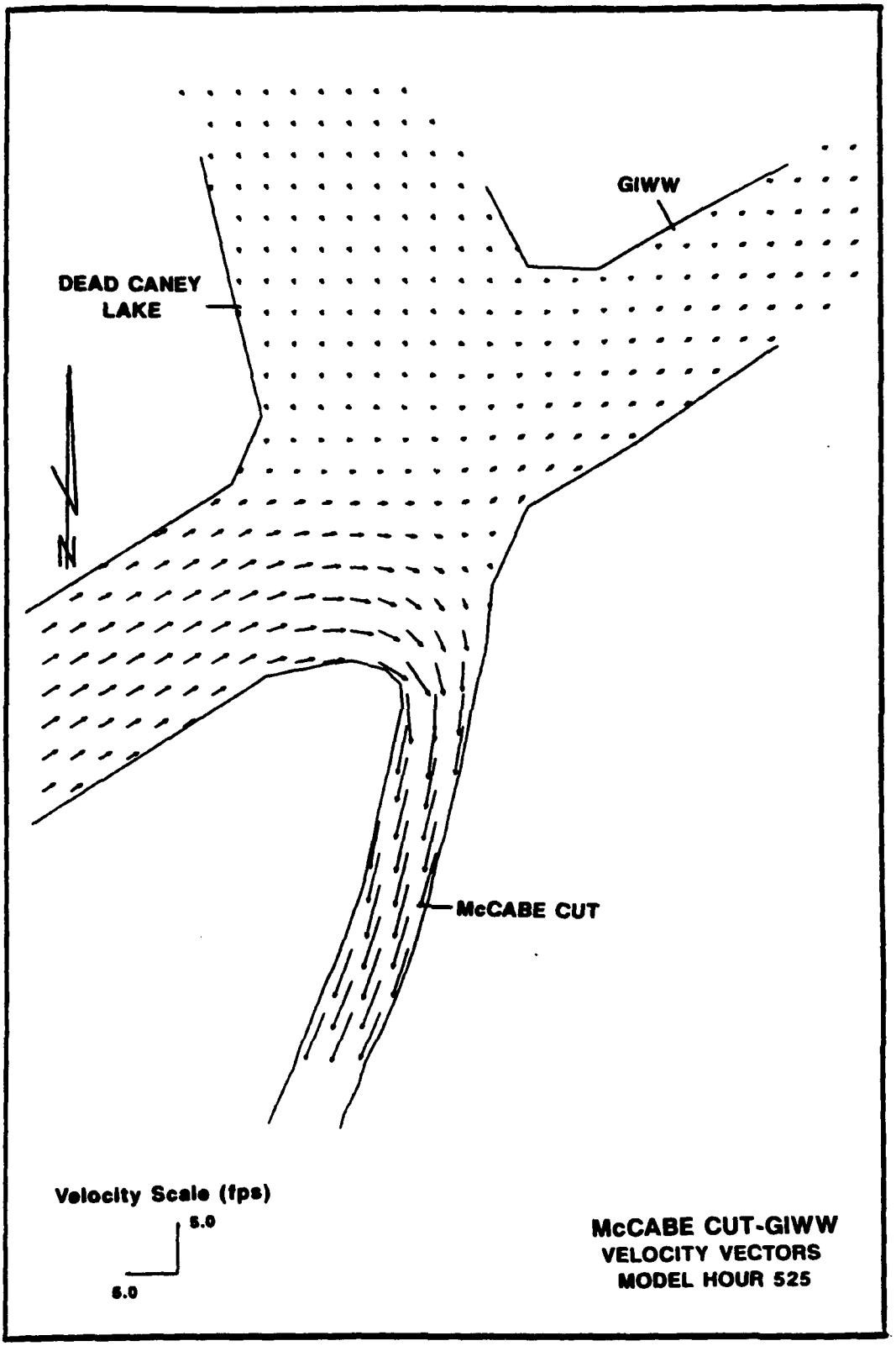

Figure 35. McCabe Cut–GIWW area simulated velocity vectors for hour 525

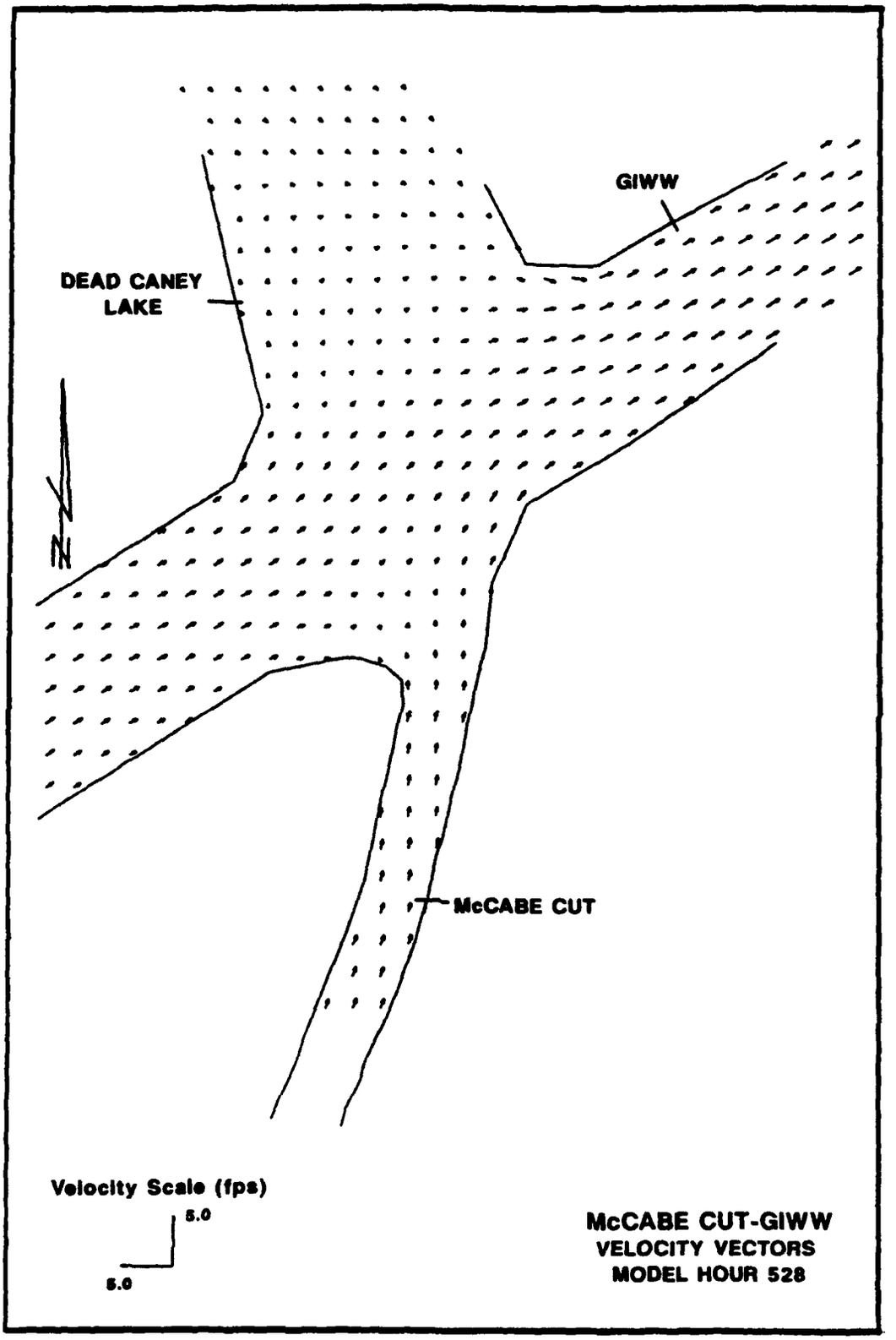

Figure 36. McCabe Cut–GIWW area simulated velocity vectors for hour 528

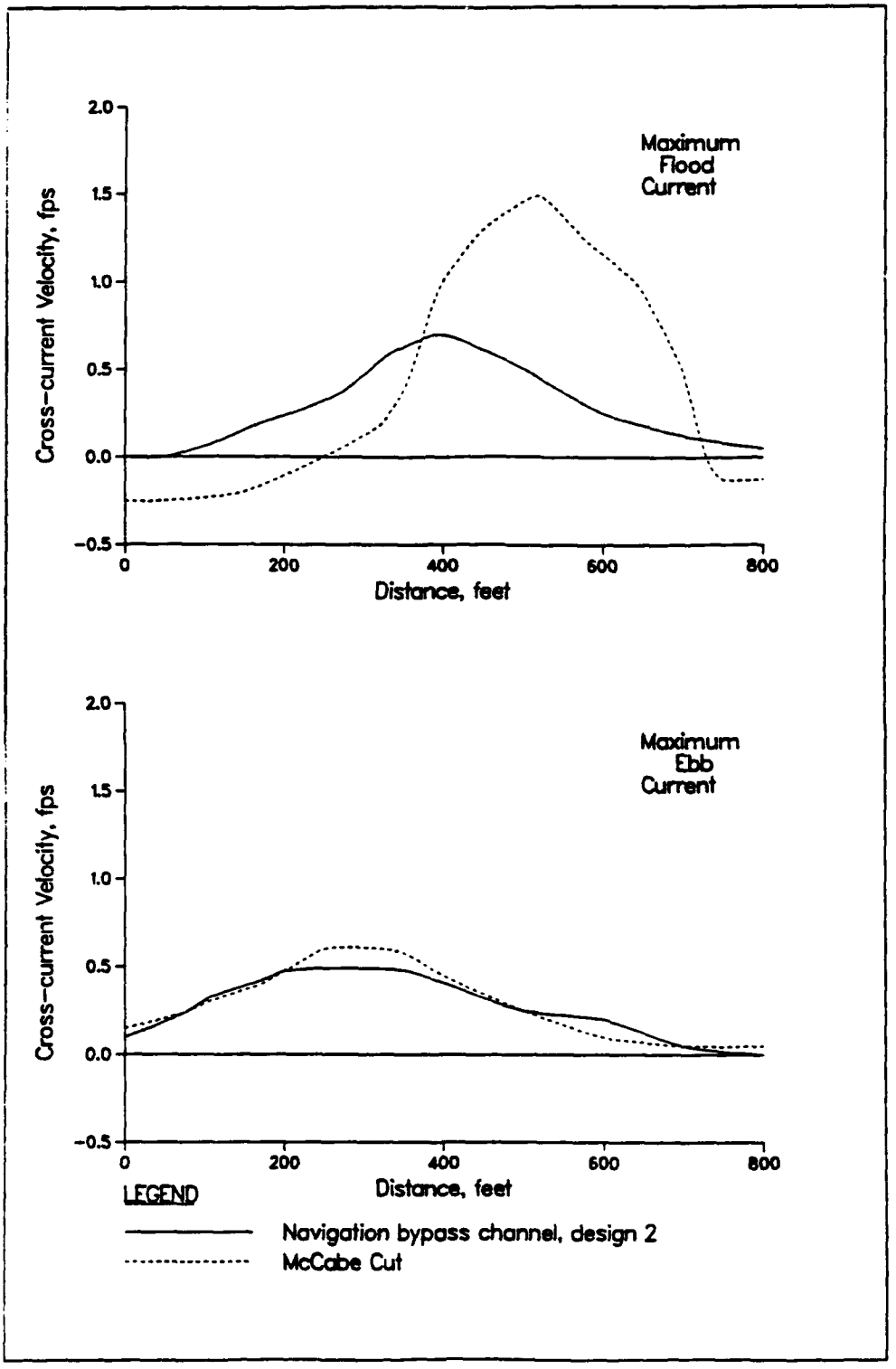

Figure 37. Comparison of simulated cross currents in GIWW at maximum flood and ebb currents

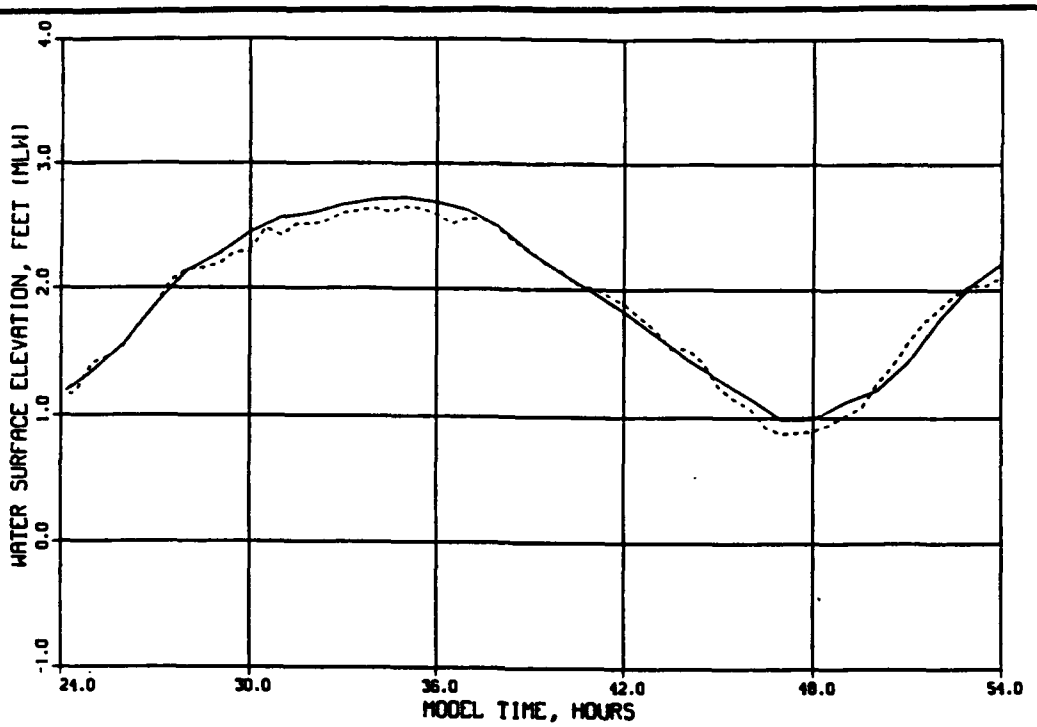

STA S3

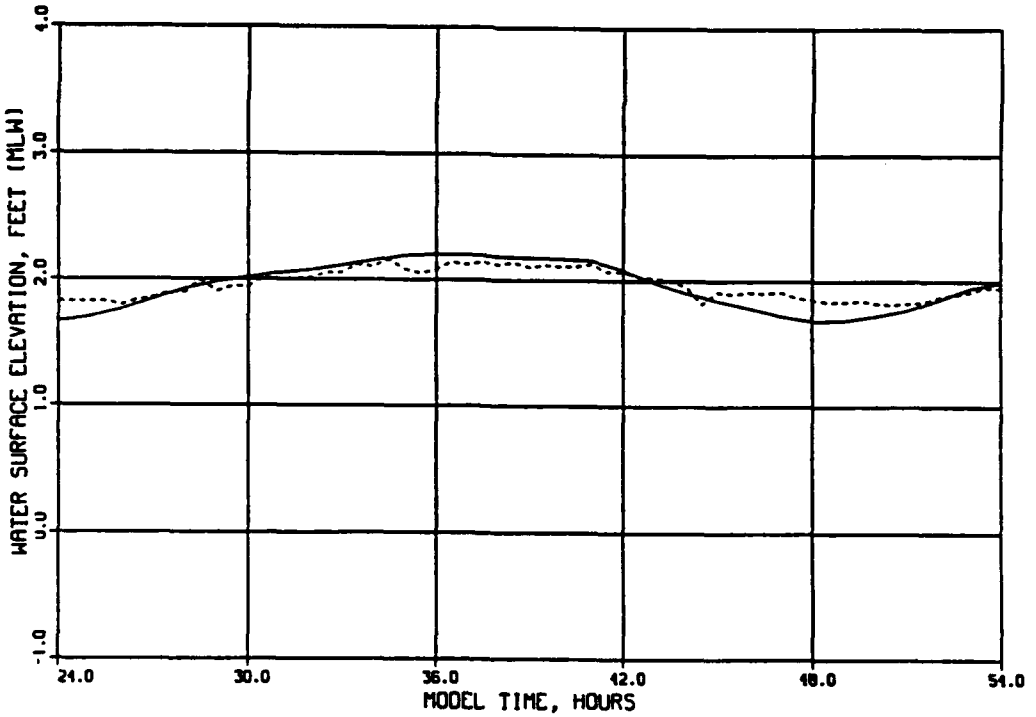

STA S4

LEGEND

— **RMA-2V**

- - - **FIELD MEASUREMENT**

WATER LEVELS
RMA-2V VERSUS FIELD DATA
25-26 MAY 1990
STA S3, S4

PLATE 1

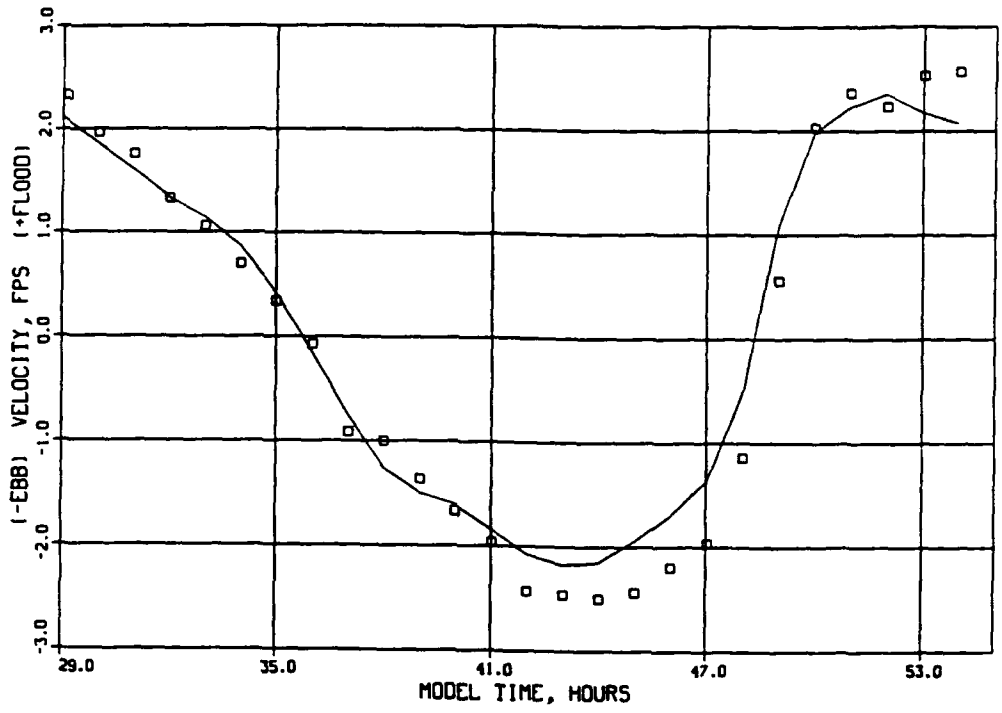

STA 1A

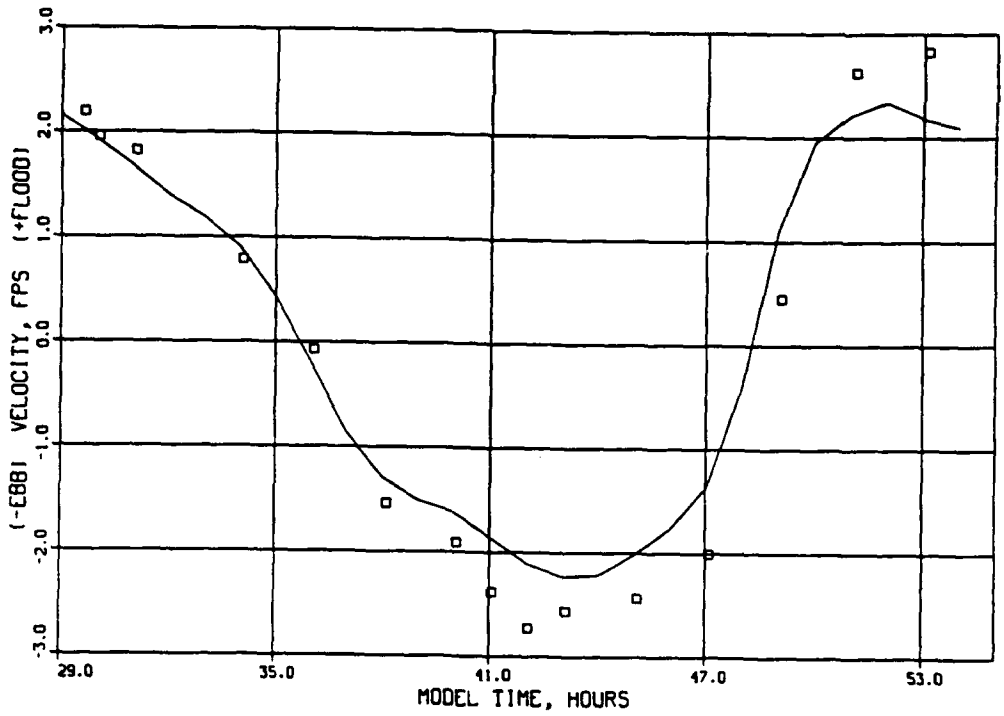

STA 1B

LEGEND

— RMA-2V

□ VERTICALLY AVERAGED FIELD DATA

VELOCITY DATA
RMA-2V VERSUS FIELD DATA
25-26 MAY 1990
STA 1A, 1B

PLATE 2

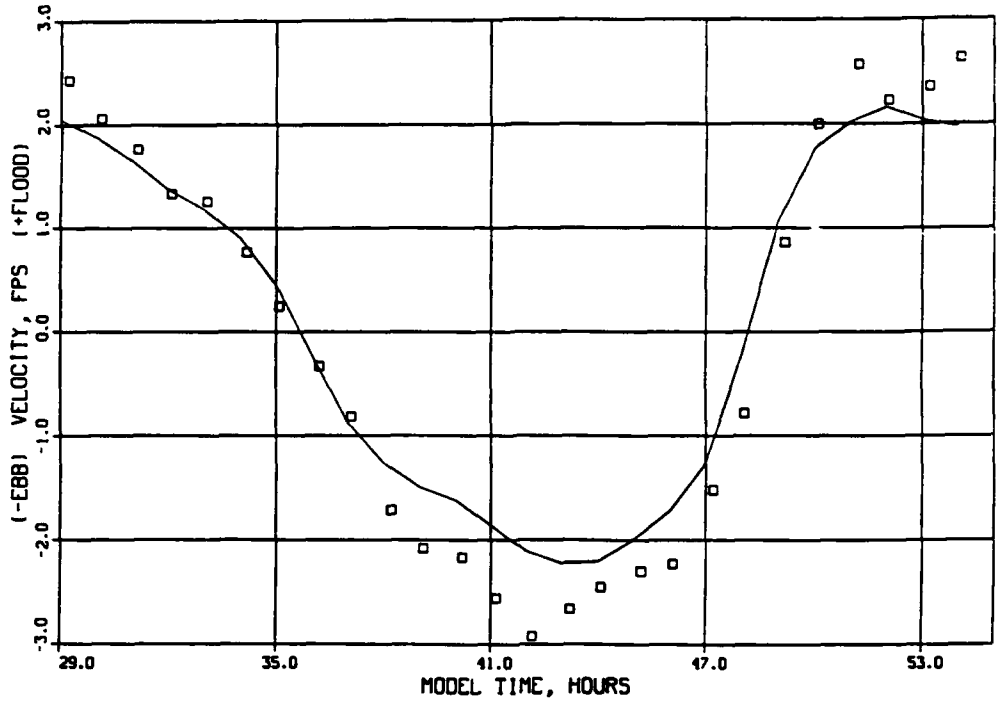

STA 1C

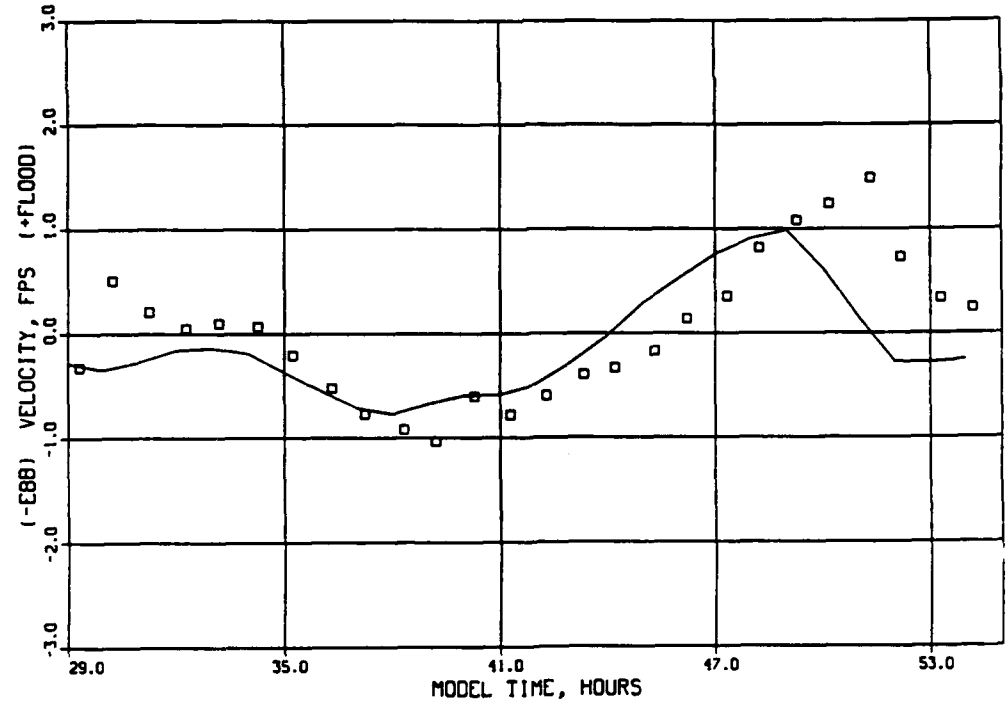

STA 2A

LEGEND

— RMA-2V

□ VERTICALLY AVERAGED FIELD DATA

VELOCITY DATA
RMA-2V VERSUS FIELD DATA
25-26 MAY 1990
STA 1C, 2A

PLATE 3

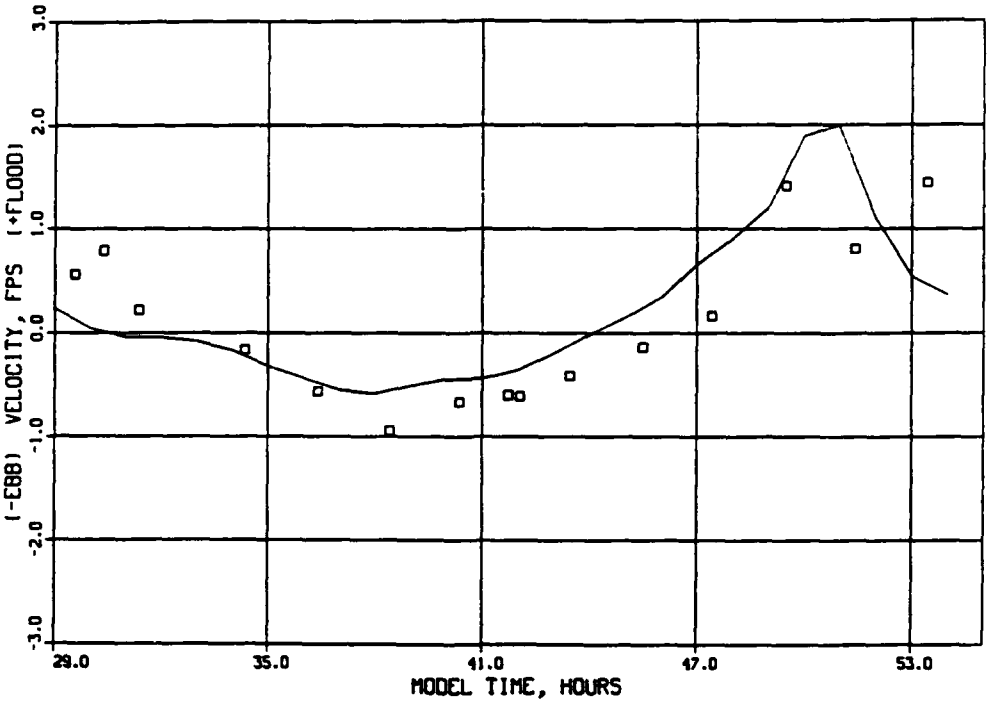

STA 2B

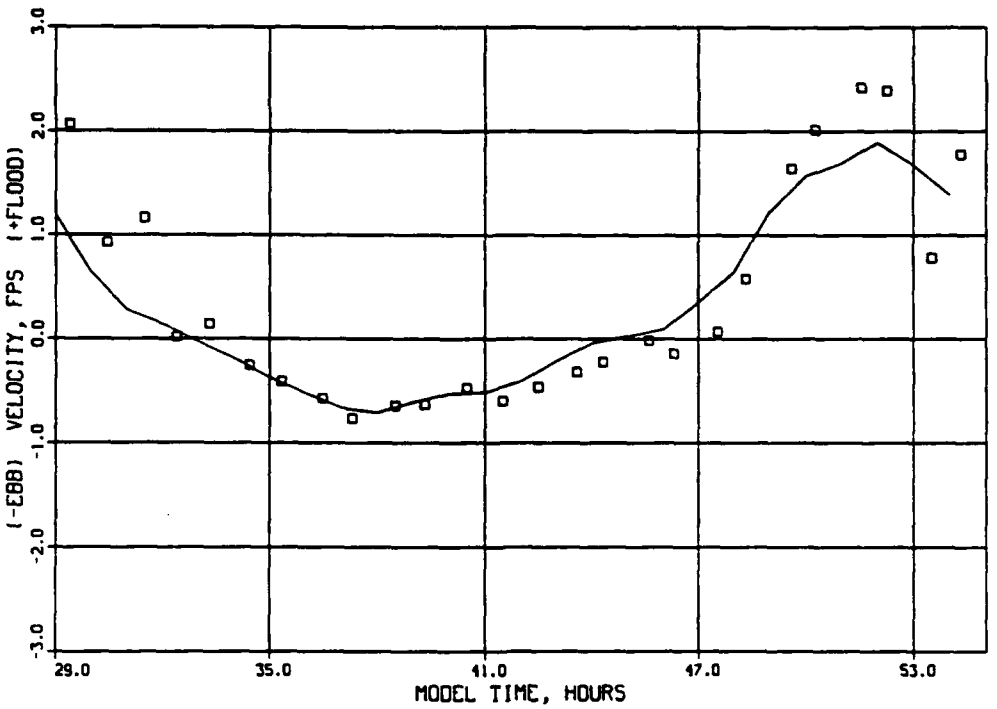

STA 2C

LEGEND

— RMA-2V

□ VERTICALLY AVERAGED FIELD DATA

VELOCITY DATA
RMA-2V VERSUS FIELD DATA
25-26 MAY 1990
STA 2B, 2C

PLATE 4

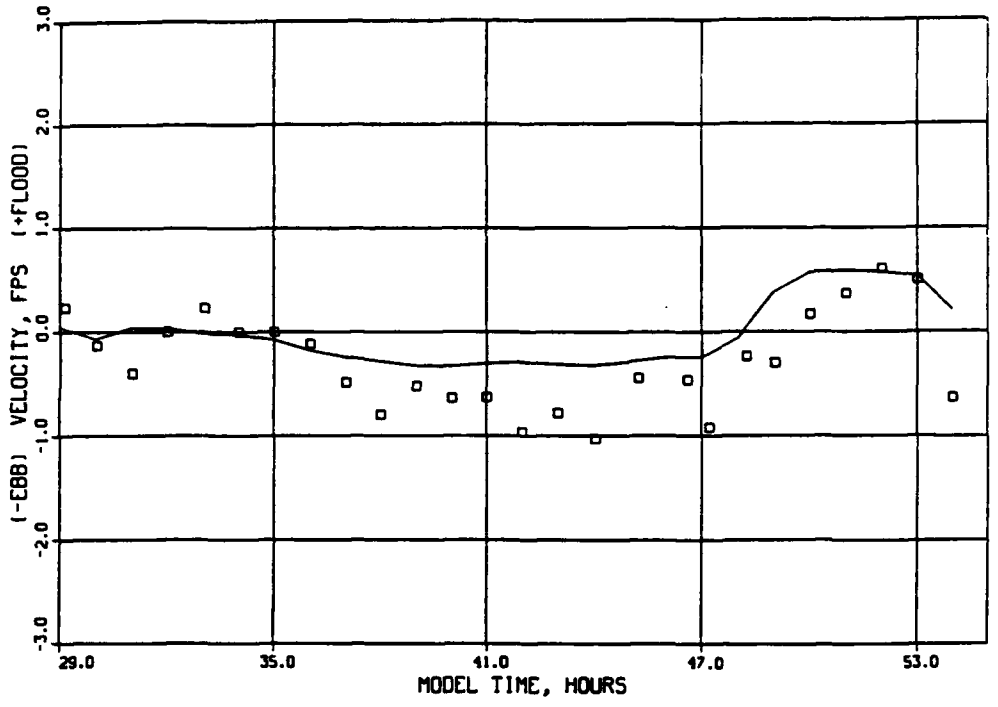

STA 3A

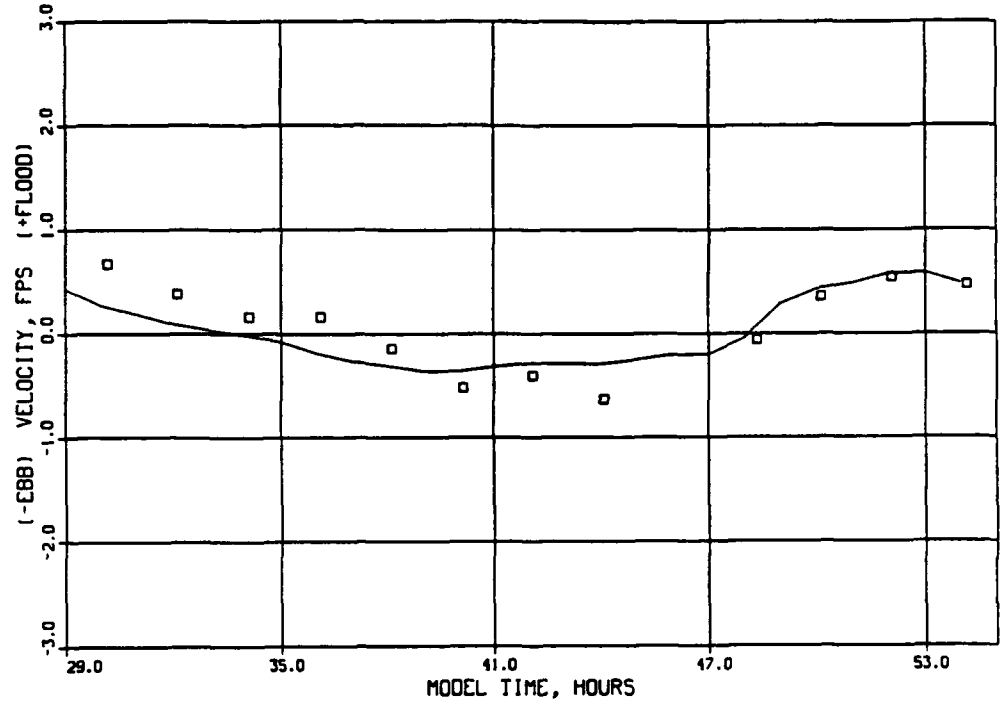

STA 3B

LEGEND

— RMA-2V

□ VERTICALLY AVERAGED FIELD DATA

VELOCITY DATA
RMA-2V VERSUS FIELD DATA
25-26 MAY 1990
STA 3A, 3B

PLATE 5

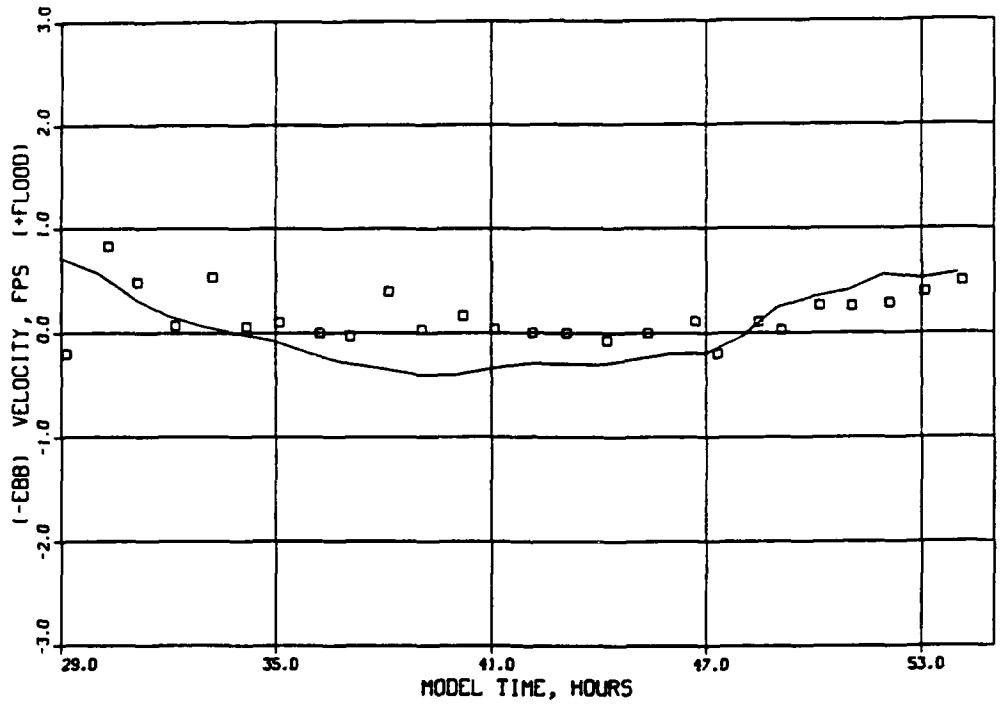

STA 3C

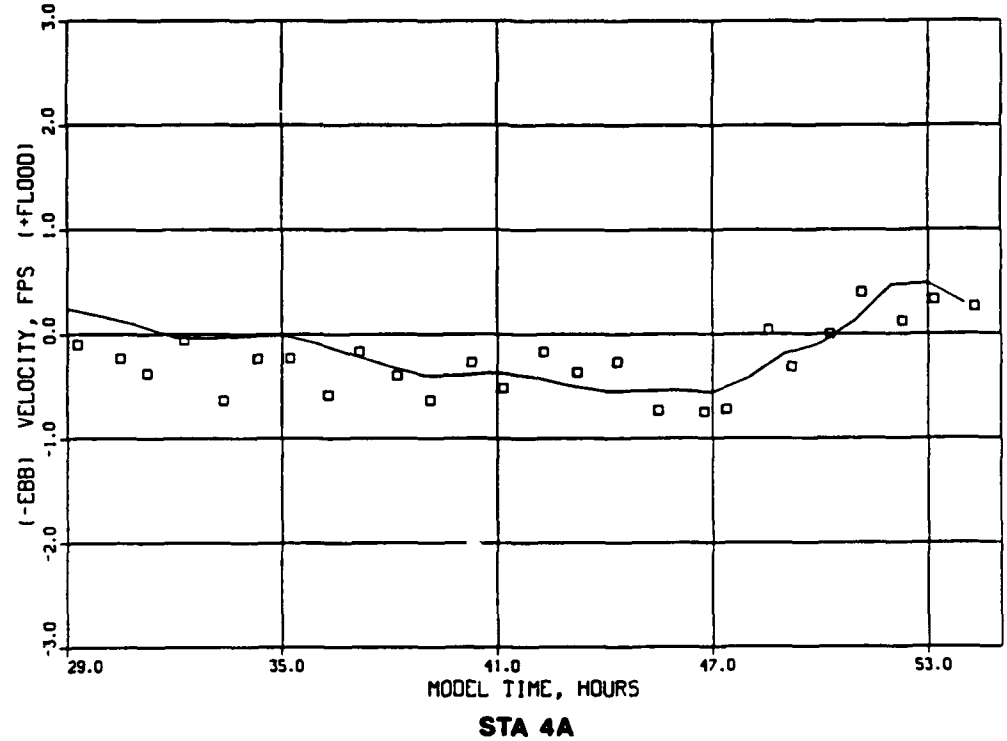

STA 4A

LEGEND

— RMA-2V

□ VERTICALLY AVERAGED FIELD DATA

VELOCITY DATA
RMA-2V VERSUS FIELD DATA
25-26 MAY 1990
STA 3C, 4A

PLATE 6

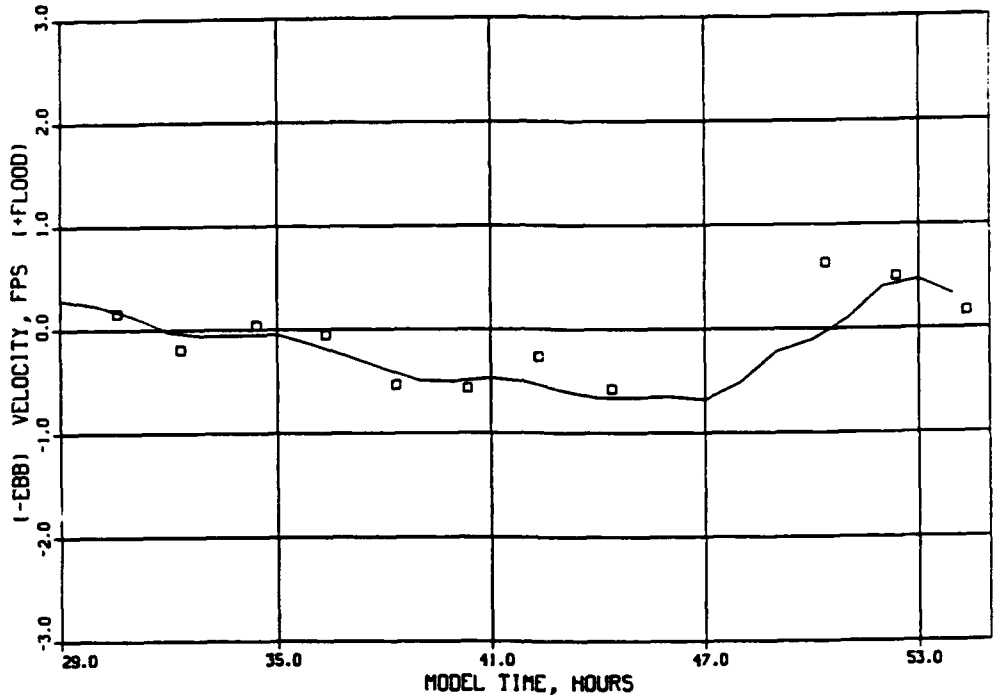

STA 4B

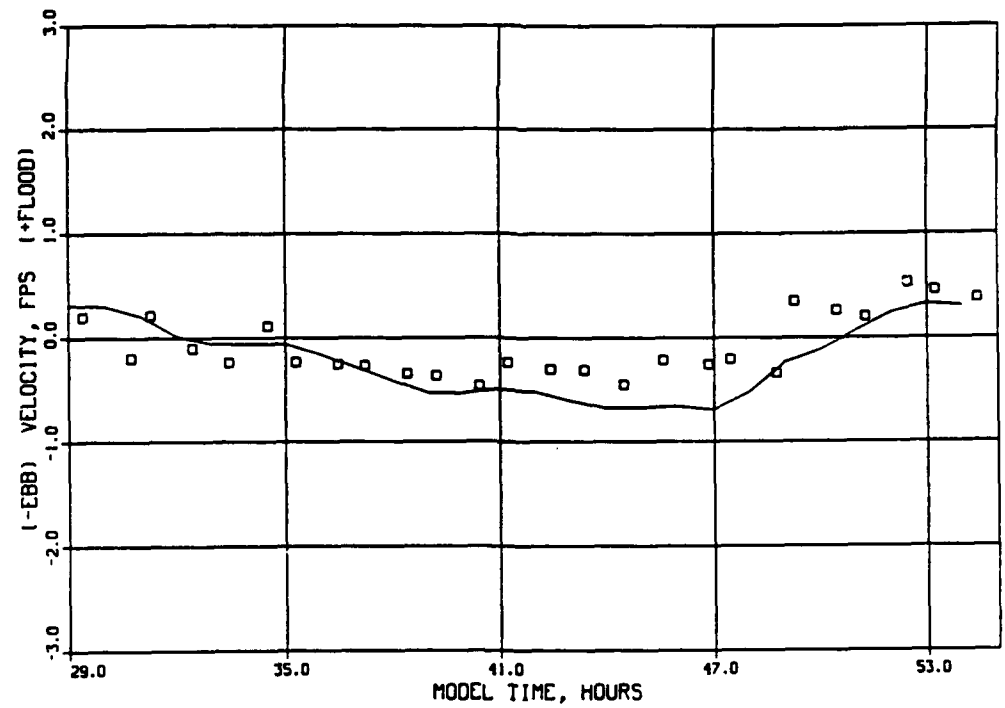

STA 4C

LEGEND

— RMA-2V

□ VERTICALLY AVERAGED FIELD DATA

VELOCITY DATA
RMA-2V VERSUS FIELD DATA
25-26 MAY 1990
STA 4B, 4C

PLATE 7

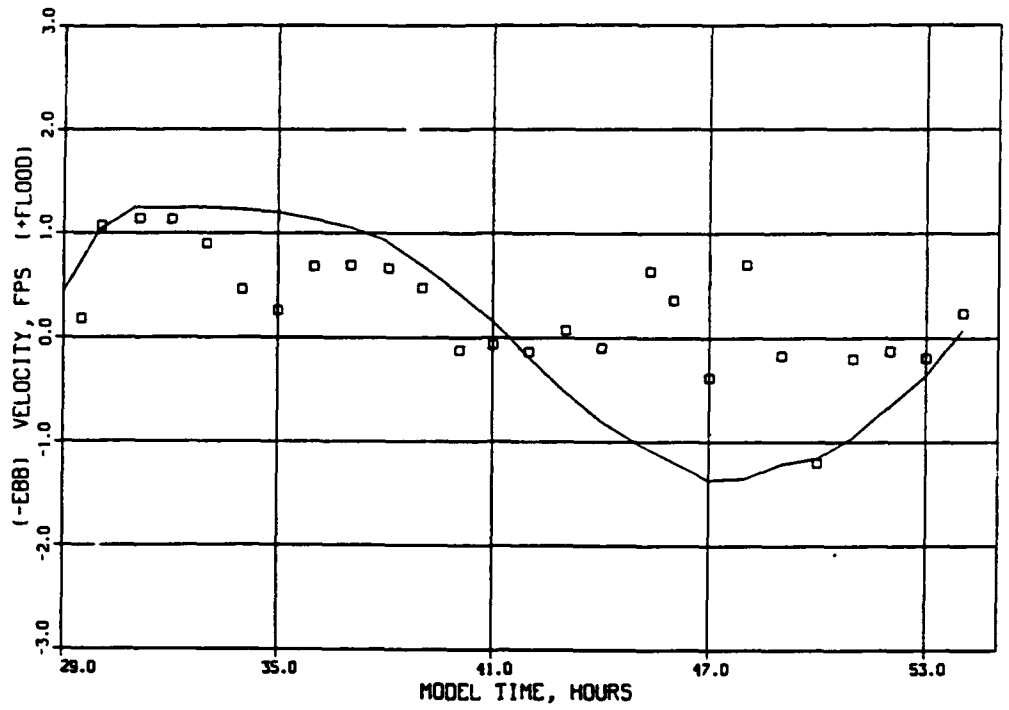

STA 5A

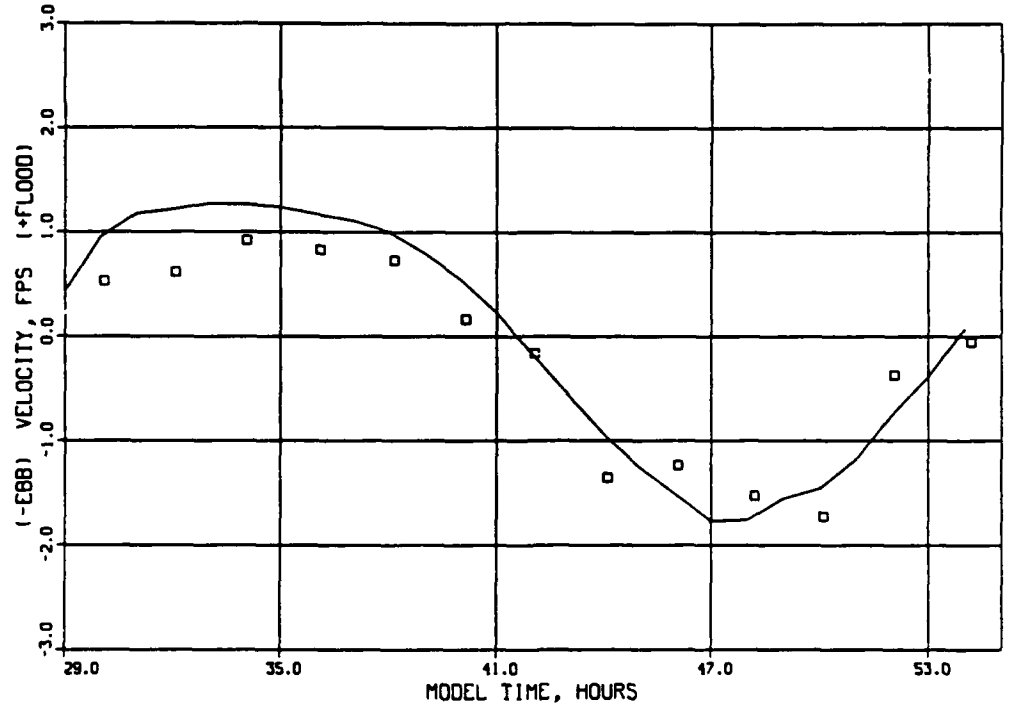

STA 5B

LEGEND

— RMA-2V

□ VERTICALLY AVERAGED FIELD DATA

VELOCITY DATA
RMA-2V VERSUS FIELD DATA
25-26 MAY 1990
STA 5A, 5B

PLATE 8

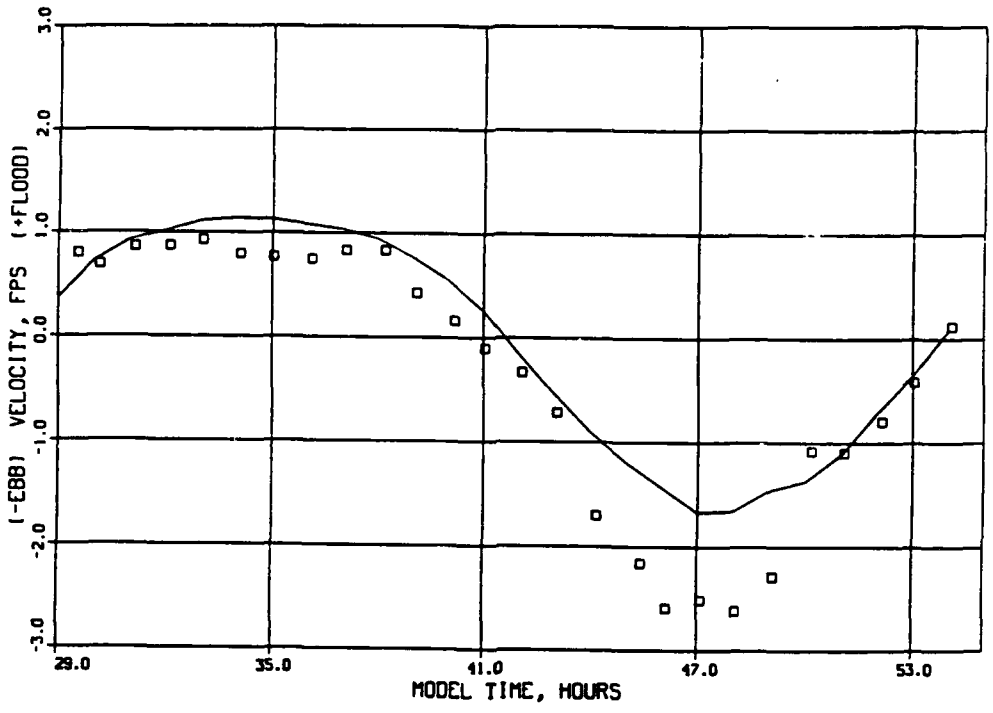

STA 5C

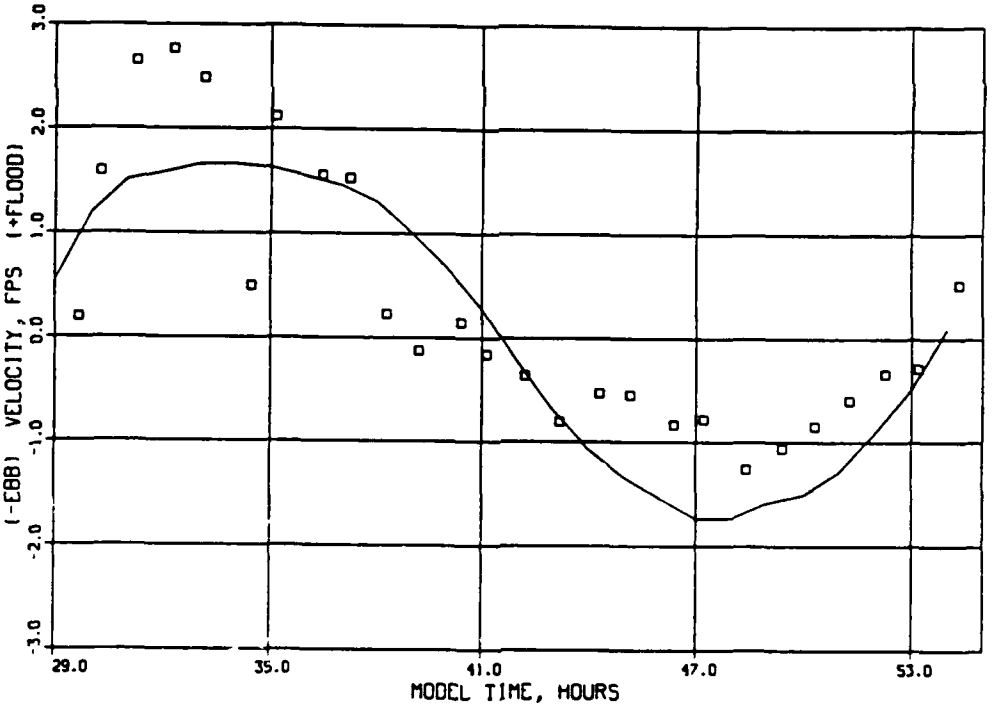

STA 6A

LEGEND

— RMA-2V

□ VERTICALLY AVERAGED FIELD DATA

VELOCITY DATA
RMA-2V VERSUS FIELD DATA
25-26 MAY 1990
STA 5C, 6A

PLATE 9

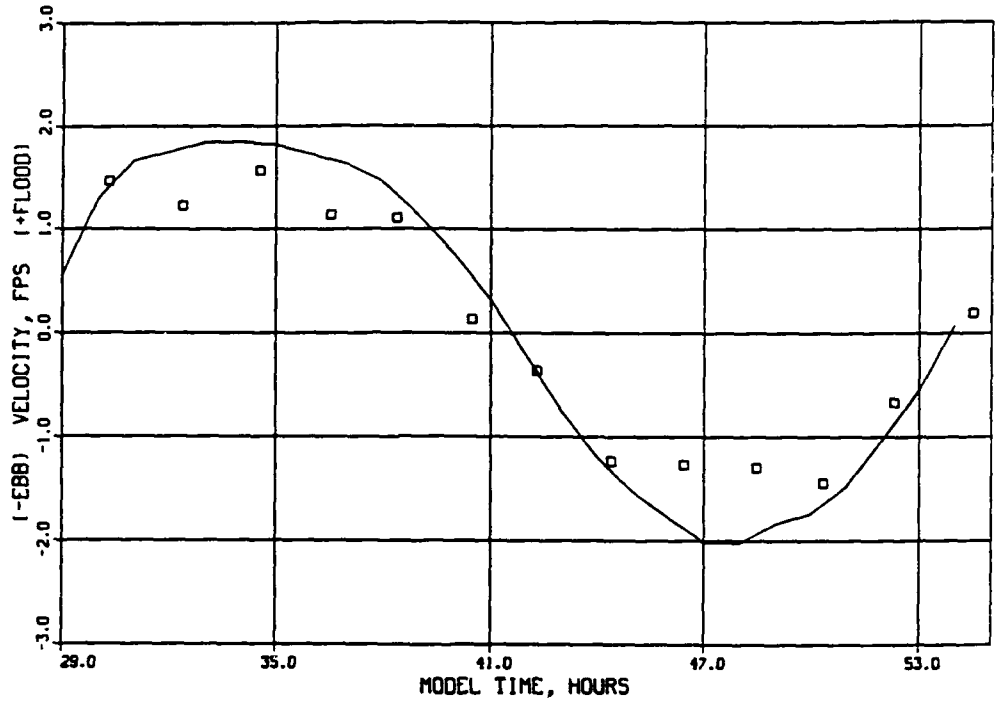

STA 6B

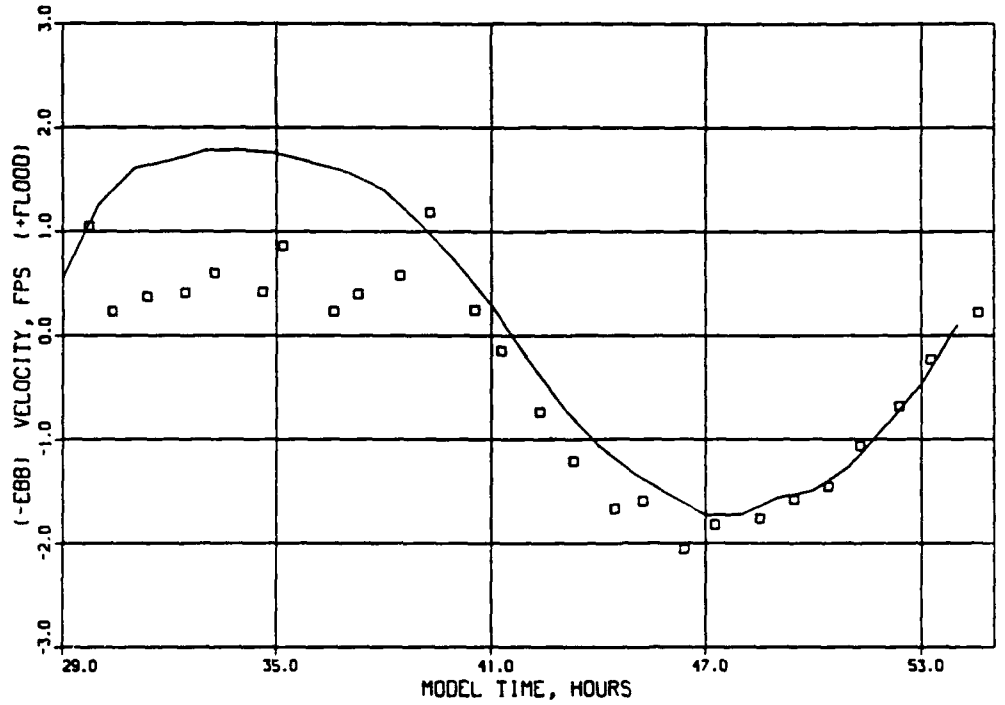

STA 6C

LEGEND

— RMA-2V

□ VERTICALLY AVERAGED FIELD DATA

VELOCITY DATA
RMA-2V VERSUS FIELD DATA
25-26 MAY 1990
STA 6B, 6C

PLATE 10

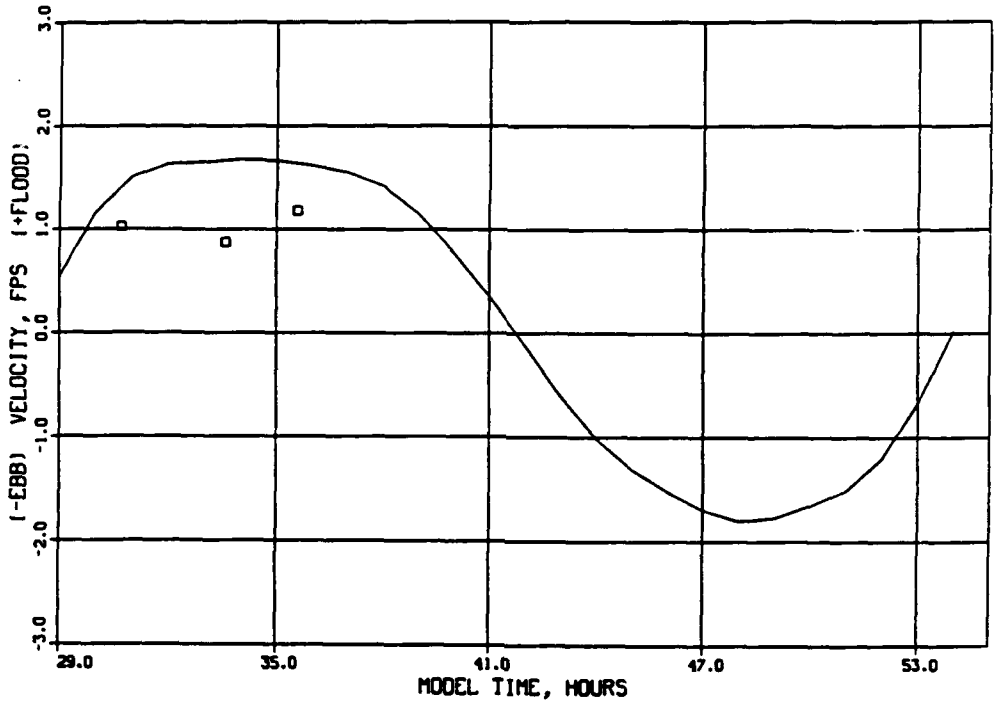

STA 7

LEGEND

— RMA-2V

□ VERTICALLY AVERAGED FIELD DATA

VELOCITY DATA
RMA-2V VERSUS FIELD DATA
25-26 MAY 1990
STA 7

PLATE 11

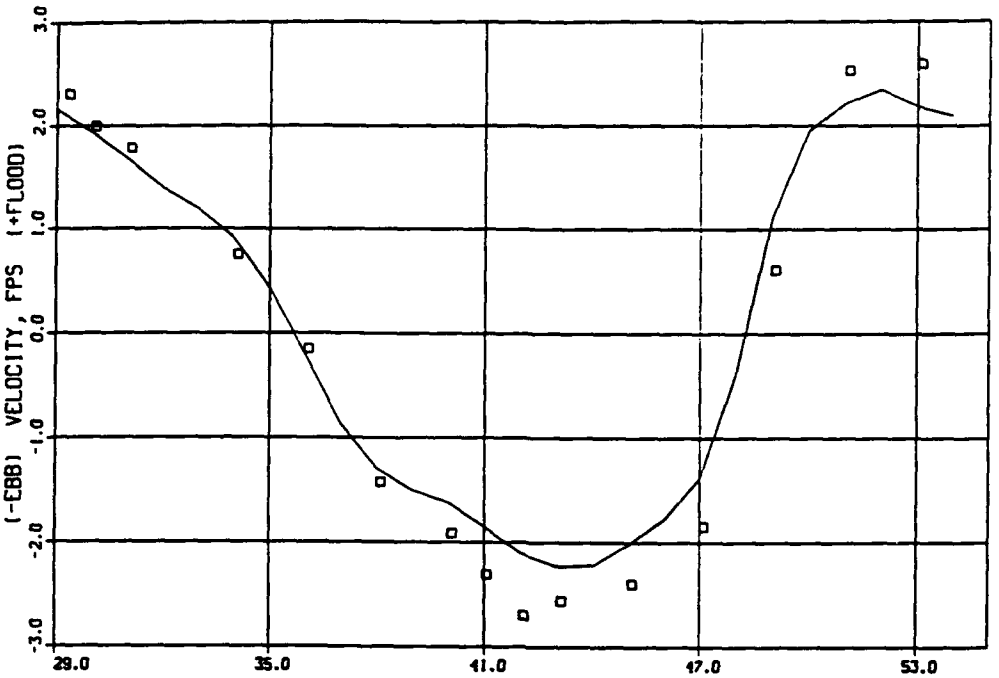

CROSS SECTION 1

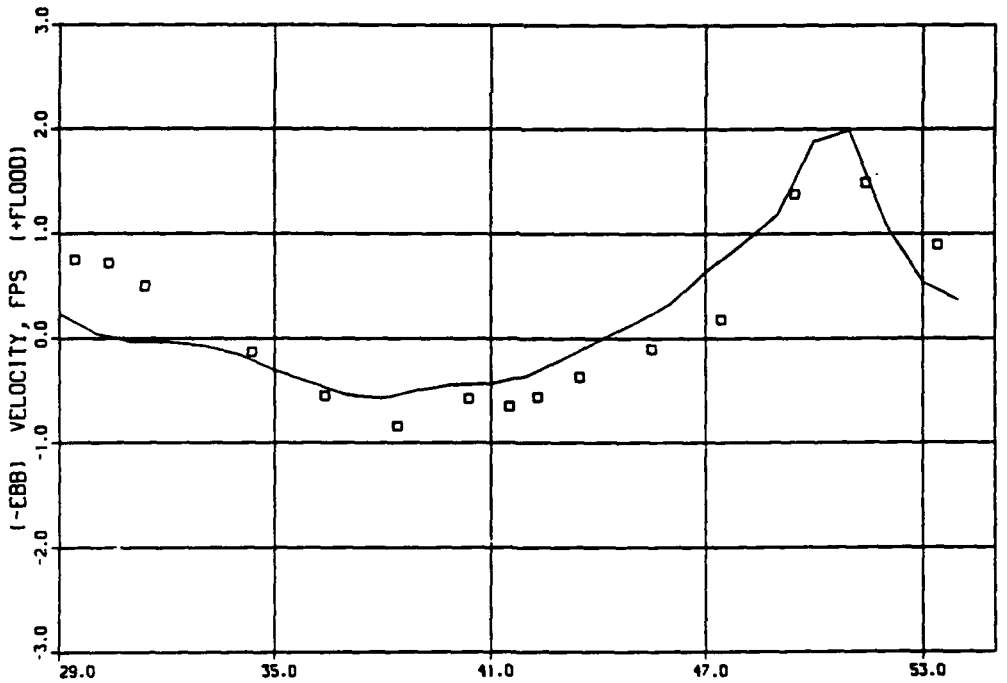

CROSS SECTION 2

LEGEND

— RMA-2V CHANNEL CENTERLINE

□ CROSS-SECTION AVERAGE FIELD MEASUREMENTS

VELOCITY DATA
RMA-2V VERSUS FIELD DATA
25-26 MAY 1990
CROSS SECTION 1, 2

PLATE 12

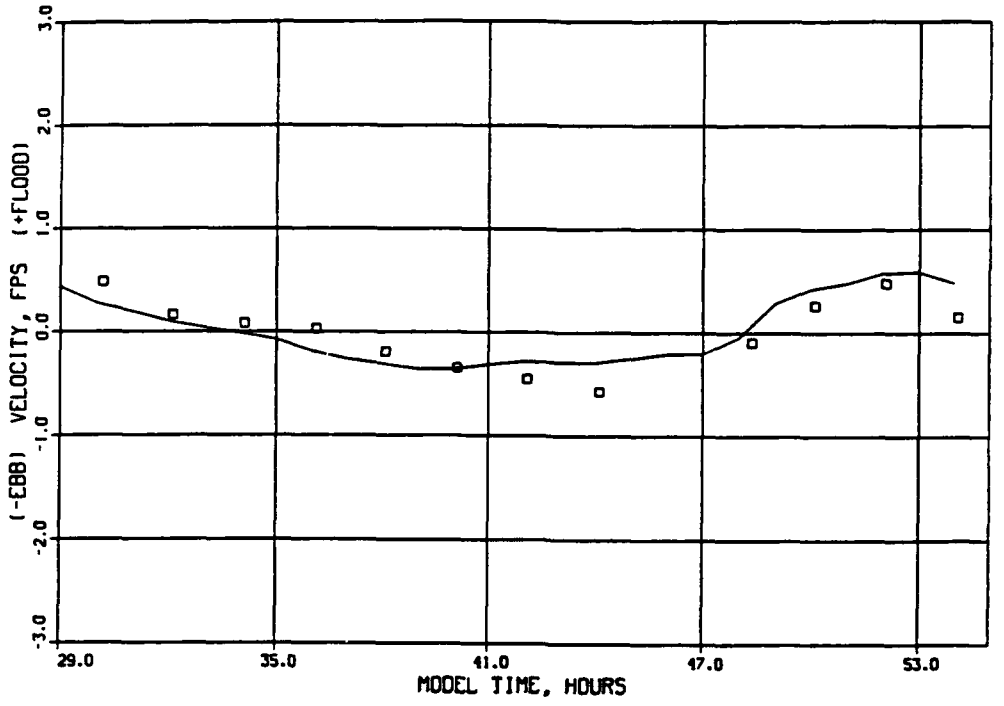

CROSS SECTION 3

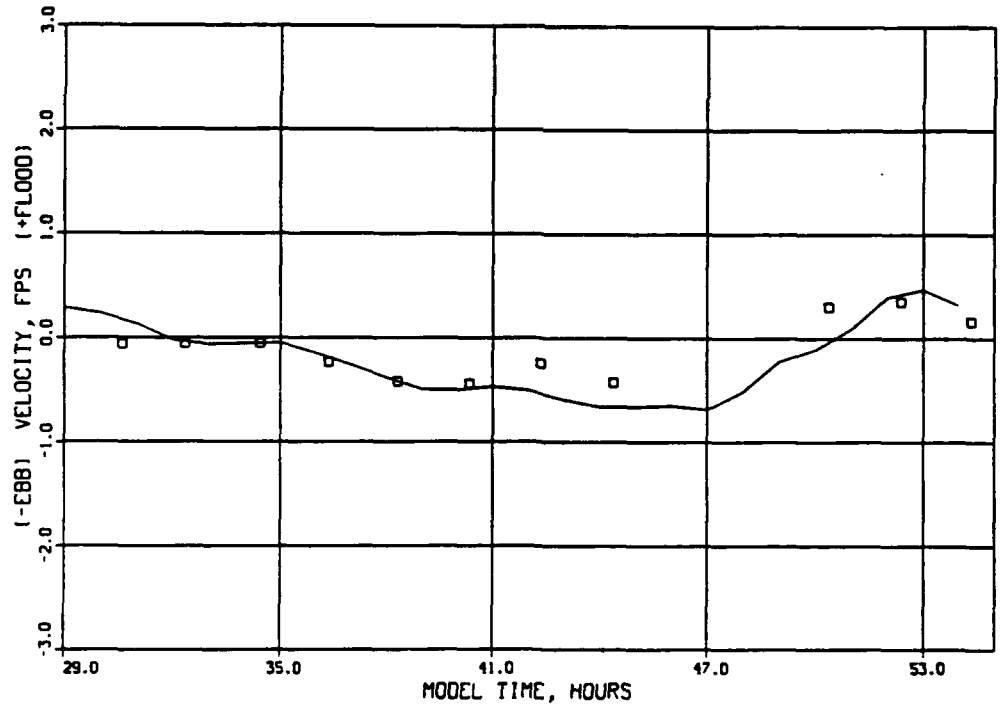

CROSS SECTION 4

LEGEND

— RMA-2V CHANNEL CENTERLINE

□ CROSS-SECTION AVERAGE FIELD MEASUREMENTS

VELOCITY DATA
RMA-2V VERSUS FIELD DATA
25-26 MAY 1990
CROSS SECTION 3, 4

PLATE 13

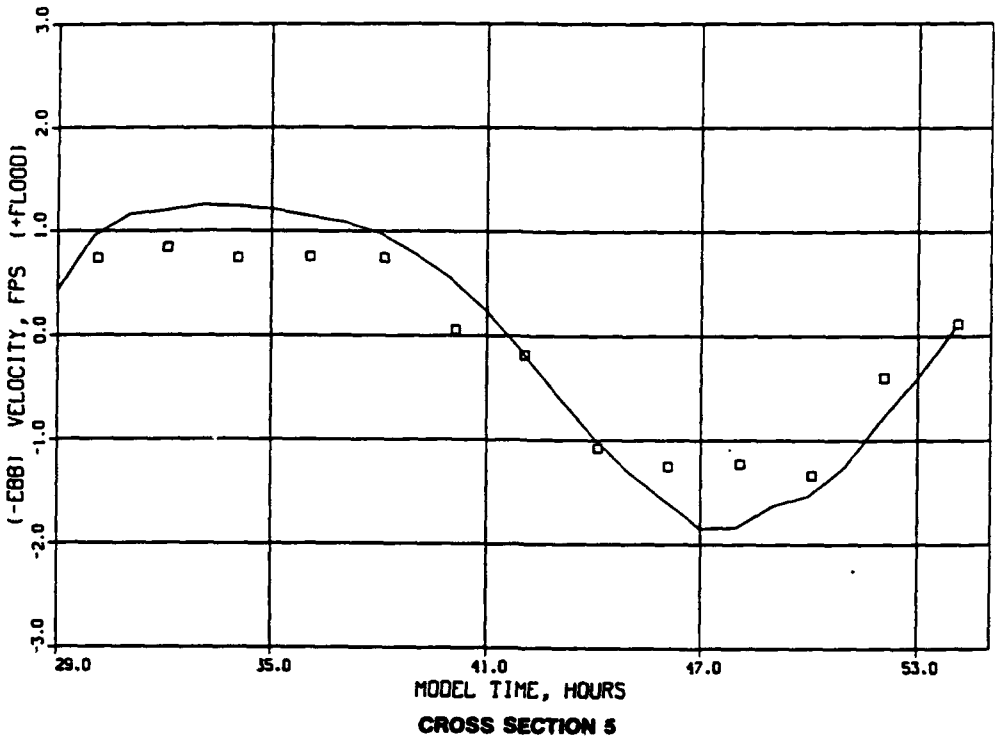

CROSS SECTION 5

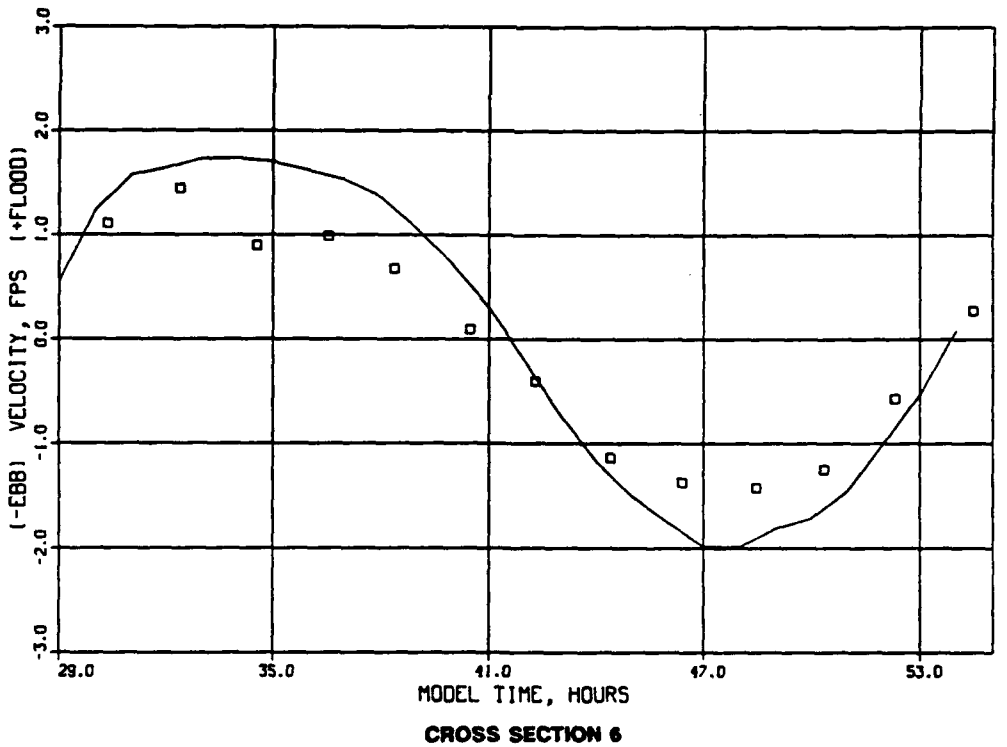

CROSS SECTION 6

LEGEND

— RMA-2V CHANNEL CENTERLINE

□ CROSS-SECTION AVERAGE FIELD MEASUREMENTS

VELOCITY DATA
RMA-2V VERSUS FIELD DATA
25-26 MAY 1990
CROSS SECTION 5, 6

PLATE 14

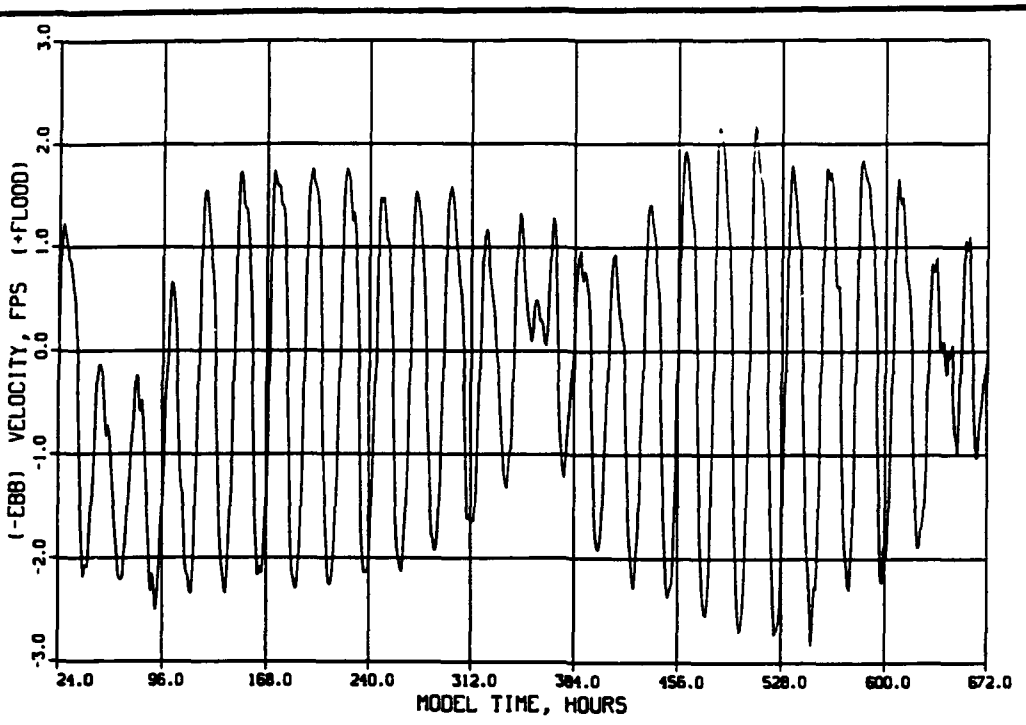

NODE 2811

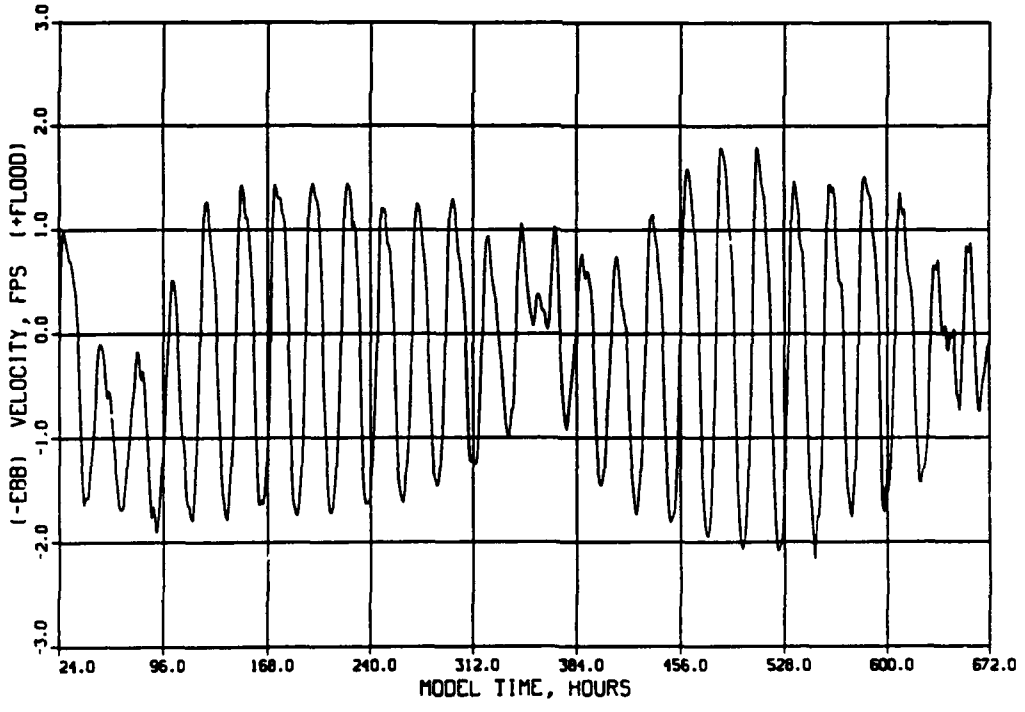

NODE 830

RMA-2V RESULTS
NAVIGATION BYPASS CHANNEL DESIGN 2
27-DAY SIMULATION
NODES 2811, 830

LEGEND
— **RMA-2V**

PLATE 15

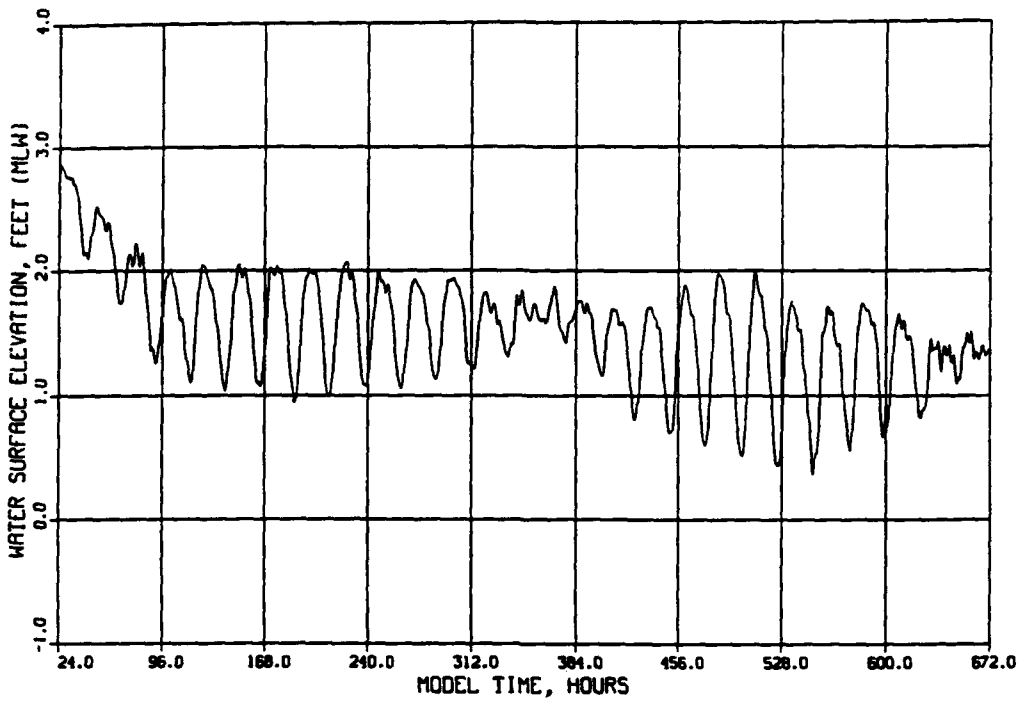

NODE 794

LEGEND

— RMA-2V

RMA-2V RESULTS
NAVIGATION BYPASS CHANNEL DESIGN 2
27-DAY SIMULATION
NODE 794

PLATE 16

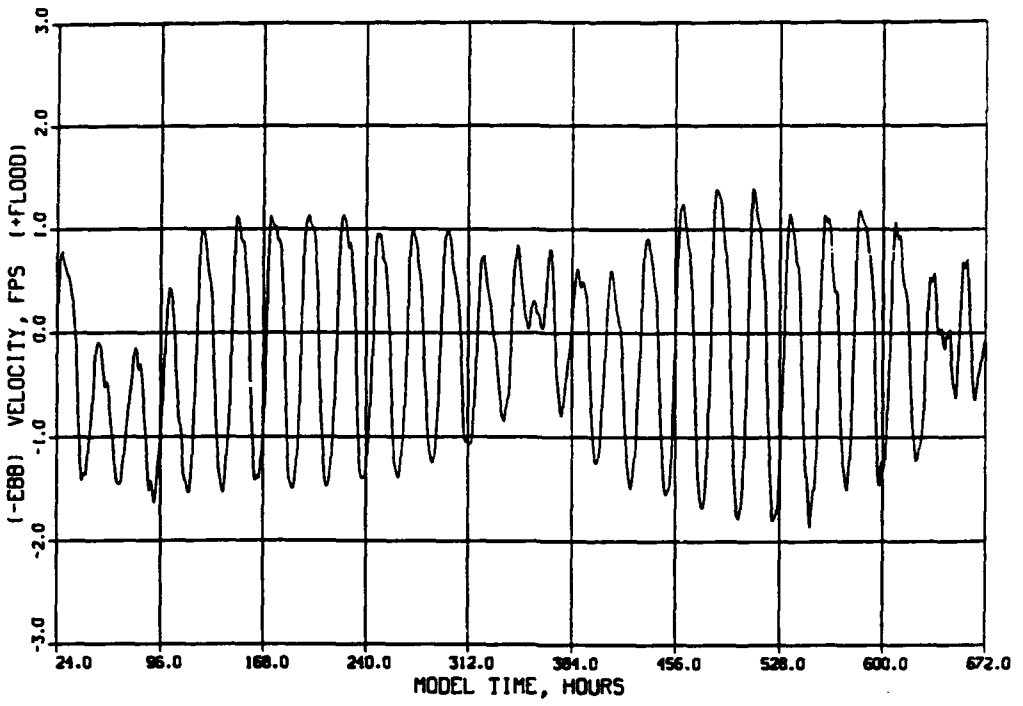

NODE 3205

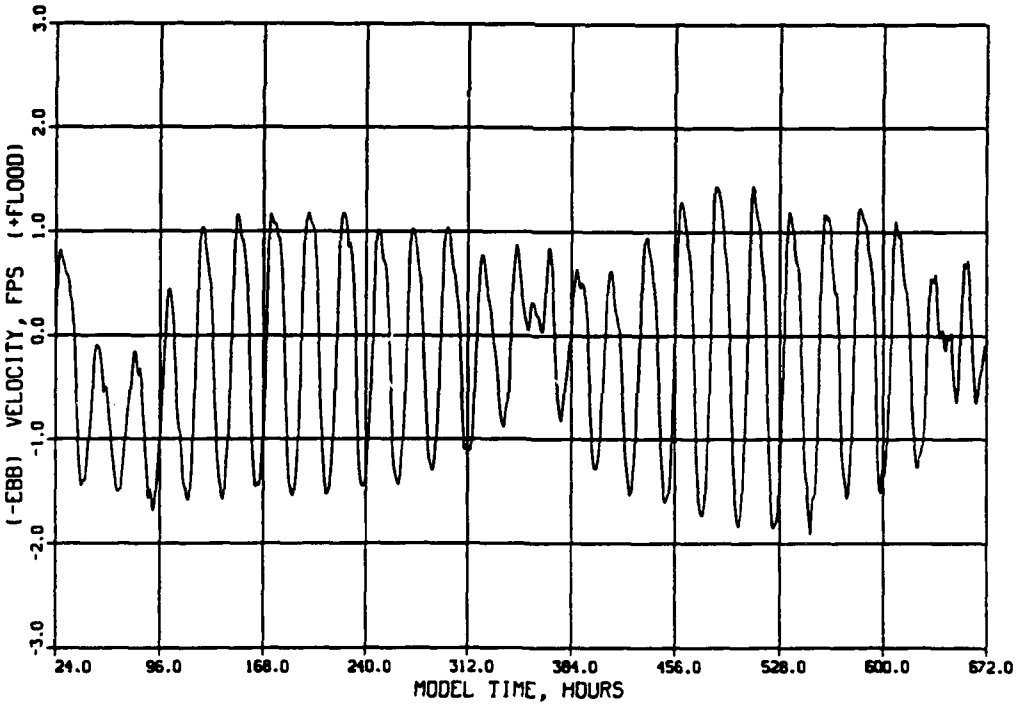

NODE 861

RMA-2V RESULTS
NAVIGATION BYPASS CHANNEL DESIGN 3
27-DAY SIMULATION
NODES 3205, 861

LEGEND
— **RMA-2V**

PLATE 17

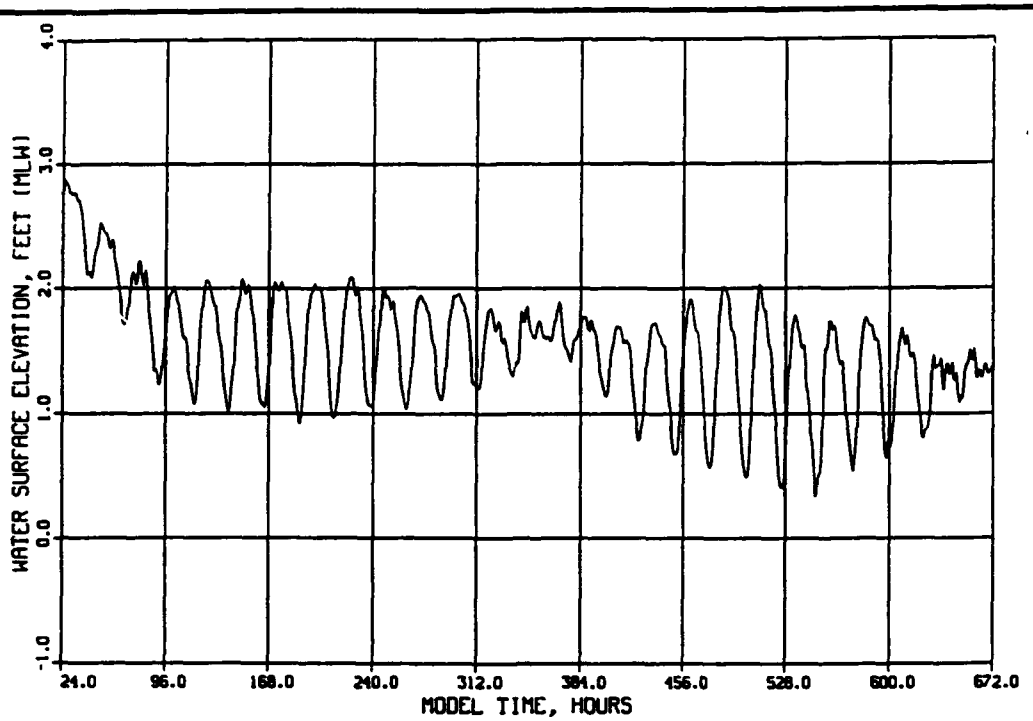

NODE 794

LEGEND

— **RMA-2V**

RMA-2V RESULTS
NAVIGATION BYPASS CHANNEL DESIGN 3
27-DAY SIMULATION
NODE 794

PLATE 18

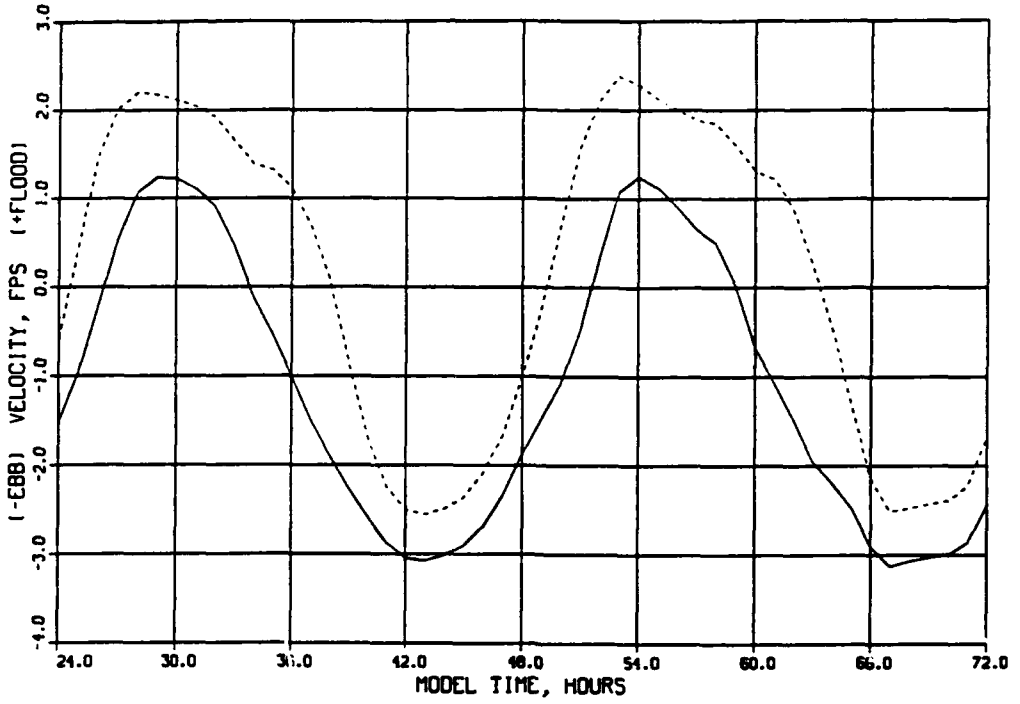

NODE 2811

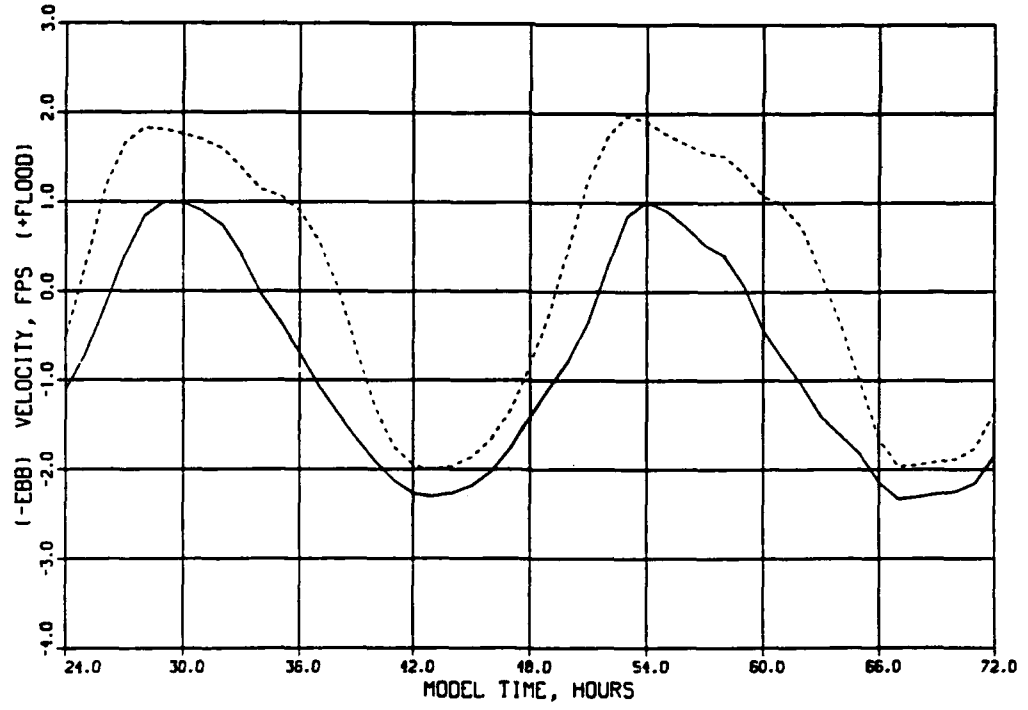

NODE 830

LEGEND

—— **RMA-2V EAST WIND**

- - - **RMA-2V WEST WIND**

RMA-2V RESULTS
SENSITIVITY TO EAST AND WEST WINDS
HIGH AMPLITUDE (TROPIC) TIDE
MODEL HOURS 24-72
NODES 2811, 830

PLATE 19

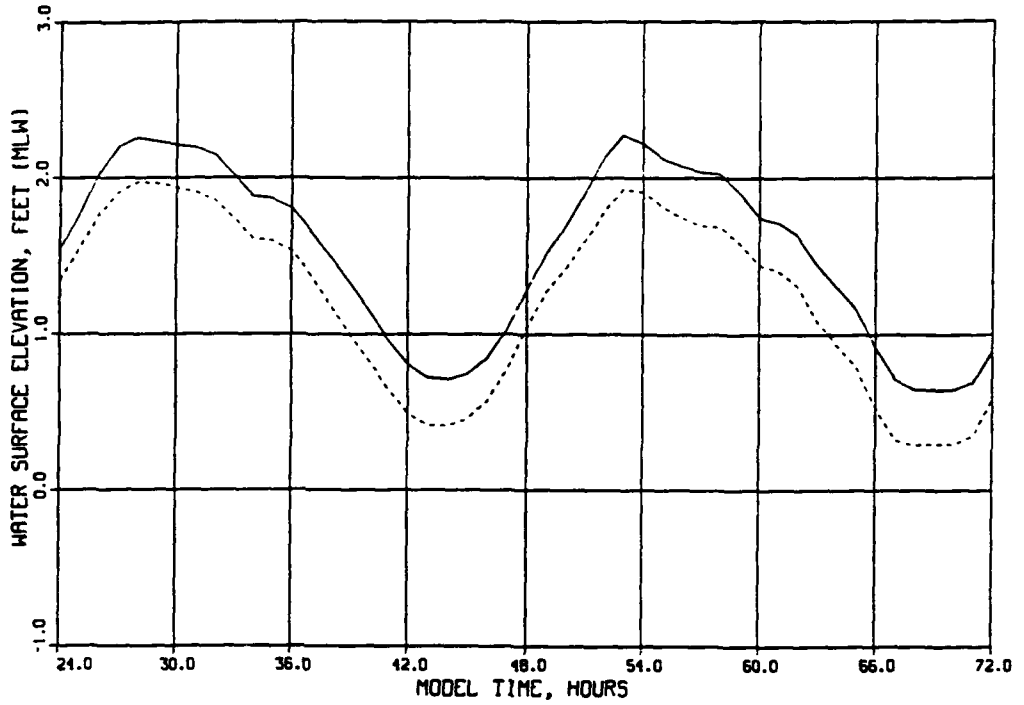

NODE 794

LEGEND

—— RMA-2V EAST WIND

- - - RMA-2V WEST WIND

RMA-2V RESULTS
SENSITIVITY TO EAST AND WEST WINDS
HIGH AMPLITUDE (TROPIC) TIDE
MODEL HOURS 24-72
NODE 794

PLATE 20

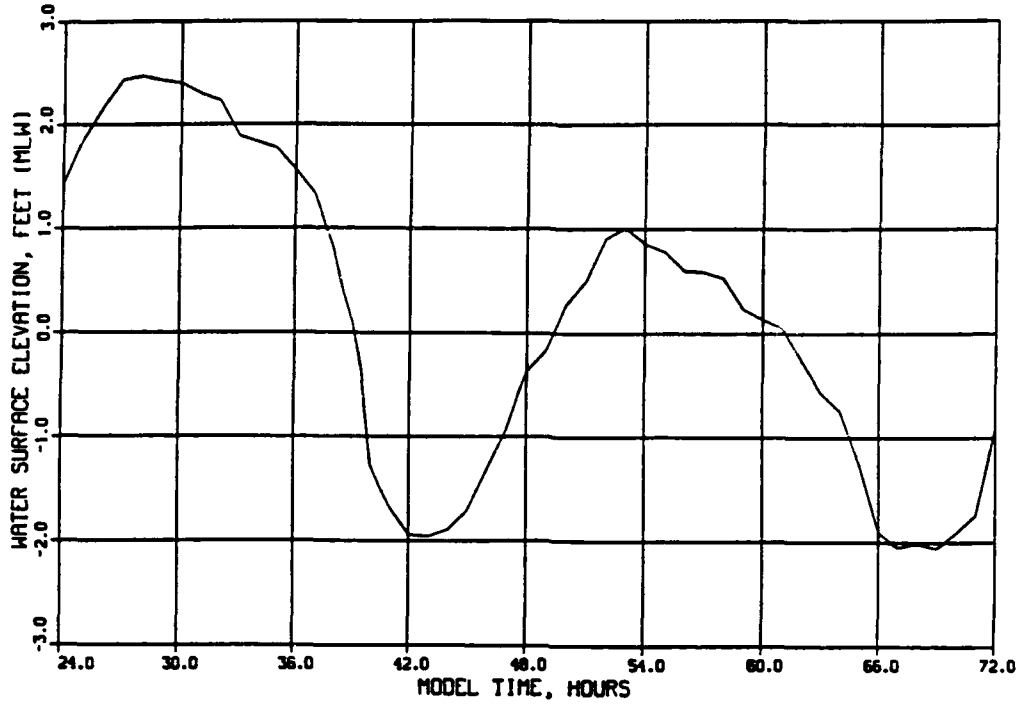

NODE 1461

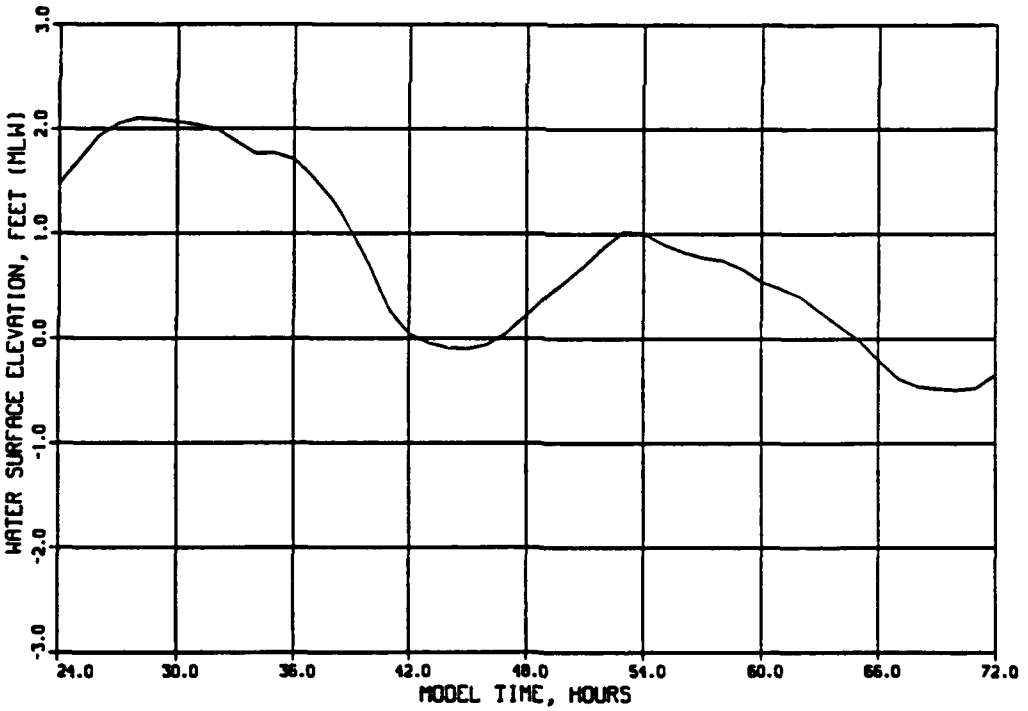

NODE 794

RMA-2V RESULTS
FRONTAL PASSAGE
HIGH AMPLITUDE (TROPIC) TIDE
MODEL HOURS 24-72
NODES 1461, 794

LEGEND
— **RMA-2V**

PLATE 21

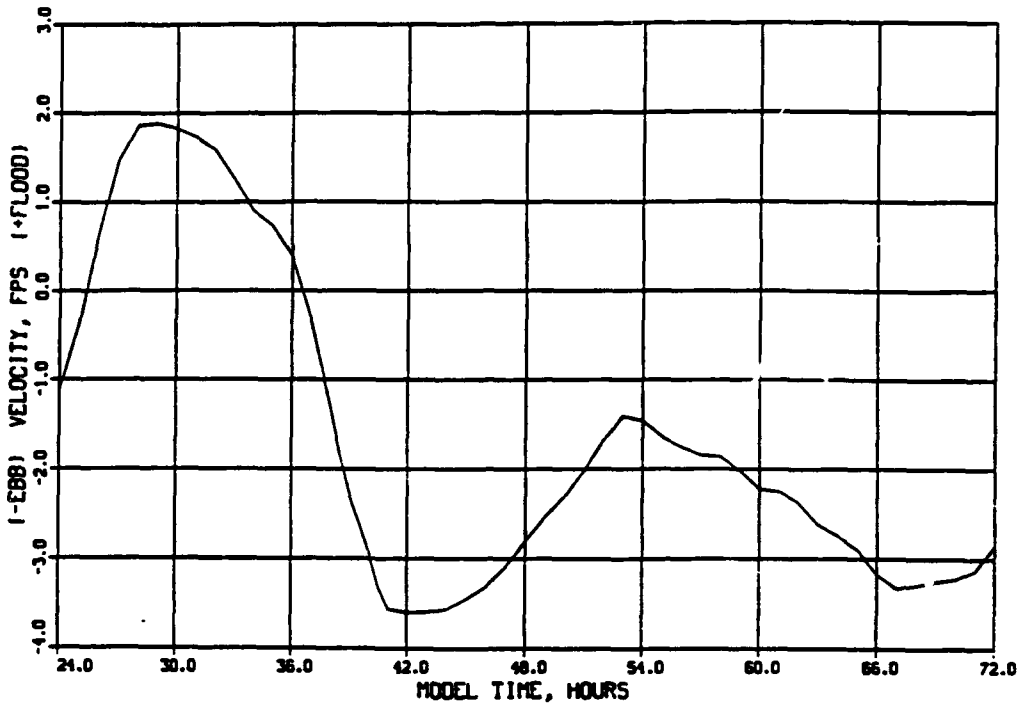

NODE 2811

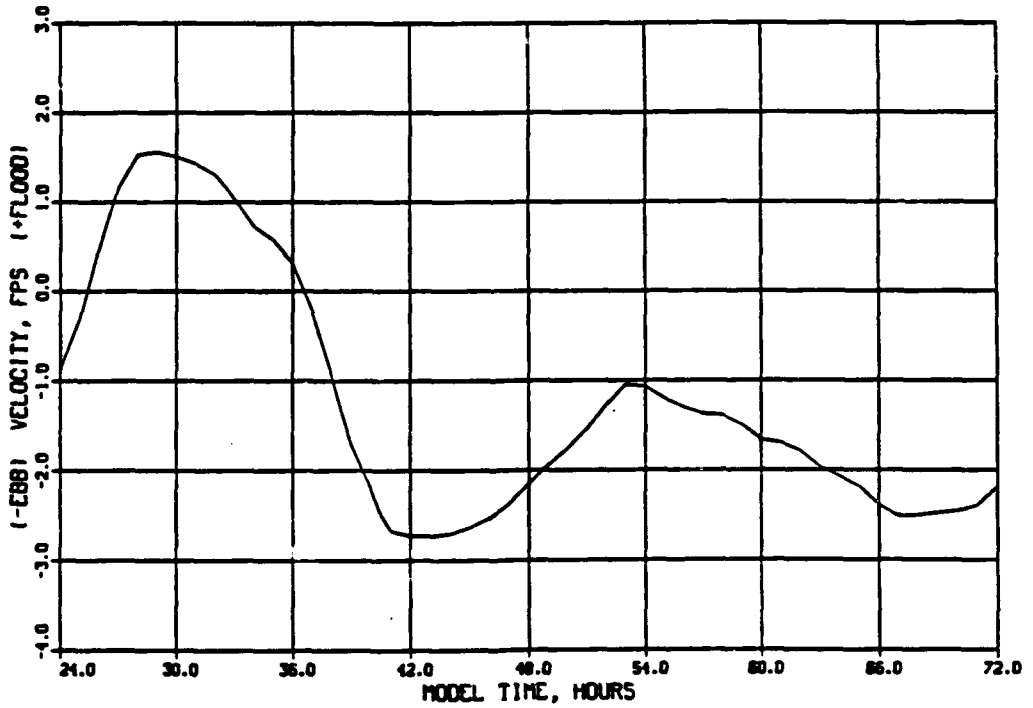

NODE 830

RMA-2V RESULTS
FRONTAL PASSAGE
HIGH AMPLITUDE (TROPIC) TIDE
MODEL HOURS 24-72
NODES 2811, 830

LEGEND
— RMA-2V

PLATE 22

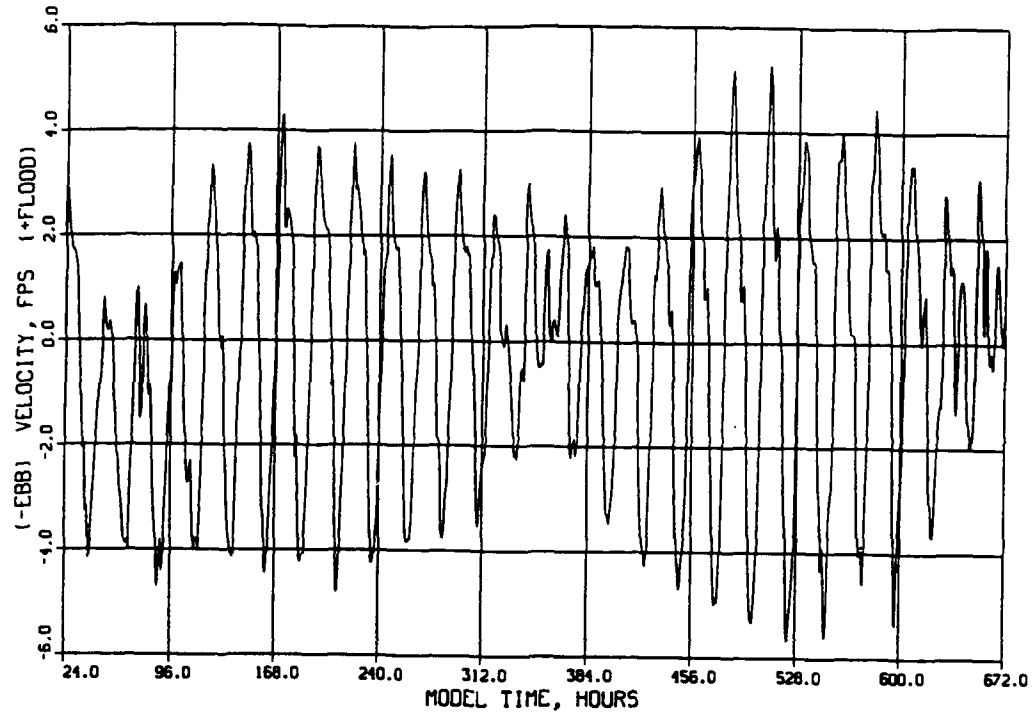

NODE 5171

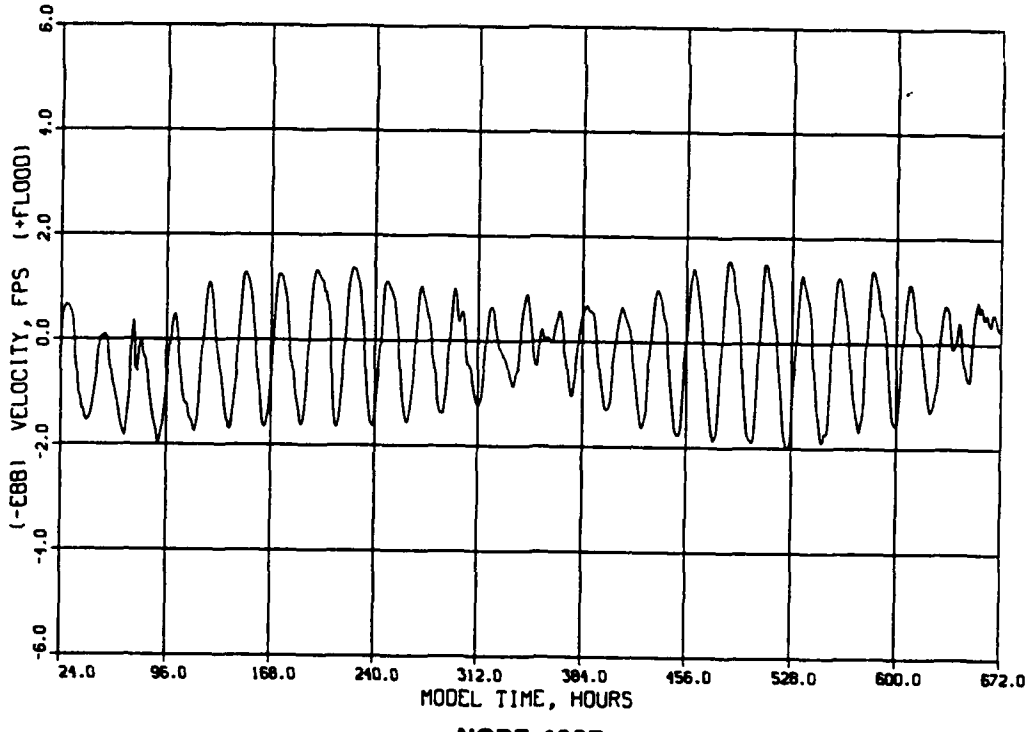

NODE 4037

LEGEND

— **RMA-2V**

RMA-2V RESULTS
McCABE CUT - GIWW
27-DAY SIMULATION
NODE 5171, 4037

PLATE 23

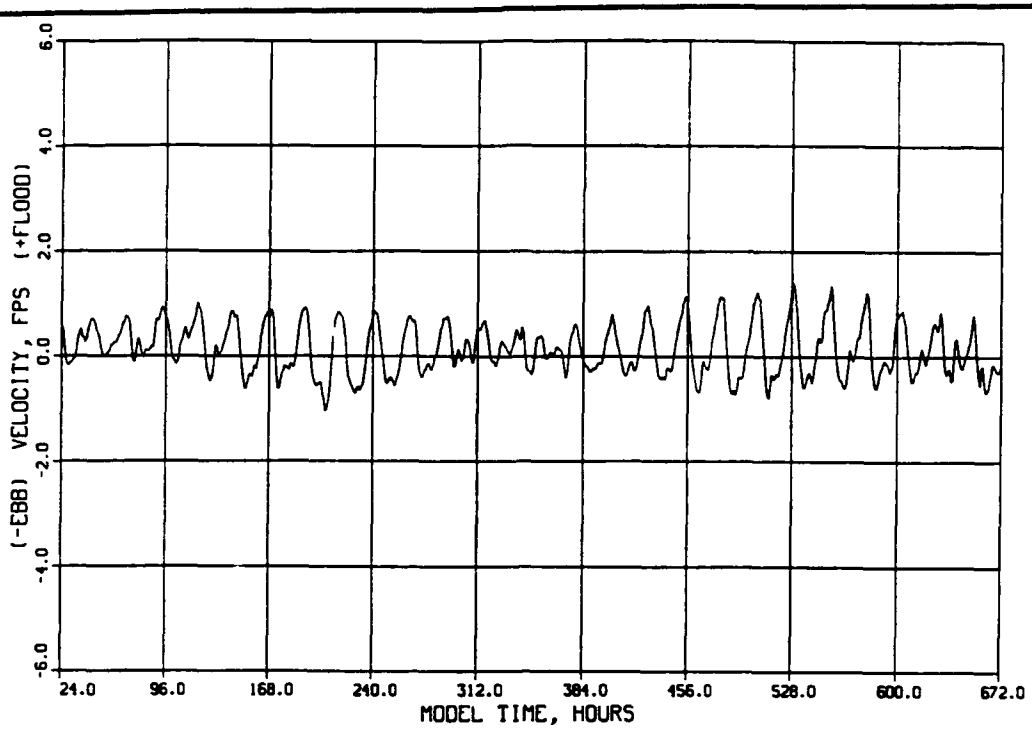

NODE 4185

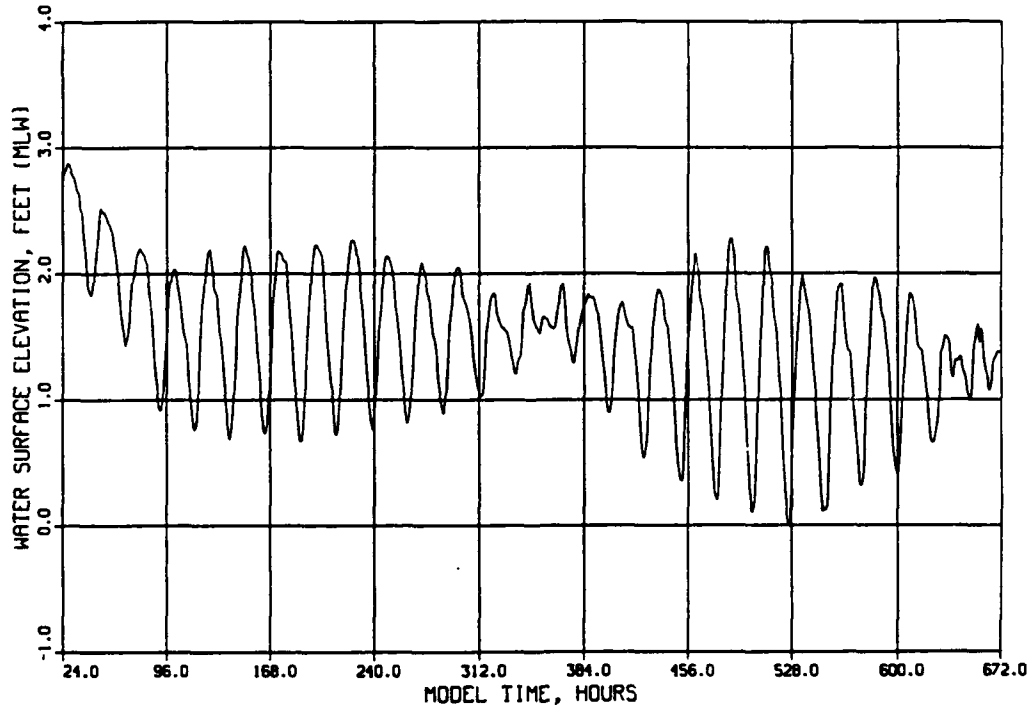

NODE 4363

RMA-2V RESULTS
McCABE CUT - GIWW
27-DAY SIMULATION
NODE 4185, 4363

LEGEND
— **RMA-2V**

PLATE 24

APPENDIX A: THE TABS-2 SYSTEM

1. TABS-2 is a collection of generalized computer programs and utility codes integrated into a numerical modeling system for studying two-dimensional hydrodynamics, sedimentation, and transport problems in rivers, reservoirs, bays, and estuaries. A schematic representation of the system is shown in Figure A1. It can be used either as a stand-alone solution technique or as a step in the hybrid modeling approach. The basic concept is to calculate water-surface elevations, current patterns, sediment erosion, transport and deposition, the resulting bed surface elevations, and the feedback to hydraulics. Existing and proposed geometry can be analyzed to determine the impact on sedimentation of project designs and to determine the impact of project designs on salinity and on the stream system. The system is described in detail by Thomas and McAnally (1985).

2. The three basic components of the system are as follows:

   a. "A Two-Dimensional Model for Free Surface Flows," RMA-2V.

   b. "Sediment Transport in Unsteady 2-Dimensional Flows, Horizontal Plane," STUDH (not used in this study).

   c. "Two-Dimensional Finite Element Program for Water Quality," RMA-4 (not used in this study).

3. RMA-2V is a finite element solution of the Reynolds form of the Navier-Stokes equations for turbulent flows. Friction is calculated with Manning's equation and eddy viscosity coefficients are used to define the turbulent losses. A velocity form of the basic equation is used with side boundaries treated as either slip or static. The model automatically recognizes dry elements and corrects the mesh accordingly. Boundary conditions may be water-surface elevations, velocities, or discharges and may occur inside the mesh as well as along the edges.

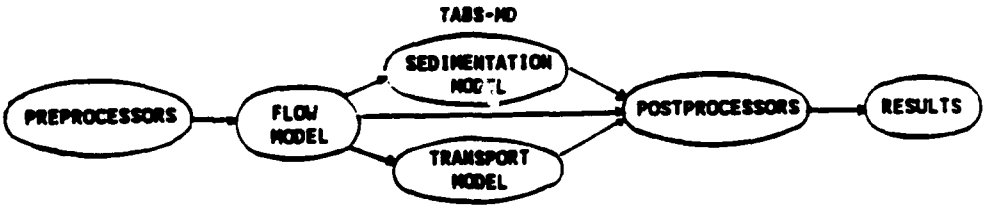

Figure A1. TABS-2 schematic

4. The sedimentation model, STUDH, solves the convection-diffusion equation with bed source terms. These terms are structured for either sand or cohesive sediments. The Ackers-White (1973) procedure is used to calculate a sediment transport potential for the sands from which the actual transport is calculated based on availability. Clay erosion is based on work by Partheniades (1962) and Ariathurai and the deposition of clay utilizes Krone's equations (Ariathurai, MacArthur, and Krone 1977). Deposited material forms layers, as shown in Figure A2, and bookkeeping allows up to 10 layers at each node for maintaining separate material types, deposit thickness, and age. The code uses the same mesh as RMA-2V.

5. Salinity calculations, RMA-4, are made with a form of the convective-diffusion equation which has general source-sink terms. Up to seven conservative substances or substances requiring a decay term can be routed. The code uses the same mesh as RMA-2V.

6. Each of these generalized computer codes can be used as a standalone program, but to facilitate the preparation of input data and to aid in analyzing results, a family of utility programs was developed for the following purposes:

a. Digitizing
b. Mesh generation
c. Spatial data management
d. Graphical output
e. Output analysis
f. File management
g. Interfaces
h. Job control language

Finite Element Modeling

7. The TABS-2 numerical models used in this effort employ the finite element method to solve the governing equations. To help those who are unfamiliar with the method to better understand this report, a brief description of the method is given here.

8. The finite element method approximates a solution to equations by dividing the area of interest into smaller subareas, which are called elements. The dependent variables (e.g., water-surface elevations and sediment

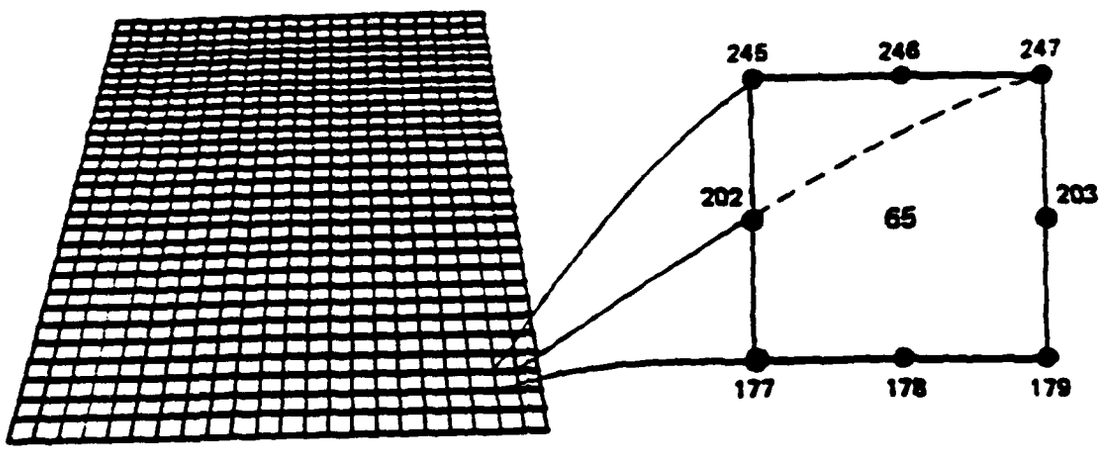

a. Eight nodes define each element

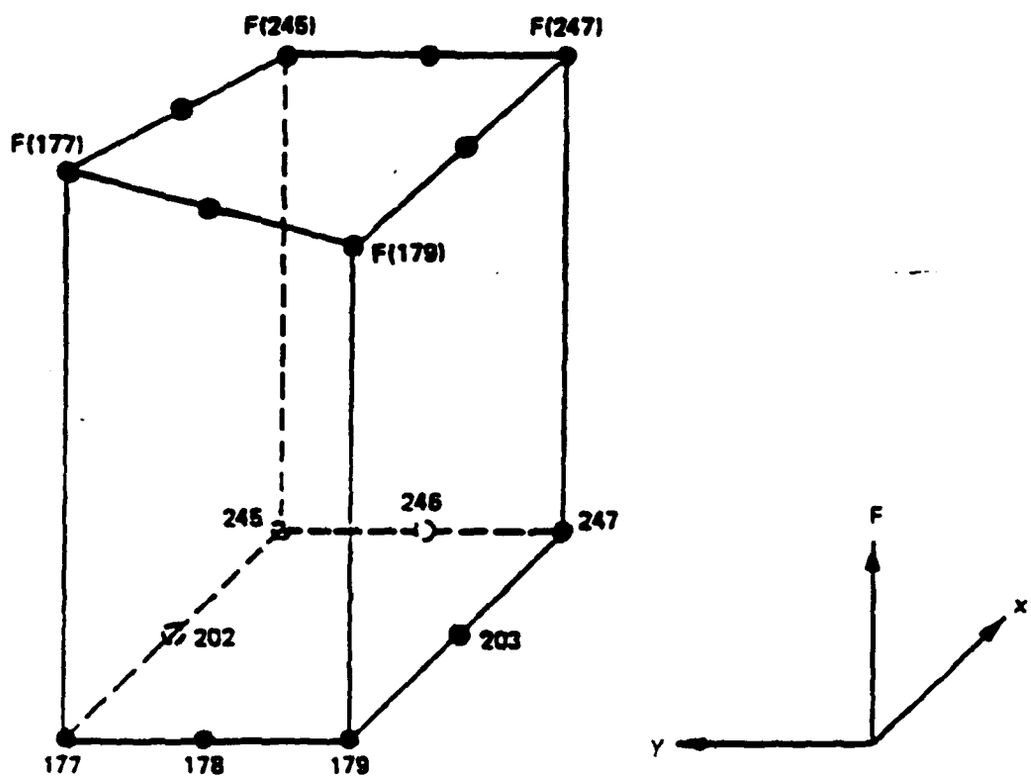

b. Linear interpolation function

Figure A2. Two-dimensional finite element mesh

concentrations) are approximated over each element by continuous functions which interpolate in terms of unknown point (node) values of the variables. An error, defined as the deviation of the approximation solution from the correct solution, is minimized. Then, when boundary conditions are imposed, a set of solvable simultaneous equations is created. The solution is continuous over the area of interest.

9. In one-dimensional problems, elements are line segments. In two-dimensional problems, the elements are polygons, usually either triangles or quadrilaterals. Nodes are located on the edges of elements and occasionally inside the elements. The interpolating functions may be linear or higher order polynomials. Figure A2 illustrates a quadrilateral element with eight nodes and a linear solution surface where F is the interpolating function.

10. Most water resource applications of the finite element method use the Galerkin method of weighted residuals to minimize error. In this method the residual, the total error between the approximate and correct solutions, is weighted by a function that is identical with the interpolating function and then minimized. Minimization results in a set of simultaneous equations in terms of nodal values of the dependent variable (e.g. water-surface elevations or sediment concentration). The time portion of time-dependent problems can be solved by the finite element method, but it is generally more efficient to express derivatives with respect to time in finite difference form.

The Hydrodynamic Model, RMA-2V

Applications

11. This program is designed for far-field problems in which vertical accelerations are negligible and the velocity vectors at a node generally point in the same directions over the entire depth of the water column at any instant of time. It expects a homogeneous fluid with a free surface. Both steady and unsteady state problems can be analyzed. A surface wind stress can be imposed.

12. The program has been applied to calculate flow distribution around islands; flow at bridges having one or more relief openings, in contracting and expanding reaches, into and out of off-channel hydropower plants, at river junctions, and into and out of pumping plant channels; and general flow patterns in rivers, reservoirs, and estuaries.

Limitations

13. This program is not designed for near-field problems where flow-structure interactions (such as vortices, vibrations, or vertical accelerations) are of interest. Areas of vertically stratified flow are beyond this program's capability unless it is used in a hybrid modeling approach. It is two-dimensional in the horizontal plane, and zones where the bottom current is in a different direction from the surface current must be analyzed with considerable subjective judgement regarding long-term energy considerations. It is a free-surface calculation for subcritical flow problems.

Governing equations

14. The generalized computer program RMA-2V solves the depth-integrated equations of fluid mass and momentum conservation in two horizontal directions. The form of the solved equations is

$$h\frac{\partial u}{\partial t} + hu\frac{\partial u}{\partial x} + hv\frac{\partial u}{\partial y} - \frac{h}{\rho}\left[\epsilon_{xx}\frac{\partial^2 u}{\partial x^2} + \epsilon_{xy}\frac{\partial^2 u}{\partial y^2}\right] + gh\left[\frac{\partial a}{\partial x} + \frac{\partial h}{\partial x}\right]$$

$$+ \frac{gun^2}{\left[1.486h^{1/6}\right]^2}\left[u^2 + v^2\right]^{1/2} - \zeta V_a^2 \cos\psi - 2h\omega v \sin\phi = 0 \qquad \text{(A1)}$$

$$h\frac{\partial v}{\partial t} + hu\frac{\partial v}{\partial x} + hv\frac{\partial v}{\partial y} - \frac{h}{\rho}\left[\epsilon_{yx}\frac{\partial^2 v}{\partial x^2} + \epsilon_{yy}\frac{\partial^2 v}{\partial y^2}\right] + gh\left[\frac{\partial a}{\partial y} + \frac{\partial h}{\partial y}\right]$$

$$+ \frac{gvn^2}{\left[1.486h^{1/6}\right]^2}\left[u^2 + v^2\right]^{1/2} - \zeta V_a^2 \sin\psi + 2\omega hu \sin\phi = 0 \qquad \text{(A2)}$$

$$\frac{\partial h}{\partial t} + h\left[\frac{\partial u}{\partial x} + \frac{\partial v}{\partial y}\right] + u\frac{\partial h}{\partial x} + v\frac{\partial h}{\partial y} = 0 \qquad \text{(A3)}$$

where

h = depth

u,v = velocities in the Cartesian directions

x,y,t = Cartesian coordinates and time

ρ = density

ϵ = eddy viscosity coefficient, for xx = normal direction on x-axis surface; yy = normal direction on y-axis surface; xy and yx = shear direction on each surface

g = acceleration due to gravity

a = elevation of bottom

n = Manning's n value

1.486 = conversion from SI (metric) to non-SI units

ζ = empirical wind shear coefficient

V_a = wind speed

ψ = wind direction

ω = rate of earth's angular rotation

ϕ = local latitude

15. Equations A1, A2, and A3 are solved by the finite element method using Galerkin weighted residuals. The elements may be either quadrilaterals or triangles and may have curved (parabolic) sides. The shape functions are quadratic for flow and linear for depth. Integration in space is performed by Gaussian integration. Derivatives in time are replaced by a nonlinear finite difference approximation. Variables are assumed to vary over each time interval in the form

$$f(t) = f(0) + at + bt^c \qquad t_0 \leq t < t \tag{A4}$$

which is differentiated with respect to time, and cast in finite difference form. Letters a , b , and c are constants. It has been found by experiment that the best value for c is 1.5 (Norton and King 1977).

16. The solution is fully implicit and the set of simultaneous equations is solved by Newton-Raphson iteration. The computer code executes the solution by means of a front-type solver that assembles a portion of the matrix and solves it before assembling the next portion of the matrix. The front solver's efficiency is largely independent of bandwidth and thus does not require as much care in formation of the computational mesh as do traditional solvers.

17. The code RMA-2V is based on the earlier version RMA-2 (Norton and King 1977) but differs from it in several ways. It is formulated in terms of velocity (v) instead of unit discharge (vh), which improves some aspects of the code's behavior; it permits drying and wetting of areas within the grid;

and it permits specification of turbulent exchange coefficients in directions other than along the x- and z-axes. For a more complete description, see Appendix F of Thomas and McAnally (1985).

References

Ackers, P., and White, W. R. 1973 (Nov). "Sediment Transport: New Approach and Analysis," Journal, Hydraulics Division, American Society of Civil Engineers, No. HY-11.

Ariathurai, R., MacArthur, R. D., and Krone, R. C. 1977 (Oct). "Mathematical Model of Estuarial Sediment Transport," Technical Report D-77-12, US Army Engineer Waterways Experiment Station, Vicksburg, MS.

Norton, W. R., and King, I. P. 1977 (Feb). "Operating Instructions for the Computer Program RMA-2V," Resource Management Associates, Lafayette, CA.

Partheniades, E. 1962. "A Study of Erosion and Deposition of Cohesive Soils in Salt Water," Ph.D. Dissertation, University of California, Berkeley, CA.

Thomas, W. A., and McAnally, W. H., Jr. 1985 (Aug). "User's Manual for the Generalized Computer Program System; Open-Channel Flow and Sedimentation, TABS-2, Main Text and Appendices A through O," Instruction Report HL-85-1, US Army Engineer Waterways Experiment Station, Vicksburg, MS.